MICROREACTORS AND MICROCAPSULES AS APPROACHES TO MULTICATALYST SYSTEMS

A Dissertation

Presented to the Faculty of the Graduate School

of Cornell University

In Partial Fulfillment of the Requirements for the Degree of

Doctor of Philosophy

by

Sarah Lihoa Poe

January 2009

MICROREACTORS AND MICROCAPSULES AS APPROACHES TO MULTICATALYST SYSTEMS

Sarah Lihoa Poe, Ph. D.

Cornell University 2009

This dissertation discusses the use of microreactors and microcapsules in the context of multicatalyst systems. The first two chapters focus on organic synthesis in microfluidic devices, whose modular design offers the possibility for performing sequential reactions in flow. In the first example, the unique behavior of fluids at small dimensions was taken advantage of in order to prevent solid products from clogging the microfluidic channels. By performing reactions in dispersed droplets surrounded by a carrier phase, the precipitated products were kept away from the channel walls, preventing channel clogging. The second chapter describes the synthesis of ibuprofen and atropine as multi-step syntheses in flow. In addition to the successful synthesis of both of these products, this project resulted in the development of a solid-supported reagent that has the potential to enable multi-step synthesis in flow. The second focus of this work involves microencapsulated catalysts. The theory behind this approach is that the encapsulation of large polymeric catalysts within polymer shells would prevent catalysts from interacting with each other, allowing for the use of multiple catalysts in one reaction vessel. The synthesis of a microencapsulated polyamine catalyst is described, and the development of a two-step, one-pot reaction is discussed. This multistep reaction, consisting of nitroalkene formation and a Michael reaction, produces γ-amino acid precursors that cannot be obtained if the polyamine catalyst in not encapsulated. In addition to catalyzing nitroalkene formation, the microencapsulated catalyst was found to enhance the rate of

the Michael addition. Initially attributed to the ureas of the polyurea capsule, it was discovered that the rate enhancement was due to the amine groups. However, a small molecule bifunctional urea was developed that was found to provide rate enhancement for the proline-catalyzed α-aminoxylation of aldehydes. Experimental evidence suggests that the origin of the rate enhancement is due to interaction between the urea and an oxazolidinone and may be general for other proline-catalyzed reactions involving aldehydes.

BIOGRAPHICAL SKETCH

Born in 1982, Sarah Lihoa Poe was raised in Duluth, Minnesota, where she learned to ski shortly after she learned to walk. After spending 17 years of her life trying not to become a chemist like her parents, she attended Wellesley College in Wellesley, Massachusetts and promptly became a chemistry major. After dabbling in biochem and P-chem labs, she joined the organic chemistry laboratory of David R. Haines, where she decided to settle down until she graduated *magna cum laude* in 2004. Despite having fallen in love with California during a summer REU at Harvey Mudd College, Sarah opted not to head to the West Coast for grad school, but rather she decided to spend the next 5(ish) years in the middle of New York state, where the snow and cold reminded her of home. There she joined the group of D. Tyler McQuade, where she focused on making synthetic chemistry more efficient by designing multicatalyst systems. Upon moving to Tallahassee with the rest of the McQuade group in September of 2007, Sarah was overwhelmed by the unfamiliar sensation of heat and humidity. Fortunately, she discovered that this could be avoided by staying in the lab during daylight hours, which, to her delight, was also conducive to completing her Ph. D. requirements.

To my parents, for everything.

ACKNOWLEDGEMENTS

Although the degree that I will receive will bear only my name, to say that I earned it alone would be a lie. I would not be where I am without the support of so many others, and this is a result of their efforts as well as mine.

None of this work would have been possible without my adviser D. Tyler McQuade, who provided me not only with a project, space, and funding, but more importantly with guidance, knowledge, and his confidence that I could do anything. In challenging me to realize my potential, he has made me grow both scientifically and otherwise. I also thank David Haines, whose insightful advice led me to grad school in the first place.

I am very fortunate to have interacted with many faculty, staff members, and students at both Cornell and Florida State University, who have helped me in ways I probably have yet to realize. Thank you to the members of the McQuade group, without whom I would have had a very lonely five years, and especially to Andrew Bogdan, who was constantly there with me and for me throughout this whole journey.

I owe so much to my parents, who have been an unfailing source of love, support, and guidance in my 26 years. They provided me with, among many other things, an amazing environment in which to discover and pursue my interests.

Finally, I am deeply grateful both to and for Muris Kobašlija, whose contributions to this work are evident in the chapters of this thesis, but whose impact on my life are not as easily put into words. For everything that we've been through and everything that we have to look forward to, thank you.

TABLE OF CONTENTS

LIST OF FIGURES

LIST OF SCHEMES

LIST OF TABLES

LIST OF EQUATIONS

CHAPTER 1

Solving the Clogging Problem: Precipitate-Forming Reactions in Flow

Preface

In early 2005, former McQuade group members Elizabeth Quevedo and Jeremy Steinbacher developed a microfluidic device consisting of syringe pumps, syringes, needles, and tubing. This device was readily adaptable, relatively inexpensive, and capable of performing interfacial polymerization in flow to produce polyamide microcapsules. The work described in this chapter builds upon their technique and has led to a method of performing precipitate-forming organic synthesis in flow.

Abstract

This work describes a method by which solids can be produced in flow. A monodisperse flow in a microreactor provides an efficient method for keeping solid products away from channel walls. The use of a carrier phase, such as mineral oil, hexane, or toluene, enables solids to be synthesized without clogging of the reactor channels. The synthesis of indigo, *N*,*N*'-dicyclohexylethylenediimine, and 4-chloro-*N*-methylbenzamide are discussed.

Introduction[*]

Techniques developed in recent decades have done little to change the fundamental processes of chemistry. Reaction vessels of a century ago continue to be

[*] Poe, S. L.; Cummings, M. A.; Haaf, M. P.; McQuade, D. T.: Solving the Clogging Problem: Precipitate-Forming Reactions in Flow. *Angew. Chem. Int. Ed.* **2006**, *45*, 1544-1548.

the standard reactors of today. Recently, however, increasing attention has been paid to chemical reactions performed in microreactors.[1-6] Reactions are performed in these microfluidic devices by flowing reactants through channels that generally range in size from 10 to 500 mm. On account of its small proportions, a flat microchannel with a width of 100 mm has a specific surface-area-to-volume ratio that is 200 times larger than that of a 100-mL flask and over 3000 times larger than a tank that occupies a cubic meter.[7] This increased surface-area-to volume ratio allows for better molecular diffusion and heat transfer properties, which allow faster and more-selective chemical reactions.[8,9]

From an industrial standpoint, microreactors are advantageous because they eliminate the need to scale up a reaction. Whereas in traditional process chemistry bench-top syntheses must be redesigned for industrial compatibility, a method known as numbering-up involves the addition of microreactors to achieve the desired throughput.[10] As every reactor is identical to the pilot reactor, there is no need to change dimensions or conditions. Other advantages include increased safety,[11] lower costs, and more environmentally friendly chemistry owing to efficient reactions that require less solvent.

Despite the numerous advantages of microreactors, they are not without their drawbacks.[12,13] Researchers in an academic setting have been slow to embrace these systems because of their cost and inflexibility.[14] The manufacture of a single microreactor can be a very time- and cost-intensive process, and once a microreactor has been developed, there is rarely any opportunity to make variations to the device.[15] Another commonly cited concern is the clogging of the channels that occurs upon precipitate formation.[16] The handling and processing of solids make up a significant proportion of laboratory and industrial processes, and current microreactor technology is not yet ready to handle these syntheses efficiently.[17] There has recently been an

increased effort to deal with this problem, although many industrial solutions come at a large expense. A less expensive approach incorporates a periodic purging step to flush out solids that have formed on the channel walls.[18] However, this method is not effective if significant solid buildup occurs before purging. A more attractive alternative involves performing reactions in droplets that travel through the microreactor channels inside a carrier phase.[19]

Fluid fields generated in microfluidic devices can control reagent mixing[20] and allow the formation of an emulsion upon the collision of two immiscible liquids. We have recently reported a simple microfluidic device that can replicate these flow phenomena.[21] Our device is composed of syringe pumps, syringes, needles, and ordinary laboratory tubing—all of which are relatively inexpensive and commercially available (Figure 1.1). Development of our microreactor to facilitate chemical syntheses would potentially ameliorate some of the problems still plaguing microreactors, namely their cost and channel clogging. By utilizing disperse-phase droplets as individual reactors, we can confine the solid products to these droplets, thus keeping them away from the tubing walls and avoiding clogged channels. Herein, we present the results of the first chemical syntheses performed in our microreactor and show that our device is practical and efficient for the production of solids in a microfluidic device.[22]

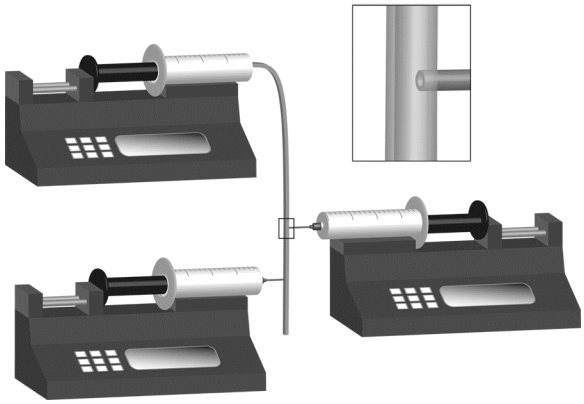

Figure 1.1. Basic design of our microfluidic reactor. The top-left syringe pump contains the carrier phase, the right pump contains the first disperse phase, and the bottom-left pump contains the second disperse phase. Reagents are injected through a 30-gauge blunt-edge needle (see inset).

Results and Discussion

By nature of its design, our microfluidic device is versatile, bearing the essential features of the reactor illustrated in Figure 1.1. Additional fluid junctions may be added as needed simply by inserting a needle anywhere along the tubing. To demonstrate the suitability of our device for the synthesis of solid particles, we chose a simple system in which aqueous reagents combine to form a solid precipitate. Having successfully demonstrated the ability to synthesize solids by interfacial polymerization in a two-flow system,[21] we took advantage of the versatility of our device and added a third fluid flow. In each case, an inert carrier fluid was employed as the continuous phase, and disperse-phase reagents were injected into the tubing through separate syringe pumps located downstream from the carrier-phase source. Reagent mixing occurred in one of two ways. If both disperse phases are immiscible with the carrier phase, the mixing of the reagents is initiated by the collision of two different reagent phase droplets (Figure 1.2a). This type of mixing was observed when mineral oil was used as the carrier phase. On the other hand, reagents that are miscible with the carrier phase are injected coaxially as the final reagent. In this case, the mixing is caused both by infusion of the second reagent into the first and by diffusion from the carrier

phase into the disperse phase (Figure 1.2b). In both of these cases, chaotic advection could be induced by passing the fluid stream through winding tubing (Figure 1.2c).[23] We used 30-gauge (0.15 mm i.d.) blunt edge needles for reagent introduction to obtain spherical droplets (Figure 1.1, inset); beveled needles do not result in clean snap-off of the droplets.

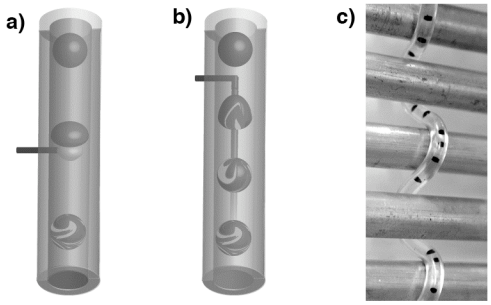

Figure 1.2. Reagents are mixed inside the tubing by droplet–droplet collision (a) or infusion followed by diffusion (b). Mixing can be enhanced by chaotic advection induced by passing the reaction stream through winding tubing (c).

A number of research groups have employed fluorinated solvents as carrier phases for microfluidic processes to minimize the possibility of side reactions.[24] These solvents, however, can be expensive and are rarely used as common laboratory reagents. Instead, we chose mineral oil, hexane (mixture of isomers), and toluene as relatively inert and readily available carrier phases.

The first reaction we performed was the synthesis of indigo (**3**), which involves a base-catalyzed aldol condensation between acetone (**1**) and 2-nitrobenzaldehyde (**2**; Scheme 1.1).

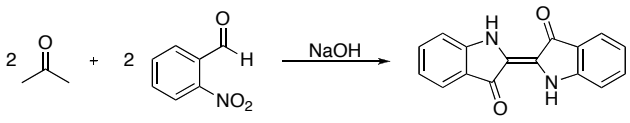

Scheme 1.1. Synthesis of indigo (**3**).

The synthesis of this dye was appealing not only because it results in the precipitation of a solid, but also because the product stains the poly(vinyl chloride) (PVC) tubing upon contact, which provides an easy means of determining the effectiveness of our method for isolating the solid from the channel walls. We found that a mineral oil flow rate of 3 mL/min produces sufficiently small droplets that are confined to the center of the tubing. Figure 1.3 illustrates the differences observed when indigo is synthesized in the presence and absence of a carrier phase. The reagent collision shown in Figure 1.2 a and b induces some mixing of the reagents. It has been shown that a further enhancement is observed when the droplets are flowed through a winding channel, which causes mixing by chaotic advection.[23] We observed a qualitatively similar phenomenon when we wound our tubing through a series of parallel horizontal bars. When the indigo synthesis was performed inside this tubing, the indigo formation (observed by a color change) occurred more rapidly than it did in straight tubing. Characterization was not performed for this reaction due to well-established purification issues.[25]

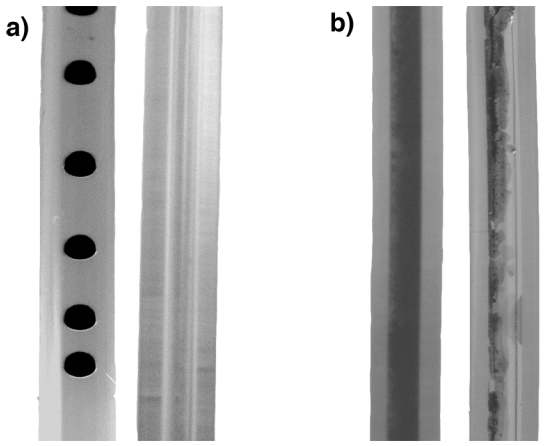

Figure 1.3. Demonstration of the effectiveness of the carrier phase in the formation of solids. Comparison of the tubing during (left tube) and after (right tube) the synthesis of indigo in the presence (a) and absence (b) of a mineral oil carrier phase.

This method of producing solids in microreactors by using a monodisperse droplet flow can be extended to carrier phases other than mineral oil. The reaction of glyoxal (**4**) with cyclohexylamine (**5**) results in the precipitation of *N*,*N*'-dicyclohexylethylenediimine (**6**; Scheme 1.2).

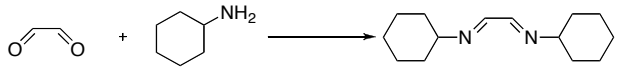

4 **5** **6**

Scheme 1.2. Synthesis of *N*,*N*'-dicyclohexylethylenediimine (**6**).

When mineral oil is used as the carrier phase, the droplet–droplet phenomenon shown in Figure 1.2a is observed. However, as **6** is soluble in mineral oil, product recovery is difficult. In contrast, the use of hexane (mixture of isomers) as the carrier phase allows both the formation of solid in the monodisperse flow as well as easier extraction of the solid. Owing to the decreased viscosity and density of the hexane carrier phase relative to mineral oil, higher flow rates are required to achieve the desired flow type. We found that a flow rate of at least 12 mL/min for the hexane phase yields desirable conditions for the formation of solid without channel blockage, although a rate as low as 5 mL/min acts as an efficient purging system by keeping the channel walls free of solids.

The final microfluidic reaction we studied was the conversion of 4-chlorobenzoyl chloride (**7**) and methylamine (**8**) into 4-chloro-*N*-methylbenzamide (**9**; Scheme 1.3).

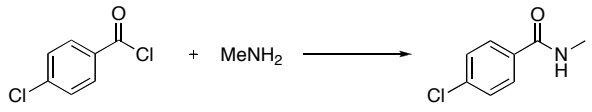

7 **8** **9**

Scheme 1.3. Synthesis of 4-chloro-*N*-methylbenzamide (**9**).

This highly exothermic reaction was performed in our microreactor with no safety concerns. The small dimensions of the device not only mitigated the violence with which the reaction took place, but they have also increased the yield of **9** (Table 1.1). The use of toluene as the carrier phase for this reaction further demonstrates the versatility of our system.

Batch syntheses were carried out as a control by stirring the reagents for the same amount of time as the microreactor experiments were allowed to run. As indicated in Table 1.1, the yields for the microreactor products are comparable to—if not greater than—those for the batch reactions. Also, space–time yields (STY) for the solids formed by microscale flow were much higher than those for solids formed in the macroscale batch reactions. High yields were obtained in the microfluidic system even when one reagent was miscible with the carrier phase. Although we expected lower yields as a result of the miscible reactant flowing into both the carrier and reactant phases, this was not observed, which suggests that diffusion is fast enough in our system to ensure reagent mixing.

Table 1.1. Synthesis of solids in our microfluidic device.

Product	System	Yield (%)[a]	Purity (%)[b]	STY[c]	STY rel
6	flow	97.0	94.5	11.44	25.55
6	batch	99.4	96.6	0.4478	1.00
9	flow	87.6	> 99	9.150	20.43
9	batch	76.9	> 99	0.7140	1.59

[a]Crude yields are reported for **6**, purified yields are reported for **9**.
[b]Purities were determined from ^{13}C satellites from ^{1}H NMR spectra. Purities of the crude product are reported for **6**, purities of the purified product are reported for **9**.
[c]Space-time yields are reported in mol/m^3•min.

Conclusion

In summary, we have reported a practical method for producing solids in microreactors. As demonstrated by the indigo synthesis, by performing these reactions

in a monodisperse droplet flow, the solid particles are effectively isolated from the walls of the tubing. Our device not only allows the practical synthesis of solids in microfluidic devices, it also retains the advantages of traditional microreactors. Its ease of use, the widespread availability of many of its components, and its versatility provide further benefits. Future work with our microfluidic device includes temperature-controlled experiments as well as multistep syntheses in a single device.

Afterword

From the interfacial polymerization performed by Elizabeth Quevedo and Jeremy Steinbacher to the work discussed here to the packed-bed microreactors developed by Andrew Bogdan, the McQuade group has shown that practical, affordable microreactors can be assembled from common laboratory equipment. This first instance of organic synthesis in our lab was a success, and it set the stage for the microfluidic ibuprofen and atropine syntheses discussed in Chapter 2.

Experimental Section

General Considerations

All materials were used as received unless otherwise noted. 4-Chlorobenzoyl chloride was recrystallized from EtOH prior to use. ^{1}H NMR and ^{13}C NMR spectra were recorded on Varian Mercury 300 MHz and Inova 400 MHz spectrometers operating at 299.763 MHz and 399.780 MHz, respectively, using residual solvent as the reference. Data are reported as s = singlet, d = doublet, bd = broad doublet. Microfluidic reactors consisted of Harvard Apparatus Standard Pump 22 syringe pumps, Hamilton syringes, 30-gauge blunt-edge needles, and 0.0625 inch (1.59 mm) internal diameter (i.d.) PVC or 0.066 inch (1.68 mm) i.d. polyethylene (PE) tubing.

Indigo (3): Mineral oil (15 mL, 3 mL/min) was used as the carrier phase in 0.0625 inch (1.59 mm) internal diameter (i.d.) PVC tubing. NaOH (1m in water, 3 mL, 0.6 mL/min) was injected into the center of the carrier phase. **2** (0.66m in acetone (**1**), 3 mL, 0.6 mL/min) was introduced into the tubing further downstream. The pumps were allowed to run for 5 minutes while the product was collected over an ice–water bath.

***N*,*N*'-Dicyclohexylethylenediimine (6)**: Hexane (mixture of isomers, 60 mL, 6 mL/min) was used as the carrier phase in 0.066 inch (1.68 mm) i.d. polyethylene (PE) tubing. glyoxal (**4**, 0.40 M in water, 12 mL, 1.2 mL/min) was injected into the center of the carrier phase. Cyclohexylamine (**5**, 4.368 M in water, 2.4 mL, 0.24 mL/min) was introduced into the tubing further downstream. The pumps were allowed to run for 10 minutes while the product was collected at room temperature. Evaporation of the solvent yielded a white solid: ^{1}H NMR (400 MHz, d_6-DMSO) δ 8.48 (bd, 1H), 7.80 (d, 2H), 7.43 (d, 2H), 2.75 (d, 3H); ^{13}C NMR (75 MHz, d_6-DMSO) δ 166.2, 136.6, 133.9, 129.6, 129.0, 26.9.

4-Chloro-*N*-methylbenzamide (9): Toluene (70 mL, 7 mL/min) was used as the carrier phase in 0.066 inch (1.68 mm) i.d. PE tubing. Methylamine (**8**, 1.44 M in water, 3 mL, 0.3 mL/min) was injected into the center of the carrier phase. 4-Chlorobenzoyl chloride (**7**, 1.0 mL, 0.1 mL/min) was introduced into the tubing further downstream. The pumps were allowed to run for 10 minutes while the product was collected at room temperature. Evaporation of the solvent and recrystallization from MeOH/H_2O afforded needles of white solid: ^{1}H NMR (300 MHz, $CDCl_3$) δ 7.91 (s, 2H), 1.20 (s, 18H); ^{13}C NMR (75 MHz, $CDCl_3$) δ 158.1, 58.8, 29.5.

REFERENCES

1. Schwalbe, T.; Kursawe, A.; Sommer, J. *Chem. Eng. Technol.* **2005**, *28*, 408.

2. Wu, T.; Mei, Y.; Cabral, J. T.; Xu, C.; Beers, K. L.; *J. Am. Chem. Soc.* **2004**, *126*, 9880.

3. Watts, P.; Haswell, S. J. *Chem. Eng. Technol.* **2005**, *28*, 290.

4. Comer, E.; Organ, M. G. *J. Am. Chem. Soc.* **2005**, *127*, 8160.

5. Zhang, X.; Stefanick, S.; Villani, F. J. *Org. Process Res. Dev*. **2004**, *8*, 455.

6. Yoshida, J. *Chem. Commun*. **2005**, 4509.

7. Taghavi-Moghadam, S.; Kleemann, A.; Golbig, K. G. *Org. Process Res. Dev.* **2001**, *5*, 652.

8. Bayer, T.; Himmler, K. *Chem. Eng. Technol*. **2005**, *28*, 285.

9. Yoshida, J.; Nagaki, A.; Iwasaki, T.; Suga, S.; *Chem. Eng. Technol*. **2005**, *28*, 259.

10. Ehrfeld, W.; Hessel, V.; Lowe, H. *Microreactors: New Technology for Modern Chemistry*, Wiley-VCH, Weinheim, 2000, p. 9.

11. Chambers, R. D.; Fox, M. A.; Holling, D.; Nakano, T.; Okazoe, T.; Sanford, G. *Chem. Eng. Technol*. **2005**, *28*, 344.

12. Delsman, E. R.; de Croon, M. H. J. M.; Elzinga, G. D.; Cobden, P. D.; Kramer, G. J.; Schouten, J. C. *Chem. Eng. Technol*. **2005**, *28*, 367.

13. Kikutani, Y.; Kitamori, T. *Macromol. Rapid Commun*. **2004**, *25*, 158.

14. Shah, K.; Shin, W. C.; Besser, R. S. *Sens. Actuators B* **2004**, 157.

15. Chambers, R. D.; Fox, M. A.; Holling, D.; Nakano, T.; Okazoe, T.; Sanford, G. *Lab Chip* **2005**, *5*, 191.

16. Boswell, C. *Chem. Mark. Rep*. **2004**, *266*, 8.

17. Roberge, D. M.; Ducry, L.; Bieler, N.; Cretton, P.; Zimmerman, B. *Chem. Eng. Technol*. **2005**, *28*, 318.

18. Thayer, A. M. *Chem. Eng. News* **2005**, *83*, 43.

19. Shestopalov, I.; Tice, J. D.; Ismagilov, R. F. *Lab Chip* **2004**, *4*, 316.

20. Zheng, B.; Tice, J. D.; Ismagilov, R. F. *Anal. Chem*. **2004**, *76*, 4977.

21. Quevedo, E.; Steinbacher, J.; McQuade, D. T. *J. Am. Chem. Soc*. **2005**, *127*, 10498.

22. Chang, Z.; Liu, G.; Tian, Y.; Zhang, Z. *Mater. Lett*. **2004** *58*, 522.

23. Chen, D. L.; Gerdts, C. J.; Ismagilov, R. F. *J. Am. Chem. Soc.* **2005**, *127*, 9672.

24. Song, H.; Tice, J. D.; Ismagilov, R. F. *Angew. Chem. Int. Ed.* **2003**, *42*, 768.

25. Kohlhaupt, R.; Bergmann, U. U.S. Patent No. 5,424,453, **1995**.

CHAPTER 2

Ibuprofen and Atropine Syntheses in Flow

Preface[*]

In early 2007, my adviser's startup company, Systanix, embarked on a joint project with Foster Miller, Inc. Funded by the Defense Advanced Research Projects Agency (DARPA), the goal of this project was to design common pathways for three active pharmaceutical ingredients (APIs), verify two of these syntheses as traditional batch reactions, and ultimately to perform these reactions in flow. Andrew Bogdan and I, along with Cornell undergraduate student Daniel Kubis, were hired as consultants for the project and spent the months of February through August refining these syntheses and putting them into flow. Much progress was made over the course of the project, however, some of the reactions remain unoptimized or incomplete due to time restraints. This chapter describes the syntheses of ibuprofen and atropine and discusses the progress we made toward performing the reactions in flow.

Abstract

We have developed syntheses containing common reaction pathways for the APIs ibuprofen and atropine. The design of these reaction routes resulted in the realization of a previously unknown iodine-mediated rearrangement in the synthesis of atropine. We have achieved both of these syntheses in flow using homogeneous reaction conditions, and we discuss progress toward the use of packed-bed microreactors for these syntheses.

[*] The author thanks Dr. Steven Broadwater, Andrew Bogdan, and Daniel Kubis for their contribution to this unpublished work.

Introduction

Pharmaceutical synthesis is currently one of the most materials- and waste-intensive sectors of the chemical industry.[1] Recent initiatives to promote more sustainable chemistry—such as the implementation of Green Chemistry awards—as well as the establishment of green chemistry-oriented academic journals and conferences indicate that this is a problem that requires attention. While these approaches have been and continue to be successful in reducing the materials and waste associated with the chemical pathways, they do not address issues such as the packaging, transport and storage of reagents and products, all of which contribute to the waste associated with pharmaceutical synthesis.[2] Funded by DARPA, the objective of this project was to design common pathways for the syntheses of different APIs in flow, with the ultimate goal being on-demand drug generation in a portable flow device. The incorporation of common reagents and reactions into these syntheses would minimize the number and types of materials needed for purification. In addition, the reactor design and reactions themselves would allow for the on-demand generation of API in an on-site flow reactor, eliminating the need for product packaging and storage. The two APIs chosen for this project were ibuprofen (**1**) and atropine (**2**), a non-steroidal anti-inflammatory drug (NSAID) and an anticholinergic agent, respectively. The BHC Company (now BASF Corporation) synthesis of ibuprofen[3,4] and a synthesis of atropine[5-7] are shown below (Schemes 2.1 and 2.2).

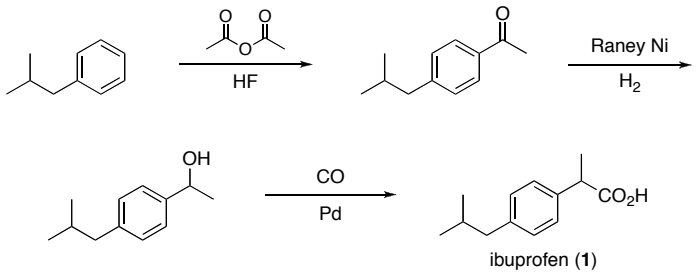

Scheme 2.1. BHC Company synthesis of ibuprofen (**1**).

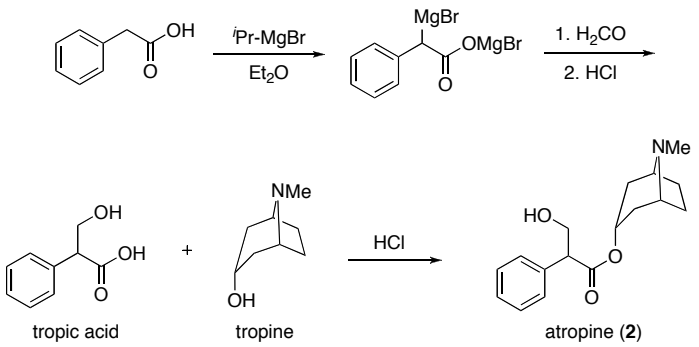

Scheme 2.2. Synthesis of atropine (**2**). Tropine is the product of a Raney Ni/H_2 reduction of tropinone, which can be synthesized *via* the Robinson tropinone synthesis.[6]

At the beginning of the project, we created synthetic designs for ibuprofen and atropine that utilize a common set of reactions. The reaction design shown in Scheme 2.3 begins with a Friedel-Crafts hydroxyalkylation between either isobutylbenzene or benzene and a pyruvate ester.

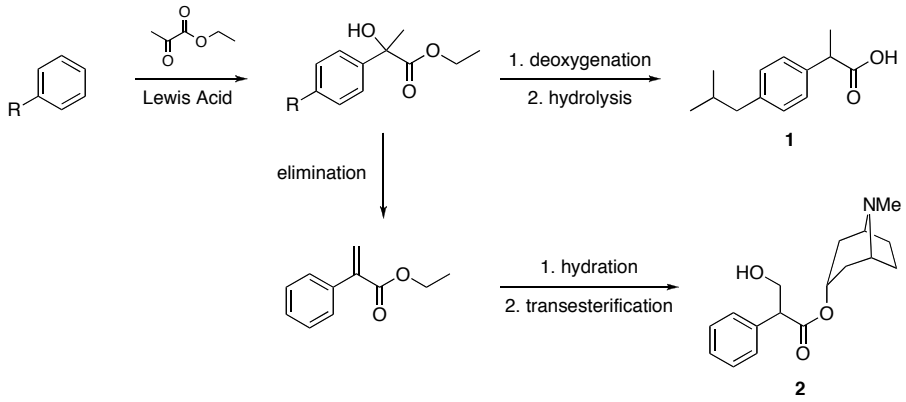

Scheme 2.3. Proposed syntheses of ibuprofen and atropine.

Friedel-Crafts reactions similar to the one described above are known; however, they typically involve more activated substrates.[8-10] This chapter discusses our attempts to achieve this as well as other Friedel-Crafts reactions. Though the synthetic routes shown in Scheme 2.3 ultimately proved to be unsuccessful, we established two new routes containing overlapping chemistry and were able to partially or fully perform these syntheses in flow.

Results and Discussion

Ibuprofen in Batch. As discussed above, we envisioned a route beginning with the Friedel-Crafts hydroxyalkylation of isobutylbenzene with a pyruvate ester, followed by deoxygenation[11] and hydrolysis. The trifluoromethanesulfonic acid (TfOH)-catalyzed Friedel-Crafts hydroxyalkylation, based on a similar reaction between substituted aromatics and ethyl 3,3,3-trifluoropyruvate,[12] was found to produce a dimer of ethyl pyruvate under a variety of conditions (Table 2.1, entries 1-4). A solid-supported TfOH catalyst yielded the same product.[13] After these unsuccessful attempts, we screened a number of Lewis acid catalysts, each of which resulted in either the wrong product or no reaction at all (Table 2.1, entries 6-12).

Having had no success with the Friedel-Crafts hydroxyalkylation of isobutylbenzene, we examined Friedel-Crafts alkylations with a variety of electrophiles that would directly yield the ester of ibuprofen. Although this would remove the shared step of the ibuprofen and atropine syntheses, it would result in a concise, two-step synthesis of ibuprofen. Such alkylations involving methyl acrylate **a**, ethyl lactate **b**, and ethyl 2-bromopropionate **c** have been reported in the literature,[14-16] but as with the ethyl pyruvate hydroxyalkylations, they generally involve more activated substrates. Unfortunately, though a variety of conditions were screened for each electrophile (Table 2.2), we were unable to obtain the desired ibuprofen ester.

Table 2.1. Reaction conditions screened for the Friedel-Crafts alkylation of isobutylbenzene with ethyl pyruvate.

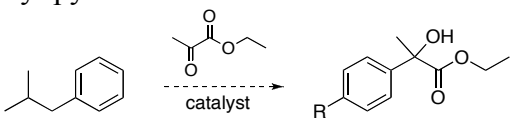

Entry	Catalyst	Conditions	Major product
1	TfOH (20 mol%)	CH_2Cl_2, reflux, overnight	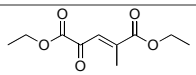
2	TfOH (20 mol%)	CH_2Cl_2, reflux slow addition of pyruvate	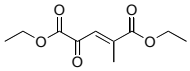
3	TfOH (20 mol%)	neat,105 °C	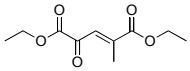
4	TfOH (20 mol%)	CH_2Cl_2, 90 °C, overnight dry sealed tube	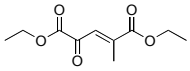
5	Solid-supported TfOH	CH_2Cl_2, reflux, overnight	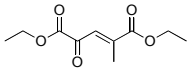
6	$SnCl_4$ (1.2 eq)	CH_2Cl_2,0 °C to rt, 3 h	undetermined[a]
7	$AlCl_3$ (1.5 eq)	CH_2Cl_2,rt, under N_2	undetermined
8	$TiCl_4$ (1.5 eq)	CH_2Cl_2,rt, under N_2	no reaction
9	BF_3OEt_2 (1 eq)	neat, rt	no reaction
10	$TiCl_4$ (1.3 eq) Al_2O_3 (1.2 eq)	CH_2Cl_2, rt	no reaction
11	BF_3OEt_2 (1.3 eq) Al_2O_3 (1.2 eq)	CH_2Cl_2,rt	no reaction
12	$AlCl_3$ (1.3 eq) Al_2O_3 (1.2 eq)	CH_2Cl_2,rt	no reaction

[a]NMR data suggests the product of the condensation of 3 eq of ethyl pyruvate.

Table 2.2. Reaction conditions screened for the Friedel-Crafts alkylation of isobutylbenzene with methyl acrylate (**a**), ethyl lactate (**b**), and ethyl 2-bromopropionate (**c**).

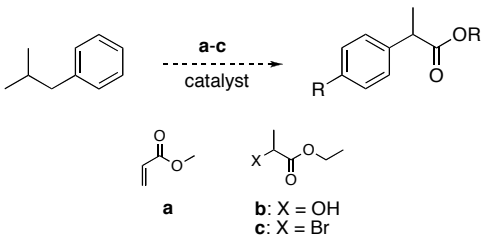

Entry	Electrophile	Catalyst	Conditions	Major product
1	**a**	$AlCl_3$ (1.5 eq)	CH_2Cl_2, rt, under N_2	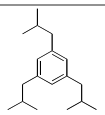
2	**a**	$AlCl_3$ (1.5 eq) HCl (g)	CH_2Cl_2, rt, under N_2	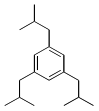
3	**a**	$AlCl_3$ (1.5 eq) HCl (aq)	CH_2Cl_2, rt, under N_2	no reaction
4	**a**	$SnCl_4$ (1.5 eq)	CH_2Cl_2, rt, under N_2	no reaction
5	**a**	$TiCl_4$ (1.5 eq)	CH_2Cl_2, rt, under N_2	no reaction
6	**a**	BF_3OEt_2 (1 eq)	neat, rt	no reaction
7	**a**	$AlCl_3$ (1.3 eq) Al_2O_3 (1.2 eq)	CH_2Cl_2, rt	undetermined
8	**b**	H_2SO_4 (aq, 80%)	75 °C, overnight	no reaction
9	**b**	$AlCl_3$ (1.3 eq) Al_2O_3 (1.2 eq)	CH_2Cl_2, rt	no reaction
10	**b**	TfOH	80 °C, overnight sealed vial	no reaction
11	**c**	$AlCl_3$ (1.5 eq)	solvent: CH_2Cl_2 room temp	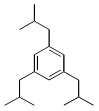
12	**c**	$AlCl_3$ (1.3 eq) Al_2O_3 (1.2 eq)	solvent: CH_2Cl_2 room temp	no reaction
13	**c**	TfOH (20 mol %)	80 °C, overnight sealed vial	no reaction

Our next approach for the synthesis of ibuprofen involved the conversion of known batch reactions into flow reactions. The synthesis we chose consisted of a Friedel-Crafts acylation of isobutylbenzene with propionyl chloride, an iodine-

mediated rearrangement,[17] and saponification (Scheme 2.4). These reactions were easily carried out in batch to obtain pure ibuprofen.

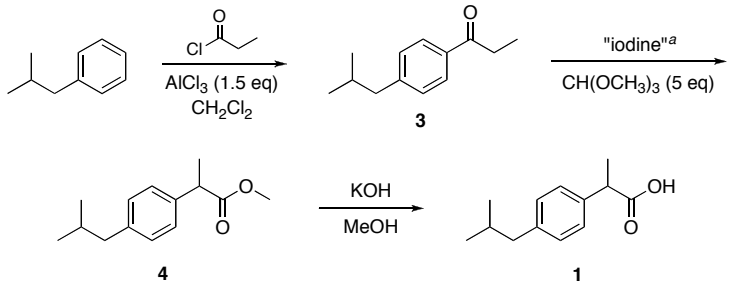

Scheme 2.4. Revised synthesis of ibuprofen. [a]"Iodine" refers to either I_2 or $PhI(OAc)_2$.[18]

Atropine in Batch. Because the Friedel-Crafts hydroxyalkylation proposed as the common first step of the ibuprofen and atropine syntheses was unsuccessful, we instead envisioned a new route that incorporated the iodine-mediated rearrangement used in the synthesis of ibuprofen (Scheme 2.5). Although this specific rearrangement is unprecedented, the success we had with the ibuprofen synthesis inspired us to pursue this route.

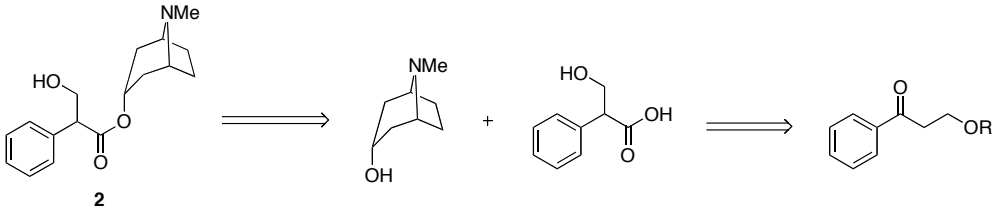

Scheme 2.5. Revised retrosynthesis of atropine.

The first step of this synthesis involved the formation of 3-methoxy-propiophenone (**5**) or 3-ethoxypropiophenone (**6**) from 3-chloropropiophenone (Scheme 2.6). This step proved to be more problematic than expected, as the elimination pathway was often dominant, resulting in the formation of phenyl vinyl ketone as a byproduct. Subsequent polymerization of this material often provided an intractable reaction mixture. It was found that the reaction proceeded with the

addition of an alcoholic solution of KOH at 0 °C as opposed to adding KOH directly to the reaction mixture. By premixing the KOH and methanol or ethanol, the exotherm was controlled and resulted in more efficient temperature control of the reaction, allowing us to obtain our desired product.

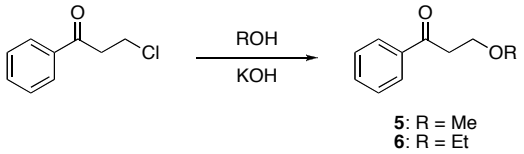

Scheme 2.6. Substitution of 3-chloropropiophenone.

Our first attempts at the iodine-mediated rearrangement of **5** or **6** also presented us with some challenges (Scheme 2.7). Treatment of **5** or **6** with $CH(OCH_3)_3$ and I_2 consistently yielded 3-methoxy-2-iodopropiophenone (**7**) rather than the desired product. However, we found that the use of $PhI(OAc)_2$ rather than I_2 furnished the rearranged product methyl 3-methoxy-2-phenylpropanoate (**8**) in 71% yield. In addition, it was discovered that this transformation could be carried out at room temperature, as opposed to the literature-reported 60 °C. In the context of carrying out chemistry in the field, room temperature reactions are advantageous because of the reduced energy requirement.

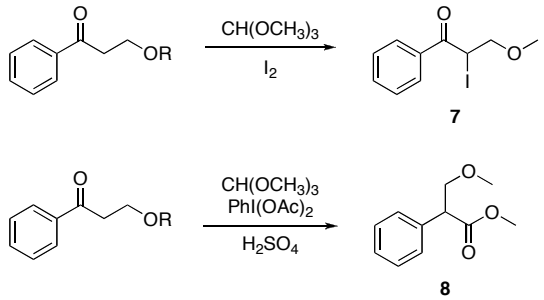

Scheme 2.7. Iodine- and iodoso-mediated rearrangement of 3-alkoxypropiophenone.

It should be noted that for both the I_2- and $PhI(OAc)_2$-mediated reactions, the respective products contained a methyl ether regardless of whether **5** or **6** was used as

the starting material. Since the original methoxy or ethoxy groups were being replaced by a methoxy group from $CH(OCH_3)_3$ during the reaction, we saw the potential for performing the substitution and rearrangement of 3-chloropropiophenone in one step. However, the attempted rearrangement 3-chloropropiophenone with either I_2 or $PhI(OAc)_2$ was unsuccessful.

With **8** in hand, we saw three approaches to the completion of the atropine synthesis. The first involved a transesterification of the methyl ester product of the iodine-mediated rearrangement (Scheme 2.8A). Subsequent cleavage of the methyl ether would liberate the unprotected alcohol and result in the formation of atropine. The second route involves saponification of the methyl ester, followed by esterification with tropine (Scheme 2.8B). Finally, the route described in Scheme 2.8C involves saponification followed by activation of the resulting carboxylic acid to facilitate ester formation with tropine.

Though a variety of conditions for transesterification (Scheme 2.8A) were screened, none were successful. For the direct esterification route (Scheme 2.8B), saponification of the methyl ester of **8** with methanolic KOH was achieved to provide the desired product **9** in 88% yield, but none of the esterification conditions we employed effected the coupling of **9** with tropine. However, the carboxylic acid **9** could be activated using thionyl chloride to produce an acid chloride (Scheme 2.8C). After removing excess thionyl chloride by distillation, the acid chloride was coupled with tropine to form the desired tropic acid ester in 52% isolated yield (Scheme 2.9).

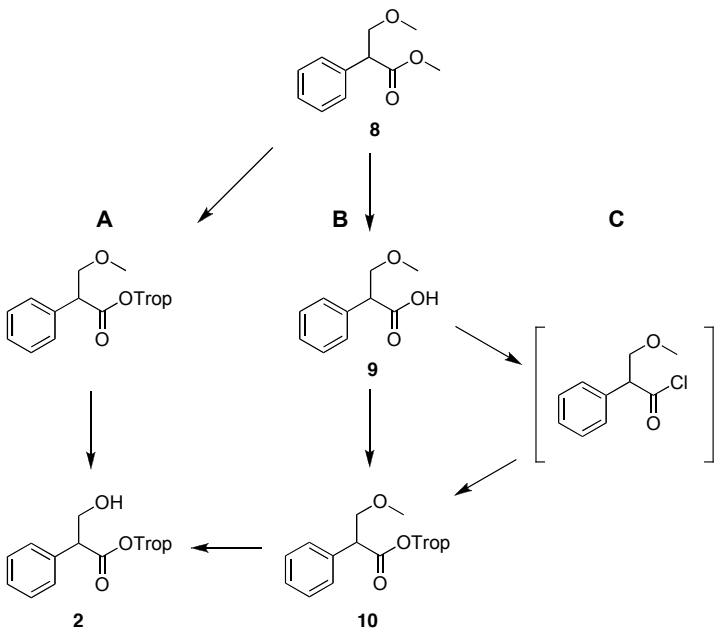

Scheme 2.8. Alternative routes for the synthesis of atropine from **8** and tropine: A) transesterification; B) esterification; C) esterification using an activated carboxylic acid.

The final step of the atropine synthesis involved a boron tribromide-mediated demethylation. Analysis of this reaction using thin layer chromatography indicated that atropine was being formed under these conditions, however no isolated yield was obtained. It is possible that the tertiary amine in the tropine moiety was slowly being methylated by the methyl bromide byproduct that is formed during the course of the reaction. This method is very promising and might be optimized (reaction time and temperature) with further development.

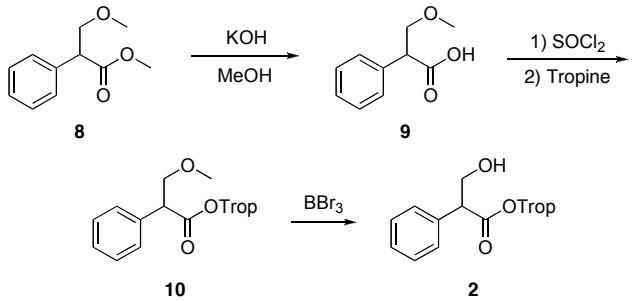

Scheme 2.9. Saponification of **8**, followed by esterification using an activated carboxylic acid.

Ibuprofen in Flow. Once the successful syntheses of ibuprofen and atropine were achieved, the next objective of this project was to find conditions that allowed the reactions to be run in flow. The majority of this development was performed by Andrew Bogdan and Daniel Kubis and will not be discussed in detail here. Instead, the optimized conditions and results for the synthesis of ibuprofen are shown below (Schemes 2.10-2.12). Typical reactor setup consisted of two syringe pumps that flowed reagents together inside poly(vinyl chloride) (PVC) tubing (Figure 2.1). Reaction times were varied by changing either the length of the tubing or the flow rates.

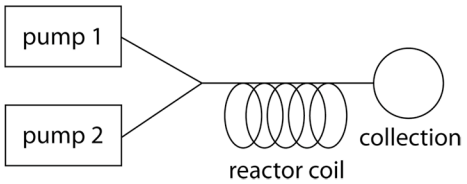

Figure 2.1. Representation of general flow reactor setup.

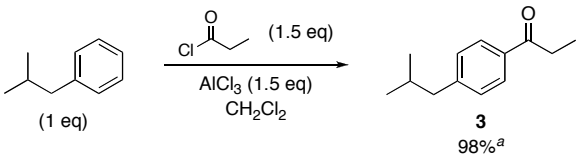

Scheme 2.10. Optimization of Friedel-Crafts acylation in flow. Pump 1: isobutylbenzene, CH_2Cl_2, 30 µL/min; pump 2: propionyl chloride, $AlCl_3$, CH_2Cl_2, 30 µL/min; room temperature. [a]Based on GC conversion.

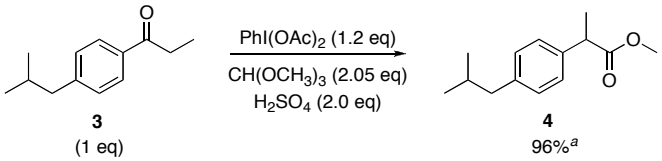

Scheme 2.11. Optimization of $PhI(OAc)_2$-catalyzed rearrangement in flow. Pump 1: 4'-isobutylpropiophenone, $PhI(OAc)_2$, $CH(OCH_3)_3$, CH_2Cl_2, 45 µL/min; pump 2: H_2SO_4, 0.85 µL/min; room temperature. [a]Based on GC conversion

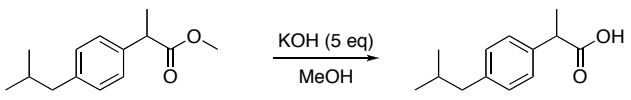

4 (1 eq) **1** 88%[a]

Scheme 2.12. Optimization of saponification in flow. Pump 1: methyl 2-(4'-isobutylphenyl)propanoate, MeOH, 25 μL/min; pump 2: KOH, MeOH, 25 μL/min; room temperature. [a]Unoptimized yield.

In addition to identifying appropriate flow conditions for the homogeneous reactions discussed above, we also looked into developing solid-supported catalysts and reagents for these transformations. Packed-bed microreactors combine the benefits of heterogeneous catalysts (ease of removal from the reaction mixture, catalyst recycling, etc…) with the high heat transfer and mixing associated with microreactors, making them an attractive option.

The first reaction that we investigated is the iodine-mediated oxidative rearrangement used in both the ibuprofen and atropine syntheses. As an alternative to using $PhI(OAc)_2$ for the rearrangement, we envisioned supporting the iodoso reagent to create a packed-bed microreactor in which the reagent can be regenerated and recycled.[19] Such a reagent could also enable multistep synthesis, as it would remain site-isolated from the components of other reactions. Others in the McQuade group have previously demonstrated that the performance of packed-bed microreactors is highly dependent on the solid support.[20] We therefore screened a variety of heterogeneous materials in our development of a solid-supported iodoso reagent.

The McQuade group has reported several examples of creating heterogeneous catalysts using Rohm and Haas's Amberzyme Oxirane (AO) as a starting material.[20,21] AO is an excellent support for continuous flow applications because it is highly solvent-tolerant and does not exhibit variable swelling behavior, therefore providing predictable flow behavior. Utilizing a published methodology, a solid-supported iodobenzene derivative (**11**) was prepared using "click chemistry" (Scheme 2.13).[20]

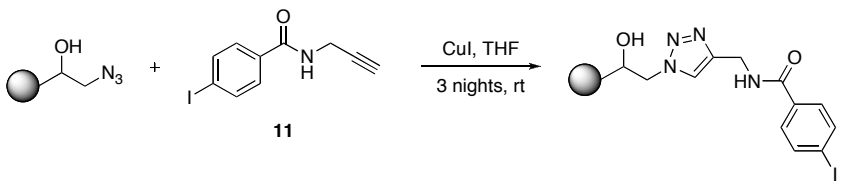

Scheme 2.13. Resin functionalization *via* Huisgen reaction.

In addition, we functionalized several amine-containing resins using standard peptide coupling procedures.[22] These resins included aminomethyl polystyrene, JandaJel (polystyrene core functionalized with poly(ethylene glycol) chains), and an amine version of AO. A third approach to preparing a heterogeneous iodobenzene reagent involved the direct iodination of unfunctionalized polystyrene resin (2% DVB) using I_2, I_2O_5, CCl_4, H_2SO_4, and nitrobenzene.[23,24]

Once prepared, each supported iodobenzene reagent was oxidized with peracetic acid to provide heterogeneous iodoso reagents. The prepared resins were analyzed for iodine content by elemental analysis and screened for activity. These reactions were carried out in batch due to the ability to set up several small-scale reactions that do not consume significant amounts of resin. It can be seen in Table 2.3 that several of the resins demonstrated activity and the AO amide was recycled successfully.

Table 2.3. Results of 4'-isobutylpropiophenone rearrangement performed in batch using various solid-supported iodoso reagents.

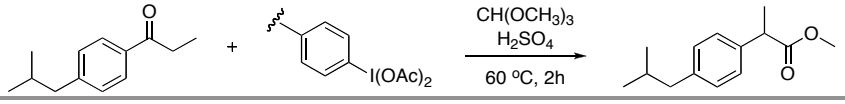

Resin	Loading (mmol/g)[a]	Activity	Recyclable
AO (Huisgen)	0.14	Yes	No
PS (amide)	1.0	Yes	No
JandaJel	Not determined	No	No
AO (amide)	0.56-0.68	Yes	Yes
PS (iodinated)	0.7	Yes	No

[a]Determined by elemental analysis.

Once we identified the AO amide resin as a functional supported reagent that could be successfully recycled, we attempted to use it in a packed-bed microreactor. The general reactor setup is shown in Figure 2.2. Because the reaction required a temperature of 60 °C, temperature control was achieved by housing the packed-bed segment of the reactor inside of an HPLC column heater. However, instead of flowing the reagents together directly inside the column heater, we found that it was necessary first to cool the reagents in an ice water bath to minimize gas generation due to heat formation when the fluid streams are mixed.

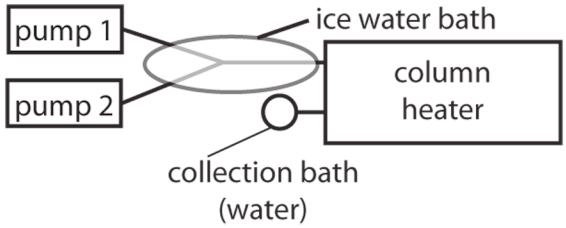

Figure 2.2. Representation of general reactor setup for rearrangement of 4-isobutylpropiophenone mediated by supported iodoso compound. Pump 1: $CH(OCH_3)_3$, 4'-isobutylpropiophenone; pump 2: H_2SO_4.

Despite the success we had with the AO amine resin in batch mode, we were unable to produce any of the rearranged product **4** in flow. Although we were achieving moderate to high conversions of the starting material **3**, we did not see any evidence that **4** was being formed. When we later attempted to optimize the reaction in batch, we found that the reactions were no longer producing **4**, rather they were forming the same unknown byproduct that we saw in the flow reactions. This observation suggests that there was a problem with our reagents or resin, not with the transition to flow mode. Although this project was over before we could solve these problems our preliminary work suggests that this might be a viable reaction once the problem is identified and the appropriate flow conditions are chosen.

Atropine in Flow. Attempts to put the atropine synthesis in flow were also met with success. Again, since the majority of this work was performed by Andrew Bogdan and Daniel Kubis, it will not be discussed in detail. The synthesis of **5** was carried out using our microreactor to provide the desired product in 98% yield. In addition, this transformation was carried out at room temperature. This obviates the need to cool the reaction, which is necessary in batch mode. The optimized conditions and results are shown in Scheme 2.14.

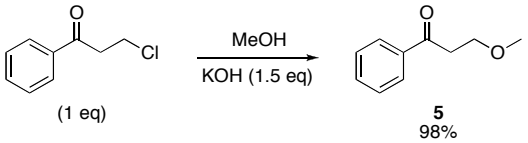

Scheme 2.14. Optimization of ether synthesis in flow. Pump 1: 3-chloro-propiophenone (0.2 M in MeOH), 65 μL/min; pump 2: KOH (0.3 M in MeOH), 65 μL/min; room temperature.

The rearrangement of 3-methoxypropiophenone was successfully performed using our microreactor. Although a high yield of 97% was achieved, this reaction was not optimized to determine what the minimal equivalents of reagents are necessary (Scheme 2.15). Given the success with the iodine-mediated rearrangement in the ibuprofen synthesis, this step has the potential for drastic improvement.

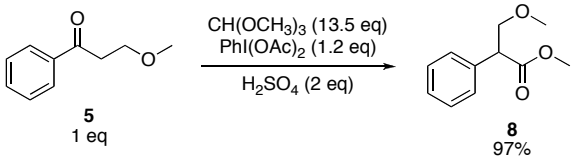

Scheme 2.15. Unoptimized rearrangement of **5** in flow. Pump 1: **5**, $PhI(OAc)_2$, $CH(OCH_3)_3$, CH_2Cl_2, 130 μL/min; pump 2: H_2SO_4, 2.45 μL/min; room temperature.

Like the saponification of **4** in flow for the ibuprofen synthesis, similar treatment of **8** with methanolic KOH in flow successfully produced **9** in an unoptimized 74% yield. In order to develop appropriate flow reaction conditions for performing the

thionyl chloride mediated ester synthesis, we opted to use phenylacetic acid and methanol as test substrates to avoid sacrificing valuable starting material (Scheme 2.16). Using only one equivalent of thionyl chloride, the acid chloride was generated and subsequently quenched into methanol to provide the desired methyl ester **12** in 96% yield.

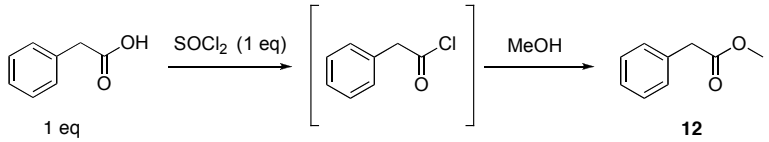

Scheme 2.16. Esterification of phenylacetic acid in flow.

Applying the conditions developed above, **9** was activated with thionyl chloride and quenched into a solution of tropine in toluene at 80 °C (Scheme 2.17). Following isolation, the desired product was obtained in a 30% yield. It is possible that the conditions for the reaction shown in Scheme 2.16 do not directly translate to these substrates. In any case, this reaction was performed successfully and further optimization of the reaction conditions would undoubtedly result in an increase in yield. It should be noted that the continuous flow conditions do not require excess thionyl chloride, and therefore removes the need for an intermediate distillation step.

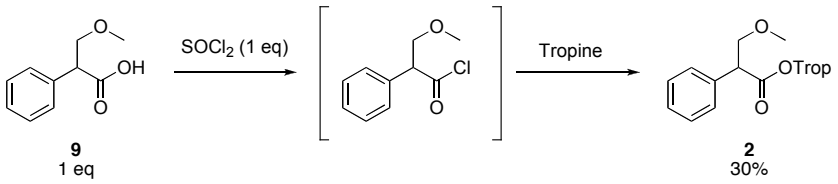

Scheme 2.17. Esterification of **9**.

The final step of the atropine synthesis in flow—cleavage of the methyl ether—was not attempted due to the time constraints that left the batch process unoptimized. However, the preliminary results for this transformation in batch are promising, and given more time, there is great potential for performing the entire atropine synthesis in

flow.

Reaction Metrics. As chemists have become more aware of the need to create more environmentally friendly reactions, a variety of metrics for determining the greenness of reactions and processes have been developed. The reaction metrics for ibuprofen and atropine have been determined as much as possible with the current state of each synthesis. It is necessary to give three brief definitions of the abbreviations that are used in this discussion:[25-32]

- Atom Economy (AE): Describes how much of the reactants remain in the final product. This does not account for stoichiometry or solvent; *higher atom economy values represent more efficient processes*.

- E-Factor: This describes the mass of waste generated per mass of product obtained; *lower E-factor values represent more efficient processes.*

- Reaction Mass Efficiency (RME): This is the percentage of the mass of reactants that remain in the final product and does account for solvent and stoichiometry; *higher RME values represent more efficient processes.*

For the purposes of this discussion, work-up conditions were not included and therefore the actual E-factors will be larger and the actual RME values will be lower. An interesting point to make about the values listed in Table 2.4 is that the E-factors for the overall ibuprofen and atropine syntheses is roughly 3- and 2-fold less for the flow synthesis in comparison to batch, respectively, which indicates the increase in chemical efficiency achieved by using microreactors.

Table 2.4. Reaction metrics for the syntheses of ibuprofen and atropine.

	Atom economy	E-factor	RME
Ibuprofen (batch)	0.19	25.4	0.04
Ibuprofen (flow)	0.19	8.3	0.11
Atropine (batch)[a]	0.20	37.2	0.03
Atropine (flow)[a]	0.20	15.9	0.06

[a]E-factor and RME for atropine syntheses were calculated for the first three steps.

Conclusion

We have successfully designed and performed syntheses of ibuprofen and atropine that contain similar reaction pathways. Through our attempts to utilize similar chemical reactions in the two syntheses, we developed a previously unreported route to atropine that employs a hypervalent iodine-mediated rearrangement. Both syntheses were validated in batch, and significant progress was made toward performing them in flow. Given more time, we expect that the syntheses for ibuprofen and atropine can be performed entirely in flow, with minimization of solvent volumes and excess reagents.

Afterword

From our perspective, the DARPA project was a success. Though we were not able to isolate and characterize atropine, we prepared the methyl ester, and there is evidence that it was successfully converted to atropine. Further work on this project may be carried out in the McQuade lab, including optimization of the atropine synthesis, and the incorporation of in-line work-up steps so that synthesis and purification can be performed entirely in flow.

Experimental Section

General Considerations

All reagents were used without purification unless otherwise noted. Microfluidic reactor components included Harvard Apparatus Standard Pump 22 syringe pumps and 0.0625 inch (1.59 mm) internal diameter (i.d.) poly(vinyl chloride) (PVC) tubing. For iodine elemental analysis, functionalized resins were sent to Robertson Microlit Laboratories for analysis (www.robertson-microlit.com). Gas chromatographic (GC) analyses were performed using a Varian CP-3800 GC equipped with a Varian CP-8400 autosampler, a flame ionization detector (FID) and a Varian CP-Sil 5CB column (length = 15 m, inner diameter = 0.25 mm, and film thickness = 0.25 μm. The temperature program for GC analysis held the temperature constant at 80 ºC, heated samples from 80 to 200 ºC at 17 ºC/min, and held at 200 ºC for 2 min. Inlet and detector temperatures were set constant at 220 and 250 ºC, respectively. Mesitylene was used as an internal standard to calculate reaction conversion. ^{1}H NMR and ^{13}C NMR spectra were recorded on Varian Mercury 300 MHz and Inova 400 MHz spectrometers operating at 299.763 MHz and 399.780 MHz, respectively, using residual solvent as the reference.. Data are reported as s = singlet, d = doublet, t = triplet, q = quadruplet, m = multiplet.

4'-Isobutylpropiophenone (3). Propionyl chloride (2.17 mL, 25 mmol) was added dropwise to a mixture of isobutylbenzene (3.95 mL, 25 mmol), $AlCl_3$ (5 g, 37.5 mmol) and CH_2Cl_2 (200 mL) and stirred at room temperature for 5 hours. The reaction was quenched with cold HCl (1 M, 100 mL) and the product was extracted with CH_2Cl_2 (3 x 100 mL). The combined organic layers were dried over Na_2SO_4 and concentrated. The product was distilled under vacuum (0.3 Torr, 78-80 °C) to produce 4'-isobutylpropiophenone as a colorless oil (4.06 g, 85% yield): ^{1}H NMR (400 MHz,

$CDCl_3$): δ 7.83 (d, 2H), 7.19 (d, 2H), 2.95 (q, 2H), 2.50 (d, 2H), 1.87 (m, 1H), 1.20 (t, 3H), 0.85 (d, 6H); ^{13}C NMR (100 MHz, $CDCl_3$): δ 200.6, 147.4, 134.9, 129.4, 128.1, 45.5, 31.8, 31.7, 30.3, 22.5, 8.5.

Methyl 2-(4-isobutylphenyl)propanoate (4). Method A: Iodine (2.5 g, 10 mmol) was added at once to a solution of 4'-isobutylpropiophenone (0.95 g, 5 mmol) in trimethyl orthoformate (2.73 mL, 25 mmol) and stirred at room temperature for 16 hours. The reaction was poured into 10% $Na_2S_2O_3$ (50 mL) and the product was extracted with $CHCl_3$ (3 x 50 mL). The combined organic layers were dried over Na_2SO_4 and concentrated. The product was purified using column chromatography (silica, 9:1 hexanes:EtOAc) to produce methyl 2-(4-isobutylphenyl)propanoate as a colorless oil (0.95 g, 86% yield).

Method B: Prepared from the general method of Tamura et al.[18] 4'-isobutyl-propiophenone (38 mg, 0.2 mmol), (diacetoxy)iodobenzene (77 mg, 0.24 mmol), trimethyl orthoformate (0.6 mL, 5.5 mmol), and H_2SO_4 (98%, 21.3 μL) were stirred at 60 °C for 10 min. The reaction was quenched with H_2O (2 mL) and the product was extracted with ether. GC analysis indicated complete conversion to methyl 2-(4-isobutylphenyl)propanoate: ^1H NMR (400 MHz, $CDCl_3$): δ 7.22 (d, 2H), 7.13 (d, 2H), 3.72 (q, 1H), 3.61 (s, 3H), 2.44 (d, 2H), 1.86 (m, 1H), 1.50 (d, 3H), 0.90 (d, 6H); ^{13}C NMR (100 MHz, $CDCl_3$): δ 175.4, 140.8, 138.0, 129.6, 127.4, 52.1, 45.3, 45.2, 30.4, 22.6, 18.9.

2-(4-Isobutylphenyl)propanoic acid (1, ibuprofen). Methyl 2-(4-isobutylphenyl)propanoate (0.33 g, 1.5 mmol) and 15% KOH in MeOH (5.3 mL) were stirred at room temperature for 16 hours. The reaction was acidified with 5 M HCl, extracted with EtOAc (3 x 20 mL), washed with brine (20 mL), dried over Na_2SO_4,

and concentrated *in vacuo* to afford ibuprofen as a white solid (309 mg, quant): ^{1}H NMR (300 MHz, $CDCl_3$): δ 7.24 (d, 2H), 7.16 (d, 2H), 3.78 (q, 1H), 2.49 (d, 2H), 1.89 (m, 1H), 1.51 (d, 3H), 0.91 (d, 6H); ^{13}C NMR (75 MHz, $CDCl_3$): δ 181.4, 141.1, 137.2, 129.6, 127.5, 45.3, 45.2, 30.4, 22.6, 18.3.

3-Methoxypropiophenone (5). KOH (1.23 g, 21.9 mmol) and MeOH (50 mL) were stirred at room temperature fully dissolved and then cooled to 0 °C. 3-Chloro-propiophenone (2.5 g, 14.8 mmol) was added and the reaction was stirred at 0 °C for 1.25 h. H_2O (25 mL) was added and the product was extracted with CH_2Cl_2 (3 x 25 mL), washed with brine (20 mL), dried over Na_2SO_4 and concentrated *in vacuo*. The product was purified using column chromatography (silica, 9:1 hexanes:EtOAc) to give 3-methoxypropiophenone as a light yellow oil (2.39 g, 98% yield): ^{1}H NMR (300 MHz, $CDCl_3$): δ 8.00 (d, 2H), 7.58 (t, 1H), 7.49 (t, 2H), 3.92 (t, 2H), 3.41 (s, 3H), 3.24 (t, 2H).

3-Ethoxypropiophenone (6). KOH (2.62 g, 46.7 mmol) and EtOH (150 mL) were stirred at room temperature until the KOH fully dissolved and then cooled to 0 °C. 3-Chloropropiophenone (5.31g, 31.5 mmol) was added and the reaction was stirred at 0 °C for 1.25 h. H_2O (75 mL) was added and the product was extracted with CH_2Cl_2 (3 x 75 mL), washed with brine (50 mL), dried over Na_2SO_4 and concentrated *in vacuo*. The product was purified using column chromatography (silica, 9:1 hexanes:EtOAc) to give 3-ethoxypropiophenone as a light yellow oil (4.47 g, 80% yield): ^{1}H NMR (300 MHz, $CDCl_3$): δ 7.98 (d, 2H), 7.57 (t, 1H), 7.49 (t, 2H), 3.90 (t, 2H), 3.54 (q, 2H), 3.28 (t, 2H), 1.20 (t, 3H).

3-Methoxy-2-iodopropiophenone (7). 3-Ethoxypropiophenone (356.5 mg, 2 mmol), $CH(OCH_3)_3$ (1.1 mL, 10 mmol), and I_2 (1.015 g, 4 mmol) were stirred at room temperature for 16 h. The reaction was poured into 10% $Na_2S_2O_3$ (20 mL) and the product was extracted with $CHCl_3$ (3 x 25 mL), dried over Na_2SO_4, and concentrated *in vacuo*. The product was purified using column chromatography (silica, 9:1 hexanes:EtOAc) to give 3-methoxy-2-iodopropiophenone: ^{1}H NMR (300 MHz, $CDCl_3$): δ 8.02 (d, 2H), 7.60 (t, 1H), 7.51 (t, 2H), 5.42 (dd 1H), 4.10 (dd, 1H), 3.89 (dd, 1H), 3.42 (s, 1H); ^{13}C NMR (75 MHz, $CDCl_3$): δ193.8, 134.3, 134.0, 129.0, 128.9, 74.1, 59.5, 21.1.

Methyl 3-methoxy-2-phenylpropanoate (8). H_2SO_4 (98%, 3 mL) was added to a mixture of 3-methoxypropiophenone (4.58 g, 27.9 mmol), $CH(OCH_3)_3$ (83.8 mL, 766 mmol), and $PhI(OAc)_2$ (10.78 g, 33.5 mmol) and the reaction was stirred at room temperature for 2.5 h. The reaction was quenched with H_2O (30 mL), extracted with Et_2O (3 x 50 mL), dried over Na_2SO_4, and concentrated. The iodobenzene that was produced was removed by vacuum distillation, and the product was purified by column chromatography (silica, 9:1 hexanes:EtOAc) to give methyl 3-methoxy-2-phenylpropanoate (3.85 g, 71% yield): ^{1}H NMR (300 MHz, $CDCl_3$): δ 7.40 (m, 5H), 4.02 (dd, 1H), 3.93 (dd, 1H), 3.77 (s, 3H), 3.61 (dd, 1H), 3.42 (s, 3H); ^{13}C NMR (75 MHz, $CDCl_3$) δ 173.1, 135.9, 129.0, 128.3, 128.0, 74.5, 59.3, 52.4, 52.1.

3-Methoxy-2-phenylpropanoic acid (9). Methyl 3-methoxy-2-phenylpropanoate (**8**, 3.85 g, 0.2 mmol) and KOH (15% in MeOH, 72 mL) were stirred at room temperature for 16 h. The reaction was diluted with water and washed with Et_2O. The aqueous layer was acidified with 5M HCl and the product was extracted with EtOAc (3 x 25 mL), dried over Na_2SO_4, and concentrated *in vacuo* to give 3-Methoxy-2-

phenylpropanoic acid (3.13, 88% yield): ^{1}H NMR ($CDCl_3$, 300 MHz): δ 7.35 (m, 5H), 3.97 (m, 2H), 3.64 (dd, 1H), 3.40 (s, 3H).

Atropine methyl ether (10). 3-Methoxy-2-phenylpropanoyl chloride (200 mg, 1.0 mmol) was dissolved in toluene (10 mL) and heated to 80 °C. Tropine (149 mg, 1.1 mmol) was added and the reaction was stirred for 4 h, during which a white solid precipitated. The solid was removed by filtration and dried under vacuum. ^{13}C NMR ($CDCl_3$, 75 MHz): δ: 171.6, 136.0, 129.0, 128.2, 127.9, 74.0, 68.0, 60.0, 59.9, 59.2, 52.6, 40.4, 36.4, 36.3, 25.5, 25.2.

4-Iodo-*N*-(prop-2-ynyl)benzamide (11). Propargylamine (0.28 mL, 4.8 mmol) and triethylamine (1.24 mL, 8.8 mmol) were added to a solution of 4-iodobenzoic acid (992 mg, 8 mmol), EDC•HCl (800 mg, 4.4 mmol), and HOBt (660 mg, 4.8 mmol) in DMF (20 mL). The reaction was stirred at room temperature for 16 h. The reaction was quenched with saturated NH_4Cl (20 mL) and the solvent was distilled off under vacuum. The product was dissolved in CH_2Cl_2 (30 mL) and washed with 10% citric acid (30 mL), H_2O (25 mL), $NaHCO_3$ (25 mL), and brine (25 mL). The organic layer was dried over Na_2SO_4 and concentrated *in vacuo* to give a white solid (0.98 g, 86% crude yield). The product was recrystallized from hexanes/EtOAc to give 4-iodo-*N*-(prop-2-ynyl)benzamide as white crystals (752 mg, 66% yield): ^{1}H NMR ($CDCl_3$, 300 MHz): δ 7.91 (d, 2H), 7.52 (d, 2H), 6.22 (bs, 1H), 4.24 (s, 2H), 2.30 (s, 1H); ^{13}C NMR (CD_3OD, 75 MHz): δ 159.8, 137.8, 133.9, 128.9, 98.9, 79.7, 71.2, 29.0.

Methyl 2-phenylethanoate (12). ^{1}H NMR ($CDCl_3$, 300 MHz): δ 7.38 (m, 5H), 3.77 (s, 3H), 3.64 (s, 2H).

Preparation of Amberzyme Oxirane Azide Resin. Amberzyme Oxirane resin (5.09) was stirred with NaN_3 (2.65 g, 40.8 mmol), NH_4Cl (1.15 g, 21.5 mmol) in MeOH/H_2O (9:1, 250 mL) at reflux for 16 h. The resin was filtered off over a glass frit, washed with H_2O, MeOH, and Et_2O, and dried under vacuum to give Amberzyme Oxirane azide resin (5.38 g).

Preparation of Amberzyme Oxirane Amine Resin. Amberzyme Oxirane azide resin (1.15 g), triphenylphosphine (1.5 g, 5.7 mmol) and THF (46 mL) were stirred gently at reflux for 6 h. H_2O (25 mL) was added and the reaction was stirred at room temperature for 1 h. The resin was washed with H_2O, MeOH, and CH_2Cl_2, and dried under vacuum to give Amberzyme Oxirane amine resin (1.05 g).

Iodination of Polystyrene Resin. Prepared according to the method of Huang et al.[22,23] Polystyrene (2% cross-linked, 2 g), I_2 (2 g, __ mmol), I_2O_5 (0.8 g, __mmol), CCl_4 (0.8 mL), H_2SO_4 (50%, 8 mL), and nitrosobenzene (24 mL) were stirred at 100 °C for 3 days. The resin was filtered off over a glass frit, washed with Et_2O, acetone, and CH_2Cl_2 and dried under vacuum to give iodinated polystyrene (2.05 g).

Functionalization of Amberzyme Oxirane Azide Resin. 4-Iodo-*N*-(prop-2-ynyl)benzamide, (0.49 g, 1.72 mmol) Amberzyme Oxirane azide resin (1.15 g), CuI (21.8 mg, 0.11 mmol), and THF (46 mL) were placed in a round bottom flask and mixed on a rotary evaporator motor under an atmosphere of N_2 for 3 days. The resin was filtered off over a glass frit, washed with THF, MeOH, and CH_2Cl_2, followed by HCl (1M), H_2O, $NaHCO_3$, and MeOH, and dried under vacuum to give the functionalized resin (1.23 g).

General Procedure for Functionalization of Amine Resins. 4-Iodobenzoic acid (496 mg, 2 mmol), HOBt (326 mg, 2.1 mmol), DIC (311.6 μL, 2 mmol), DMF, and the appropriate amount of resin were mixed on a rotary evaporator motor at room temperature for 2 days. Pyridine (40.3 μL) and acetic anhydride (47.3 μL) were added to acylate the remaining free amines and the reaction continued to mix for 3 h. The resin was filtered off over a glass frit, washed with DMF and MeOH, and dried under vacuum.

Aminomethyl polystyrene: Prepared according to the general procedure with 0.67 mg resin (~1.5 mmol/g, prepared by Brian P. Mason) and 10 mL DMF.

Aminomethyl JandaJel: Prepared according to the general procedure with 1.0 g resin (100-200 mesh, 2% cross-linked, 1 mmol/g) and 20 mL DMF.

Amberzyme Oxirane Amine: Prepared according to the general procedure with 0.8 g resin (~1.25 mmol/g) and 10 mL DMF.

Oxidation of Supported Iodobenzenes. The resins were oxidized with peracetic acid (10 mL per 1.25 g resin) at 40 °C for 16 h. The resins were filtered off over a glass frit and dried under vacuum. Final reagent loading was determined by iodine elemental analysis.

Preparation of Peracetic Acid. Prepared according to the method of Ficht et al.[21] Acetic anhydride (20 mL) and H_2O_2 (30%, 5.83 mL) were mixed at 0 °C for 4 h.

General Procedure for Rearrangement of 4'-Isobutylpropiophenone Using Supported Iodoso Reagents. 4'-Isobutylpropiophenone (31.5 mg, 0.17 mmol), $CH(OCH_3)_3$ (3 mL, 27.4 mmol), and the supported iodoso reagent (0.2 mmol, determined by elemental analysis) were cooled to 0 °C. H_2SO_4 was added and the reaction was mixed at 60 °C for 2 h. The reaction was quenched with H_2) and the product was extracted with Et_2O. Reaction conversion was determined by GC analysis.

REFERENCES

1. Sheldon, R. A.; *J. Chem. Tech. Biotechnol.* **1997**, *68*, 381.

2. Personal communication with Berkeley W. Cue, Jr., Green Chemistry Institute.

3. Elango, V.; Murphy, M. A.; Smith, B. L.; Davenport, K. G.; Mott, G. N.; Zey, E. G.; Moss, G. L. U.S. Patent No. 4,981,995, **1991**.

4. Lindley, D. D.; Curtis, T. A.; Ryan, T. R.; de la Garza, E. M.; Hilton, C. B.; Kenesson, T. M. U.S. Patent No. 5,068,448, **1991**.

5. Blicke, F. F.; Raffelson, H.; Barna, B. *J. Am. Chem. Soc.* **1952**, *74*, 253.

6. Robinson, R. *J. Chem. Soc.* **1917**, *111*, 762.

7. Finar, I.L. *Organic Chemistry Vol. 24th. Edn.* Longman 1965, p. 636.

8. Si, Y.-G.; Chen, J.; Li, F.; Li, J.-H.; Qin, Y.-J.; Jiang, B. *Adv. Synth. Catal.* **2006**, *348*, 898.

9. Zhuang, W.; Gathergood, N.; Hazell, R. G.; Jørgensen, K. A. *J. Org. Chem.* **2001**, *66*, 1009.

10. Bigi, F.; Casiraghi, G.; Casnati, G.; Sartori, G.; Soncini, P.; Fava, G. G.; Belicchi, M. F. *Tetrahedron Lett.* **1985**, *26*, 2021.

11. Kusuda, K.; Inanaga, J.; Yamaguchi, M. *Tetrahedron Lett.* **1989**, *30*, 2945.

12. Prakash, G. K. S.; Yan, P.; Török, B.; Olah, G. A. *Synlett* **2003**, *4*, 527.

13. *Polym. Advan. Technol.* **2002**, *13*, 169; *Polym. Advan. Technol.* **2003**, *14*, 360

14. Matsumoto, T.; Periana, R. A.; Taube, D. J.; Yoshida, H. *J. Mol. Catal. A-Chem.* **2002**, *180*, 1.

15. Matsumoto, T.; Taube, D. J.; Periana, R. A.; Taube, H.; Yoshida, H. *J. Am. Chem. Soc.* **2000**, *122*, 7414.

16. Arai, K.; Ohara, Y.; Takakuwa, Y.; Iizumi, T. U.S. Patent No. 4,577,025, **1986**.

17. Yamauchi, T.; Hattori, K.; Nakao, K; Tamaki, K. *J. Org. Chem.* **1988**, *53*, 4858.

18. Tamura, Y.; Yakura, T.; Shirouchi, Y.; Haruta, J.-I. *Chem. Pharm. Bull.* **1985**, *33*, 1097.

19. Togo, H.; Nogami, G.; Yokoyama, M. *Synlett* **1998**, 534

20. Bogdan, A. R.; Mason, B. P.; Sylvester, K. T.; McQuade, D. T. *Angew. Chem. In. Ed.* **2007**, *46*, 1698.

21. Rohm and Haas. "AMBERZYME Oxirane Enzyme Immobilization Polymeric Support." http://www.advancedbiosciences.com/Bioprocessing_doc/us_english/amberzyme.pdf (Accessed November 24, 2008).

22. Ficht, S.; Mülbaier, M.; Giannis, A. *Tetrahedron* **2001**, *57*, 4863.

23. Huang, X.; Zhu, Q. *J. Chem. Res.* **2000**, *5*, 300.

24. Huang, X.; Zhu, Q. *Syn. Comm.* **2001**, *31*, 111.

25. Trost, B. M. *Science*, **1991**, *254*, 1471.

26. Trost, B. M. *Acc. Chem. Res.* **2002**, *35*, 695.

27. Trost, B. M. *Angew. Chem. Int. Ed.* **1995**, *34*, 259.

28. Sheldon, R. A. *Pure. Appl. Chem.* **2001**, *72*, 1233.

29. Sheldon, R. A. *Chemtech.* **1994**, *24*, 38.

30. Sheldon, R. A. *Chem. Ind.* **1997**, 12.

31. Curzons, A. D.; Constable, D. J. C.; Mortimer, D. N.; Cunningham, V. L. *Green Chem.* **2001**, *3*, 1.

32. Andraos, J. *Org. Proc. Res. Dev.* **2005**, *9*, 149.

CHAPTER 3

Microcapsule Enabled Multicatalyst System

Preface

When I joined the McQuade group in 2004, they had developed the techniques to microencapsulate catalysts, but had not yet incorporated them into multicatalyst systems. One of the first projects given to me by my adviser was to synthesize the drug pregabalin. Though pregabalin itself is not a very complicated target, the challenge was that the synthesis needed to feature a multicatalyst system. Muris Kobašlija had been doing some unrelated work with encapsulated polyamines. These microcapsules turned out to be a catalyst for the first step of pregabalin synthesis. Paired with a nickel-based catalyst for the second step, these two catalysts worked in tandem to produce a precursor to pregabalin, and the McQuade group's first multicatalyst system was born.

Abstract[*]

We present a new microencapsulated catalyst and report its use in a tandem multicatalyst reaction. Using an encapsulation technique, we developed an active, site-isolated amine catalyst that is capable of catalyzing the addition of nitromethane to an aldehyde. When a second Lewis acid catalyst is added, the nitroalkene intermediate is trapped and converted to the corresponding Michael adduct. We show that if the amine catalyst is not encapsulated, the two catalysts cannot function together to produce the desired product. Moreover, if the two reactions are performed

[*] Reproduced in part with permission from: Poe, S. L.; Kobašlija, M.; McQuade, D. T. *J. Am. Chem. Soc.* **2006**, *128*, 15586. Copyright **2006** American Chemical Society.

in sequence rather than in tandem, the first reaction results in an undesired dinitro product and the desired Michael adduct is not formed.

Introduction

One-pot multistep reactions are effective at reducing the waste and cost of a synthetic route because they decrease the number of work-ups and purifications, as well as the volume of solvent used.[1-3] These reactions are especially useful when multiple catalysts are used so that one traps an unstable intermediate formed by the other. Though a variety of these reactions have been reported, they are limited to a relatively small number of systems where the catalysts are compatible with each other.[1,4,5] The work of Patchornik in 1981 demonstrated that this limitation can be overcome by immobilizing incompatible catalysts on solid supports.[6] Though this strategy has since been used to prevent catalyst interactions,[7] it often results in the loss of catalytic activity and in effect lowers efficiency.[8,9] Recently, one-pot multicatalyst reactions have been facilitated by site-isolated catalysts that diverge from the traditional solid support paradigm.[10-16] These examples show how materials such as sol-gels and star-polymers render incompatible catalysts compatible. However, the reactions featured are relatively simple and yield the same result when run stepwise. In addition, such successful examples are few and not easily generalized for new catalysts. It is therefore desirable to develop other techniques to site-isolate catalysts for use in one-pot multicatalyst reactions.

We recently reported the successful encapsulation of a polymeric catalyst *via* interfacial polymerization of an oil-in-water emulsion.[17,18] We demonstrated that because of the unique microenvironment created by our isolation technique, our catalyst showed greater catalytic activity than a comparable solid-supported catalyst. Herein, we extend the scope of our technique by reporting a microencapsulated amine

catalyst and demonstrate its utility by applying it to a tandem reaction sequence involving an otherwise incompatible Lewis acid catalyst (Figure 3.1). We also increase the complexity of such reactions by using the second catalyst to trap an intermediate from the first, forming a product that cannot be accessed when the reactions are performed sequentially.

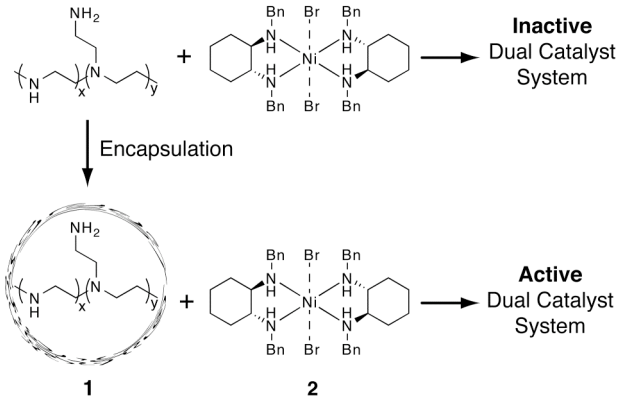

Figure 3.1. Encapsulation of a polymeric catalyst enables a tandem reaction. The two catalysts are microencapsulated PEI (**1**) and a nickel-based Michael addition catalyst (**2**).

Results and Discussion

A tandem amine-Lewis acid system was selected as a model because they are incompatible catalysts without site-isolation and because this two-catalyst system would be synthetically useful (*vide infra*). A brief screen of the literature suggested that we focus on nitroalkene formation as half of our tandem reaction sequence. This amine-catalyzed reaction often produces a mixture of nitroalkene and dinitro products, the latter being the result of a second addition of nitroalkane.[19-21] If we were able to prepare a site-isolated amine catalyst, we could trap the nitroalkene intermediate with a Lewis acid catalyst in order to direct it toward a second product rather than letting it proceed to the dinitro product. The Lewis acid we chose for this role is the nickel-based Michael catalyst (**2**) reported by Seidel and Evans to convert nitroalkenes to the

corresponding Michael adduct in high yields.[22] By combining these two reactions in one pot, we hoped to achieve a higher yield of Michael adduct than we could if the reactions were run sequentially.

With the Lewis acid catalyst chosen, we assessed the necessity for developing an encapsulated amine catalyst[23] by screening a variety of commercially available amine-based catalysts for the reaction between benzaldehyde (**3**) and nitromethane. Small, soluble amines were found to catalyze the reaction, producing both trans-β-nitrostyrene (**4**) and 1,3-dinitro-2-phenyl-propane (**5**), but when used in tandem with **2** and dimethyl malonate (DMM), the two catalysts complexed and precipitated. On the other hand, amine catalysts attached to solid supports such as MCM-41 or polystyrene beads showed no activity toward nitroalkene formation under room temperature conditions suitable for catalyst **2**. Rather, they required elevated temperatures between 60 and 90 °C to achieve nitroalkene formation.

We sought to encapsulate the polymeric amine poly(ethyleneimine) (PEI) to address the compatibility and activity problems we encountered with the commercially available catalysts. The catalyst was prepared by dispersing a methanolic PEI solution into a nonpolar cyclohexane phase with the help of a stabilizer. Upon emulsification, 2,4-tolylene diisocyanate (TDI) was added to the continuous phase to initiate cross-linking that occurs only at the interface of the emulsion droplets between TDI and PEI. After polymerization, microcapsules containing PEI chains were isolated for use in a reaction after drying.

We tested our new encapsulated (μcap) amine (**1**) as a catalyst for nitroalkene formation. In this experiment, the μcaps were swollen with methanol for 5 min before the remaining reagents were added. The reaction was performed at room temperature, and reaction progress was monitored by GC. Like the free amines, the μcap catalyst produces both **4** and **5** (Scheme 3.1). We currently propose that the retention of our

catalyst's activity as compared to the traditionally solid-supported amines is due to the unique microenvironment that the capsules possess.[17,18] A second phenomenon we observed is that the PEI-capsule walls capture intermediate **4** in an irreversible Michael-type addition, resulting in lowered reaction yields.[25-27]

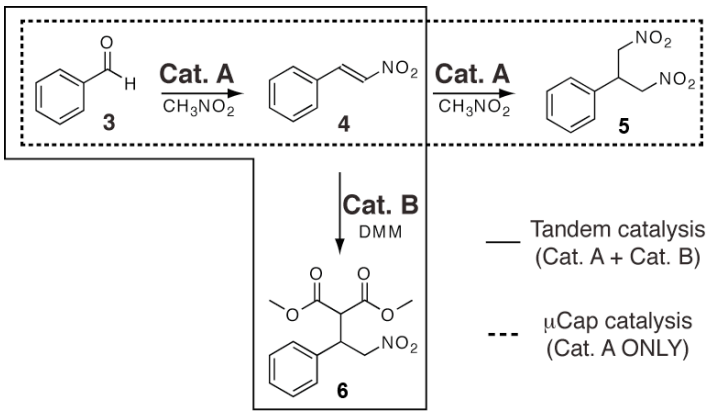

Scheme 3.1. Single-catalyst dinitro product formation (dashed) versus double-catalyst Michael adduct formation (solid).

The two undesired side reactions of **4** described above presented the opportunity to exploit a one-pot multistep reaction to its fullest potential: by adding a second catalyst to the system, we hoped to trap the transient nitroalkene intermediate and direct it toward the desired Michael adduct. The tandem reaction was carried out by first swelling the encapsulated amine catalyst in methanol for 5 min and then suspending it in toluene. The remaining catalyst and reagents were added, and reaction progress was monitored by GC. Initial formation of nitroalkene intermediate was followed by its conversion to the desired Michael adduct (**6**) rather than undesired **5** (Scheme 3.1). The Michael adduct was formed in 80% yield after 24 h. It should be noted that **6** *is not formed if only one of the catalysts is present or if the reactions are performed sequentially,* as it was demonstrated above that the first reaction alone resulted in two unproductive situations. This series of reactions is performed

efficiently only when the amine catalyst is encapsulated and the reactions are run in one pot (Table 3.1).

Table 3.1. Conversion of **3** and yield of **6** after 24 h.

Catalyst System	Conversion of **3** (%)	Yield of **6** (%)[a]
μcap amine (**1**) + Ni catalyst (**2**)	95	80.2
μcap amine (**1**) alone	67	2.1
Ni catalyst (**2**) alone	61	8.5
Free PEI + Ni catalyst (**2**)	96	5.4

[a]Yields were determined by GC areas. For cases in which the product was isolated, isolated yields agree with GC yields.

In order to assess the site isolation of the two catalysts, we investigated whether commercially available unencapsulated PEI could replace the encapsulated catalyst. We found that the two catalysts (PEI and **2**) produce the Michael adduct in only 5.4% yield (Table 3.1, entry 4). On the basis of literature precedence, we initially speculated that free PEI strongly chelates Ni, making it inactive.[28] This hypothesis was supported by the observation that the nickel-catalyzed Michael addition did not occur when performed in the presence of high levels of PEI (Figure 2.2). In addition, by monitoring UV-Vis absorbance of **2** in the presence and in the absence of μcaps, we determined that the poisoning of **2** occurs only to a small extent (see Supporting Information). However, when we lowered the PEI concentration to the loading present in the one-pot reaction, we found that the Michael addition proceeded in high yields, indicating that at these concentrations, the two catalysts do not foul each other (Figure 2.2). The observation that the two catalysts are not incompatible at these loadings presents the possibility that the microcapsule shell may not provide site isolation in this multicatalyst system. However, the benefit provided by the microcapsule shell is not negligible; though the Michael addition alone proceeds in the presence of free PEI, the tandem reaction does not function under these conditions. Table 3.1 clearly demonstrates that PEI encapsulation is necessary for the tandem

reaction to proceed in good yield. Whether or not the microcapsule shell provides site isolation, it plays a necessary role in this multicatalyst system.

Conclusion

We have demonstrated the potential for and subsequent development of an active, site-isolated amine catalyst. Our encapsulation method results in a catalytically active species that remains site-isolated during a one-pot multistep reaction, allowing it to be used in tandem with an otherwise incompatible catalyst. This example demonstrates the capabilities of tandem catalysis to trap and direct reaction intermediates efficiently. The Michael adduct formed by this reaction sequence can be used to access pharmaceutical agents such as baclofen, rolipram, and pregabalin, as well as other γ-amino acid analogs. The results of this catalyst system can likely be made general and applied to a variety of amine-Lewis acid tandem reactions as well as other incompatible catalyst systems. The efficiency of organic synthesis will improve significantly as both site-isolation techniques and tandem reactions are developed.

Afterword

The results presented in this chapter were a product of a true collaborative effort. When I needed a site-isolated polyamine catalyst, we discovered that the microcapsules that Muris Kobašlija was already working with were effective for nitroalkene formation. Furthermore, catalyst encapsulation plays a necessary role in this one-pot multicatalyst system, allowing us to access products that we could not access if the catalyst were not isolated or if the reactions were performed sequentially. The unexpected result that a second catalyst diverts the intermediate in the tandem catalytic reaction only increases the value of these findings. Our initial hypothesis that the role of the microcapsule was to prevent incompatible catalysts from interacting

needs to be revisited. Our more recent observations that low concentrations of unencapsulated PEI do not foul the second step, but prevents the overall reaction from proceeding suggests a more complicated and potentially more interesting role for the microcapsules.

Experimental Section

General Considerations

Dimethyl malonate (Acros, 97%), trifluoroacetic anhyhdride (Acros, 99+%), (±)-*trans*-1,2-diaminocyclohexane (Aldrich, 98%), mesitylene (Aldrich, 98%), *trans*-β-nitrostyrene (Aldrich, 99%), polyisobutylene (Aldrich, MW 400, 000), tolylene 2,4-diisocyanate (Aldrich, technical grade, 80%), chloroform (J. T. Baker), nitromethane (J. T. Baker, 99%), acetic anhydride (Mallinckrodt), cyclohexane (Mallinckrodt), methanol (Mallinckrodt), toluene (Mallinckrodt), poly(ethyleneimine) (Polysciences, Inc., 10,000 MW), and Span 85 (Sigma) were used as received. Benzaldehyde (Aldrich, 99.5%) was washed with saturated $NaHCO_3$, distilled, and dried over Na_2SO_4 prior to use. Reactions were rocked on a Thermolyne Speci-Mix test tube rocker. For ^{19}F elemental analysis, μcaps acylated with trifluoroacetic anhydride were sent to Robertson Microlit Laboratories for analysis (www.robertson-microlit.com). Gas chromatographic (GC) analyses were performed using a Varian CP-3800 GC equipped with a Varian CP-8400 autosampler, a flame ionization detector (FID) and a Varian CP-Sil 5CB column (length = 15 m, inner diameter = 0.25 mm, and film thickness = 0.25 μm. The temperature program for GC analysis held the temperature constant at 80 ºC, heated samples from 80 to 200 ºC at 17 ºC/min, and held at 200 ºC for 2 min. Inlet and detector temperatures were set constant at 220 and 250 ºC, respectively. Mesitylene was used as an internal standard to calculate reaction conversion. ^1H NMR and ^{13}C NMR spectra were recorded on a Varian Inova-400

(400 MHz) spectrometer and are reported in ppm using solvent as an internal standard ($CDCl_3$ at 7.26 ppm). Data are reported as s = singlet, d = doublet, t = triplet, quin = quintet, m = multiplet. Scanning electron microscopy images were obtained on a Leica 440 SEM at the Cornell Center for Materials Research. Capsules were characterized at 25 kV after sputter coating with palladium-gold. Optical microscopy images were obtained on an inverted Leica DMIL with a mounted Sony DSC-F717 digital camera and ebq100 UV source.

Synthesis of Microencapsulated Poly(ethyleneimine) Catalyst (1). The microcapsule catalyst was prepared by interfacial polymerization of oil-in-oil emulsions, in a slightly different manner than what was described by Kobašlija and McQuade.[29] To cyclohexane (50 mL, η = 9.5 cp) and Span 85 mixture (2% v/v) stirred at 1500 rpm with a magnetic stirrer, the disperse phase (1.5 mL PEI in 6.0 mL methanol and 1.5 mL chloroform) was added at once. After 2 minutes of stirring, 2,4-tolylene diisocyanate (TDI, 1.0 mL in 9.0 mL cyclohexane) was added at once and the stirring was reduced to 500 rpm. After 1 minute, polymerization was stopped by the addition of cyclohexane (30 mL). The resulting capsules were left to settle, further washed with hexanes, and left to air-dry overnight.

Determination of Catalyst Loading. Loading of the microcapsule catalyst active sites was determined via labeling with fluorine and a subsequent fluorine elemental analysis. To microcapsule catalyst (100 mg), loaded in a syringe equipped with a frit, methanol (5 mL) was added to swell them. After 5 minutes the excess methanol was removed and the solution containing trifluoroacetic anhydride (1 mL) in methanol (5 mL) was drawn into the syringe. The mixture was rocked at room temperature overnight. Fluorine labeled microcapsule catalysts were extensively washed with

methanol, dried under stream of N_2 and sent for fluorine elemental analysis. To ensure that all the active site were acylated, the microcapsules were checked for the activity in nitro-aldol reaction. As expected for fully acylated microcapsules, they have shown no activity. Results of fluorine elemental analysis suggest that the loading of the catalytically active sites is 4.7 mmol/g.

Ni(II)–bis[(±)-*trans* -N,N'-Dibenzylcyclohexane-1,2-diamine]Br_2 (2). Prepared according to the method of Evans et al.[22] (±)-*trans*-1,2-Diaminocyclohexane (3 g, 26.3 mmol) was dissolved in MeOH (16 mL) and the solution was heated to reflux. Benzaldehyde (5.4 mL, 53.2 mmol) was added dropwise and the reaction was stirred at reflux for 30 min. The reaction was allowed to cool to room temperature and was left to sit overnight, during which the product precipitated out of solution. The solid was isolated by filtration and recrystallized from petroleum ether to afford (±)-*trans*-dibenzylidenecyclohexane-1,2-diamine as white crystals (6.57 g, 86% yield): ^{1}H NMR ($CDCl_3$, 300 MHz): δ 8.22 (s, 2H), 7.61 (m, 4H), 7.34 (m, 4H), 3.42 (m, 2H), 1.89 (m, 8H), 1.50 (m, 2H); ^{13}C NMR ($CDCl_3$, 75 MHz): δ 161.3, 136.6, 130.4, 128.6, 128.2, 74.0, 33.2, 24.7.

(±)-*trans*-Dibenzylidenecyclohexane-1,2-diamine (6.57 g, 22.6 mmol) was dissolved in MeOH (55 mL) and cooled to 0 °C. $NaBH_4$ (1.8 g, 47.6 mmol) was added slowly, after which the reaction was stirred at reflux for 15 min. Once cool, the solution was acidified with 5 M HCl and washed with CH_2Cl_2. The layers were separated and 1 M NaOH was added to the aqueous layer until pH = basic. The product was extracted with CH_2Cl_2 (3 x 50 mL) and the combined organic layers were dried over Na_2SO_4, concentrated, and dried under vacuum to give (±)-*trans*-dibenzylcyclohexane-1,2-diamine as a white solid (6.58 g, 99% yield): ^{1}H NMR ($CDCl_3$, 400 MHz): δ 7.30-7.19

(m, 10H), 3.90 (d, 2H), 3.63 (d, 2H), 2.31 (m, 2H), 2.18 (d, 2H), 1.72 (m, 2H), 1.23-1.03 (m, 4H); ^{13}C NMR ($CDCl_3$, 100 MHz): δ 141.1, 128.6, 128.4, 128.3, 127.0, 61.1, 51.1, 31.7, 25.2. (±)-*trans*-dibenzylcyclohexane-1,2-diamine (3.66 g, 12.4 mmol) was dissolved in acetonitrile (150 mL). $NiBr_2$ (1.26 g, 5.8 mmol) was added and the reaction was stirred at reflux for 6 h, during which the reaction turned purple. Upon cooling, the blue solution was filtered through a glass frit and concentrated *in vacuo*. The crude product was recrystallized from CH_2Cl_2 and acetonitrile to give Ni(II)–bis[(±)-*trans* -N,N'-dibenzylcyclohexane-1,2-diamine]Br_2 as blue crystals (3.46 g, 74% yield).

General Procedure for Multicatalyst Reaction. Microencapsulated PEI catalyst **1** was swollen in methanol before use. Catalyst(s), benzaldehyde (101.6 μL, 1 mmol), nitromethane (0.54 mL, 10 mmol), dimethyl malonate (114.3 μL, 1 mmol), methanol (0.5 mL), toluene (1 mL), and mesitylene (13.9 μL) were placed in a 4 mL glass vessel and sealed with a screw cap. The reaction was rocked at room temperature on a rocker. Reaction conversion was monitored by withdrawing aliquots from the reaction at different time intervals, diluting with methylene chloride, and analyzing by GC with reference to mesitylene.

Tandem catalysis: PEI catalyst **1** (15 mg) and nickel catalyst **2** (60 mg, 7.4 mol %) were used in the reaction described above.

Encapsulated PEI catalyst (**1**) only: PEI catalyst **1** (15 mg) was used in the reaction described above.

Nickel catalyst (**2**) only: Nickel catalyst **2** (60 mg, 7.4 mol %) was used in the reaction described above.

Free PEI and nickel catalyst **2**: PEI (10,000 MW, 25 mg) and nickel catalyst **2** (60 mg, 7.4 mol %) were used in the reaction described above.

***trans*-β-Nitrostyrene (4).** The product can be commercially obtained from Aldrich for comparison purposes. ^{1}H NMR (400 MHz, $CDCl_3$) δ 7.90 (d, J = 13.65 Hz, 1H), 7.53 (d, J = 13.65 Hz, 1H), 7.48-7.35 (m, 5H); ^{13}C NMR (100 MHz, $CDCl_3$) δ 139.1, 137.1, 132.2, 130.1, 129.4, 129.3.

1,3-Dinitro-2-phenyl-propane (5). The product can be purified by column chromatography (20%EtOAc/hexanes) to give a brown oil. ^{1}H NMR (400 MHz, $CDCl_3$) δ 7.36-7.29 (m, 3H), 7.2-7.17 (m, 2H), 4.76-4.65 (m, 4H), 4.3-4.22 (quin, J = 7.21 Hz, 1H); ^{13}C NMR (100 MHz, $CDCl_3$) δ 134.5, 129.7, 129.2, 127.6, 76.9, 41.9.

Methyl 2-carboxymethoxy-4-nitro-3-phenyl-butyrate (6). The product can be purified by column chromatography (20% EtOAc/hexanes) to give a white solid. ^{1}H NMR (400 MHz, $CDCl_3$) δ 7.33-7.26 (m, 3H), 7.24-7.21 (m, 3H), 4.95-4.84 (m, 2H), 4.24 (dt, J = 5.1 Hz, 9.0 Hz, 1H), 3.86 (d, J = 9.16, 1H), 3.75 (s, 1H), 3.54 (s, 1H); ^{13}C NMR (100 MHz, $CDCl_3$) δ 168.1, 167.5, 136.4, 129.3, 128.7, 128.1, 77.6, 54.9, 53.3, 53.1, 43.2.

Supporting Information

Experimental methods and catalyst preparation and characterization are located in Appendix 1.

REFERENCES

1. Broadwater, S. J.; Roth, S. L.; Price, K. E.; Kobašlija, M.; McQuade, D. T. *Org. Biomol. Chem*. **2005**, *3*, 2899

2. Wasilke, J. C.; Obrey, S. J.; Baker, R. T.; Bazan, G. C. *Chem. Rev*. **2005**, *105*, 1001.

3. Enders, D.; Hüttl, M. R. M.; Grondal, C.; Raabe, G. *Nature* **2006**, *441*, 861.

4. Tietze, L. F. *Chem. Rev*. **1996**, *96*, 115.

5. Bruggink, A.; Schoevaart, R.; Kieboom, T. *Org. Process Res. Dev*. **2003**, *7*, 622.

6. Cohen, B. J.; Kraus, M. J.; Patchornik, A. *J. Am. Chem. Soc*. **1981**, *103*, 7620.

7. Benaglia, M.; Puglisi, A.; Cozzi, F. *Chem. Rev*. **2003**, *103*, 3401.

8. Deratani, A.; Darling, G. D.; Fréchet, J. M. J. *Polymer* **1987**, *28*, 825

9. Selkala, S. A.; Tois, J.; Pihko, P. M.; Koskinen, A. M. P. *Adv. Synth. Catal*. **2002**, 344, 941.

10. Voit, B. *Angew. Chem. Int. Ed*. **2006**, *45*, 2.

11. Gelman, F.; Blum, J.; Avnir, D. *J. Am. Chem. Soc*. **2000**, *122*, 11999.

12. Gelman, F.; Blum, J.; Avnir, D. *Angew. Chem. Int. Ed*. **2001**, *40*, 3647.

13. Gelman, F.; Blum, J.; Avnir, D. *New J. Chem*. **2003**, *27*, 205.

14. Helms, B.; Guillaudeu, S. J.; Xie, Y.; McMurdo, M.; Hawker, C. J.; Fréchet, J. M. J. *Angew. Chem. Int. Ed*. **2005**, *44*, 6384.

15. Motokura, K.; Fujita, N.; Mori, K.; Mizugaki, T.; Ebitani, K.; Kaneda, K. *J. Am. Chem. Soc*. **2005**, *127*, 9674.

16. Phan, N. T. S.; Gill, C. S.; Nguyen, J. V.; Zhang, Z. J.; Jones, C. W. *Angew. Chem. Int. Ed*. **2006**, *45*, 2209.

17. Price, K. E.; Mason, B. P.; Bogdan, A. R.; Broadwater, S. J.; Steinbacher, J. L. *J. Am. Chem. Soc*. **2006**, *128*, 10376.

18. Price, K. E.; Broadwater, S. J.; Bogdan, A. R.; Keresztes, I.; Steinbacher, J. L.; McQuade, D. T. *Macromolecules* **2006**, *39*, 7681.

19. Sartori, G.; Bigi, F.; Maggi, R.; Sartorio, R.; Macquarrie, D. J.; Lenarda, M.; Storaro, L.; Coluccia, S.; Martra, G. *J. Catal*. **2004**, 410.

20. Ballini, R.; Bosica, G.; Fiorini, D.; Palmieri, A. *Synthesis* **2004**, *12*, 1938.

21. Kisanga, P. B.; Verkade, J. G. *J. Org. Chem*. **1999**, *64*, 4298.

22. Evans, D. A.; Seidel, D. *J. Am. Chem. Soc*. **2005**, *127*, 9958.

23. In our attempts to find a catalyst that was compatible with **2**, we tried both unsupported amines (diethylenetriamine and tris(2-aminoethyl)-amine) and supported amines (diethylenetriamine, polystyrene bound; tris-(2-aminoethyl)-amine, polystyrene bound; PEI on silica gel; PEI on Amberzyme; and MCM-41 functionalized with N-(2-aminoethyl)-3-aminopropyl groups).

24. Bernasconi, C. F.; Renfrow, R. A.; Tia, P. R. *J. Am. Chem. Soc*. **1986**, *108*, 4541.

25. Lough, C. E.; Currie, D. J. *Can. J. Chem*. **1966**, *44*, 1563.

26. Mouhtaram, M.; Jung, L.; Stambach, J. F. *Tetrahedron* **1993**, 49, 1391.

27. Worrall, D. E. J. *Am. Chem. Soc*. **1927**, *49*, 1598.

28. Horn, D. In *Polymeric Amines and Ammonium Salts*, Pergamon Press: New York, 1980, pp. 333-356.

29. Kobašlija, M.; McQuade, D. T. *Macromolecules* **2006**, *39*, 6371.

CHAPTER 4

Mechanism and Application of a Microcapsule Enabled Multicatalyst Reaction

Preface

The development of the reaction described in Chapter 3 provided us with our first multicatalyst system. It also presented us with a number of answered questions as to why and how the reaction worked. The work presented in this chapter addresses some of these questions, exploring both the conditions required by the microencapsulated catalyst as well as the kinetics of the one-pot reaction.

Abstract[*]

In this paper, we describe the development and application of a multistep one-pot reaction that is made possible by catalyst encapsulation. We prepared a microencapsulated amine catalyst by interfacial polymerization and used it in conjunction with a nickel-based catalyst for the transformation of an aldehyde to a Michael adduct *via* a nitroalkene intermediate. The amine-catalyzed conversion of an aldehyde to a nitroalkene was found to proceed through an imine rather than a nitroalcohol. Kinetic studies indicated that the reaction is first order in both the nickel catalyst and the shell of the encapsulated amine catalyst. Furthermore, we present kinetic data that demonstrates that there is a rate enhancement of the Michael addition due to the presence of the microencapsulated catalyst. We applied our one-pot reaction to the development of a new synthetic route for pregabalin that proceeds with an overall yield of 74%.

---

[*] Reproduced in part with permission from: Poe, S. L.; Kobašlija, M.; McQuade, D. T. *J. Am. Chem. Soc*. **2007**, *129*, 9216. Copyright **2007** American Chemical Society.

Introduction

Catalyst isolation techniques that enable one-pot multistep reactions hold great potential for increasing the efficiency of chemical synthesis. Performing multiple reactions simultaneously in a single reaction vessel offers possibilities for reduced waste and increased safety as well as manipulation of equilibria.[1-3] Although many site-isolated catalysts have been developed, the focus has been largely on catalyst recovery rather than on tandem catalysis. Indeed, since the pioneering work of Patchornik over 25 years ago[4] the sol-gel materials developed by Avnir and Blum have been the only catalyst supports used in the context of one-pot multistep catalysis until recently.[5-7] In the past few years, Fréchet et al. introduced a multicatalyst system that employed star polymers for catalyst isolation,[8] while Jones et al. showed that catalysts supported on polymer resins and magnetic particles could be used together while avoiding catalyst fouling.[9] In another approach Kaneda et al. immobilized two incompatible catalysts in mesoporous clays to achieve site isolation.[10] All of these examples demonstrate the effective separation of otherwise incompatible catalysts. Though each of these examples promises the possibility for application to more sophisticated systems, the full potential of multicatalyst systems will remain unrealized until applications to more complex molecules are demonstrated.

With this need in mind, we recently reported a microcapsule (μcap) enabled multicatalyst system that produces a synthetically useful product.[7] Though the goal of microencapsulation was for the microcapsule shell to provide site-isolation, we discovered that in practice, the two catalysts may interact after all. Regardless, we demonstrated that microencapsulation is necessary for a functional two-catalyst system, and despite the potential absence of site-isolation, we were able to develop a tandem reaction that would not otherwise be possible. The reaction involves the amine-catalyzed transformation of an aldehyde to a nitroalkene followed by a

transition-metal-catalyzed Michael addition in the same reaction vessel (Scheme 4.1). Typically, amine catalysts and nickel complexes are incompatible due to their tendency to chelate and render each other inactive.[11] However, microencapsulation of PEI forms catalyst **1**, which can successfully be used in tandem with the nickel-based catalyst **2** developed by the Evans group.[12]

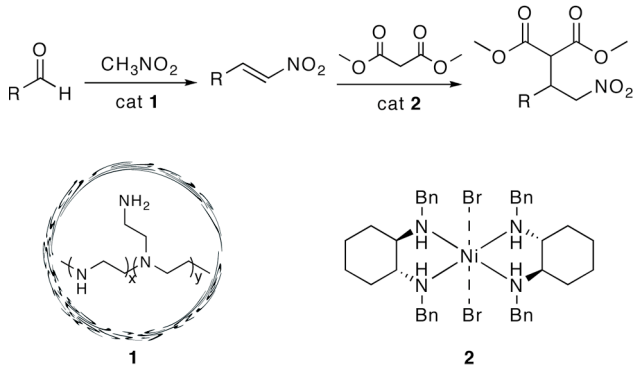

Scheme 4.1. Transformation of an aldehyde to a nitroalkene and subsequent Michael addition of a malonate ester can be performed in tandem through the use of microencapsulated catalyst **1** and nickel catalyst **2**.

Not only do these two reactions both form C-C bonds, but together they create a versatile synthetic building block. For instance, the nitroalkane can be converted into an amine via reduction or a carbonyl via the Nef reaction, while the ester groups can be transformed into a single carboxylate via hydrolysis-decarboxylation or a diol via reduction. Such subsequent reactions could provide access to a wide range of useful intermediates, such as those found en route to pharmaceuticals ranging from rolipram to baclofen to pregabalin (**3**, Scheme 4.2).

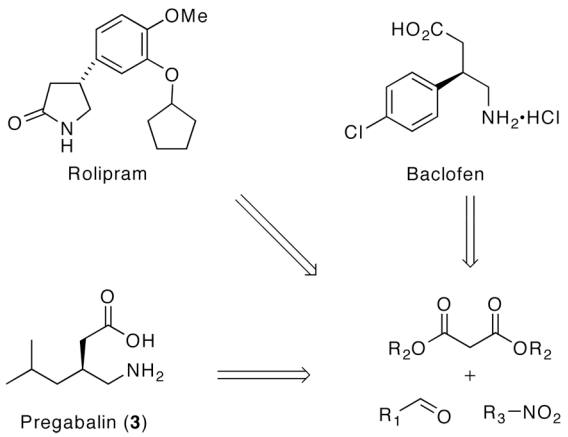

Scheme 4.2. Pharmaceutical agents that incorporate an aldehyde, a nitroalkane, and a malonate ester.

With this work, we show the generality of this reaction while providing mechanistic insight for our microencapsulated catalyst. We also discuss the application of this system to a pharmaceutically relevant problem: an efficient chemical synthesis of pregabalin.

Results and Discussion

Synthesis and Characterization of Microencapsulated Catalyst.

Encapsulation of an amine-based Henry reaction catalyst was achieved via the interfacial polymerization of oil-in- oil emulsions, as described in our previous work. Poly(ethyleneimine) (PEI) was encapsulated by dispersing a methanolic PEI solution into a continuous cyclohexane phase. Upon emulsification, 2,4-tolylene diisocyanate (TDI) was added to initiate cross-linking at the emulsion interface, forming polyurea shells that contain free chains of PEI. The microcapsules crenate when dry and swell when placed in such solvents as methanol and DMF, suggesting a hollow capsule rather than a solid sphere (Figure 4.1).[13] Catalyst loading was determined to be 1.6 mmol/g[14] by acylation of the catalytic amines with trifluoroacetic anhydride followed by fluorine elemental analysis. Oxygen elemental analysis placed the upper limit on

urea content of the μcap shells at 5.6 mmol/g (the upper limit assumes no water retention).

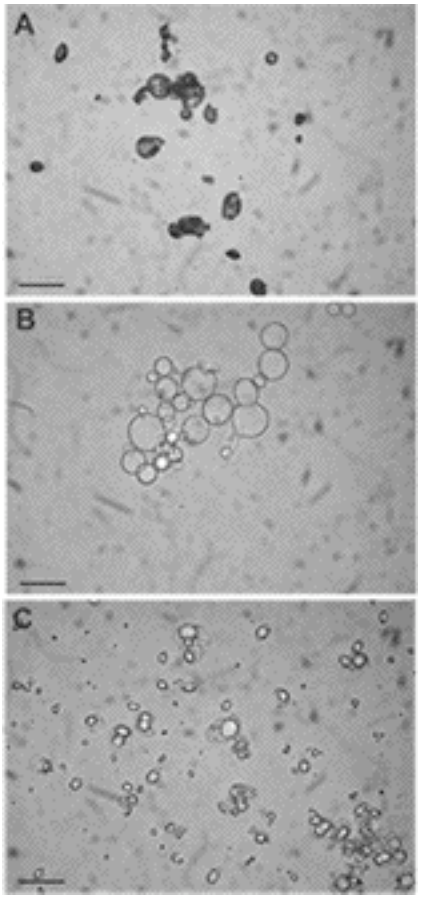

Figure 4.1. Optical micrographs of dry μcaps (a); μcaps in methanol, a swelling solvent (b); and μcaps in toluene, a nonswelling solvent (c). The scale bar is 30 μm.

Activity and Mechanism of Microencapsulated Catalyst. To better understand the importance of μcap swelling, the reaction between benzaldehyde (**4**) and nitromethane was performed in a range of different solvents.[15] Swelling effects were separated from solvent effects by using both free and encapsulated PEI as catalysts for formation of trans-β-nitrostyrene (**5**) and 1,3-dinitro-2-phenyl-propane (**6**). Figure 4.2 shows benzaldehyde conversion after 6 h for each catalyst.

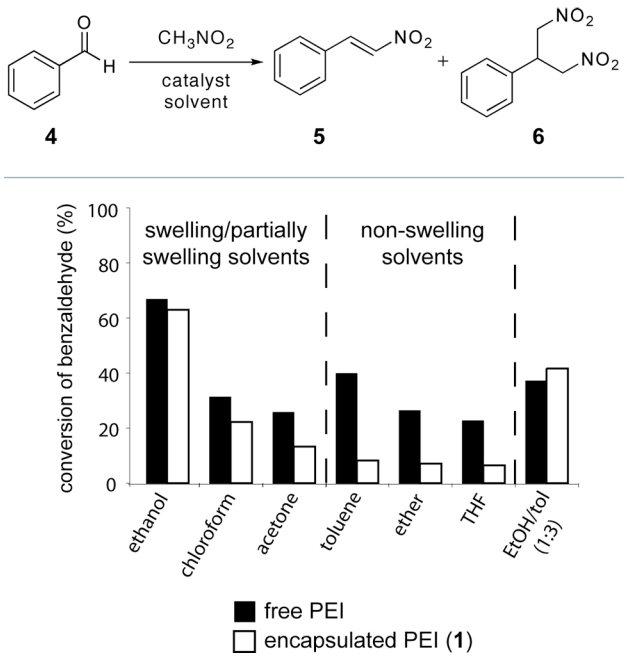

Figure 4.2. Conversion of benzaldehyde (**4**) after 6 h for the amine-catalyzed reaction between benzaldehyde and nitromethane. Catalysts for the reaction were free PEI (black bars, 4.6 mol %) and encapsulated PEI (white bars, 4.6 mol %).

The results for the reactions catalyzed by free PEI (black bars) are not affected by swelling or by the kinetic barrier introduced by the microcapsule shell and therefore indicate how effective each solvent is for this reaction. If the differences in conversion for the reactions catalyzed by encapsulated PEI (white bars) were based exclusively on solvent, we would expect the two cases to show the same trends. This is the case for both swelling and partially swelling solvents; for each catalyst conversions are high for ethanol, moderate for chloroform, and low for acetone. However, this is not true for non-swelling solvents. While the free PEI-catalyzed reactions revealed that toluene, ether, and THF were relatively good, moderate, and poor solvents, respectively, encapsulated PEI did not produce the same results. Despite the moderate conversion produced by free PEI in toluene, encapsulation resulted in an 80% decrease in catalytic activity in the same solvent. These results suggest that the solvent dependence of this reaction is two-fold; not only must the

solvent be favorable for the PEI-catalyzed reaction, but it also must be able to swell the microcapsules. Acetone swells the capsules but is a poor solvent for the reaction, while toluene is a good solvent for the reaction but is unable to swell the μcaps.

Both of these cases result in poor conversions of benzaldehyde when encapsulated PEI is used as the catalyst. Only ethanol, a good solvent for the reaction that is also able to swell the capsules, is able to produce high conversions with both free and encapsulated PEI. Furthermore, in some cases catalytic activity is retained for capsules that are swollen in a swelling solvent and then placed in a bulk non-swelling solvent (Figure 4.2). We are currently pursuing the reasons for and implications of this phenomenon.[16]

With a better understanding of the conditions required for catalytic activity, we turned our attention to the mechanism of the μcap catalyst. Transformation of an aldehyde to a nitroalkene can occur via two different pathways. The first involves nitroalcohol formation through a traditional Henry reaction, which is then followed by elimination to form the double bond. The second proceeds through an imine intermediate rather than the nitroalcohol. This latter mechanism has been suggested for cases in which the catalyst contains both primary and tertiary amino groups as well as for solid supported catalysis.[17,18] Being that our catalyst exhibits both of these features, we predicted that μcap-enabled nitroalkene formation goes through an imine intermediate rather than the nitroalcohol. Indeed, when we followed the μcap-catalyzed condensation of benzaldehyde with nitromethane over time, we did not observe the nitroalcohol at any point in the reaction. However, the nitroalcohol was found to be present during the course of the one-pot reaction, possibly having been formed by the amine ligands of the nickel catalyst. This evidence precludes the possibility that elimination occurs as soon as the nitroalcohol is formed and suggests that the reaction might follow the latter route. To further support this hypothesis,

when the nitroalcohol is placed in the presence of swollen μcaps, no nitroalkene formation is observed. The inability of the μcap catalyst to convert this potential intermediate to the final product provides further evidence against the nitroalcohol-elimination pathway. A proposed mechanism for μcap-catalyzed nitroalkene formation is shown in Scheme 4.3.

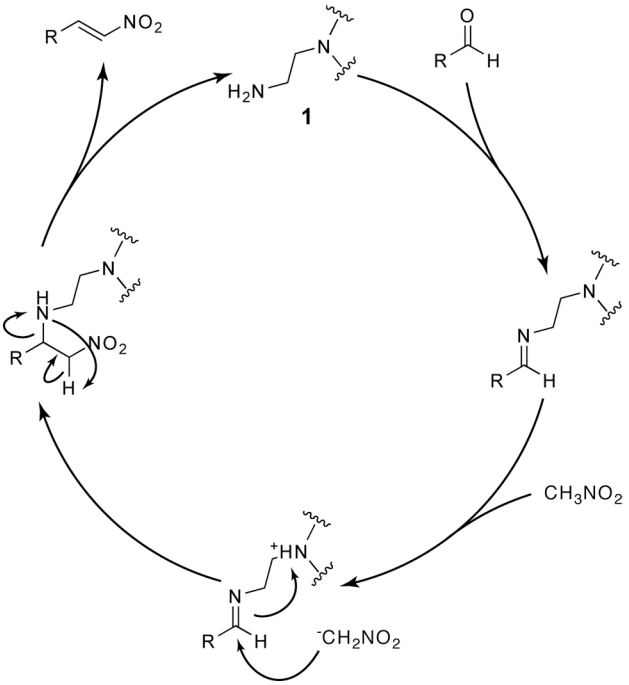

Scheme 4.3. Proposed catalytic system of μcap-catalyzed nitroalkene formation. Though the mechanism for nitroalkene formation and regeneration of the primary amine (left) is believed to occur intermolecularly, it is shown intramolecularly for clarity.

One-Pot Reaction. We reported that there is the possibility for the nitroalkene intermediate to either form the dinitro product or go through a Michael-type addition with the encapsulated PEI when subjected to the reaction discussed above. However, we have also shown that when the reaction is run in the presence of a second catalyst-reagent pair, this intermediate can be trapped and directed to a different reaction pathway (Scheme 4.4).

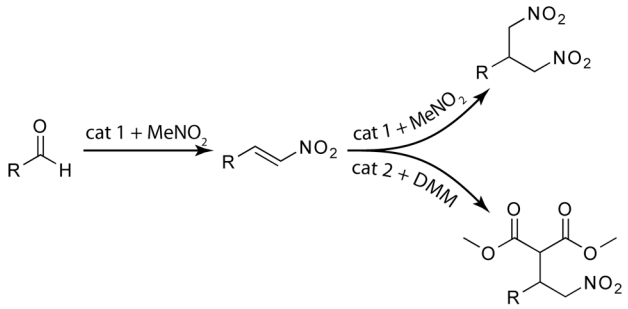

Scheme 4.4. Single-catalyst addition of nitromethane (top) versus double-catalyst addition of dimethyl malonate (DMM) (bottom).

Furthermore, because μcaps swollen in methanol retain their catalytic activity when placed in toluene, the reaction can be run in a mixture of two different solvents. This allows both the μcaps and the nickel catalyst to operate in their respective ideal solvents of methanol and toluene. To demonstrate the scope of this one-pot reaction, we performed this reaction with a variety of aromatic and aliphatic aldehydes. The results are shown in Table 4.1. It is evident that though the system tolerates both aromatic and aliphatic aldehydes, introduction of electron-withdrawing substituents on the aromatic substrates results in decreased yields. This effect is most pronounced in entries 6 and 7 for which the cyano- and nitro-substituted benzaldehydes yield minimal product formation. Assuming that the μcap-catalyzed step proceeds through an imine intermediate, this phenomemon can be rationalized by the observations of Santerre et al., who compared the rates of uncatalyzed imine formation between substituted benzaldehydes and aliphatic amines at room temperature.[19] It was found that the rate is maximal for unsubstituted benzaldehyde and steadily decreases as the substituents' σ values diverge in either direction on the Hammett plot. It is possible that the cyano and nitro substituents are too electron-withdrawing to allow for any appreciable imine formation.

Table 4.1. Scope of the one-pot reaction.

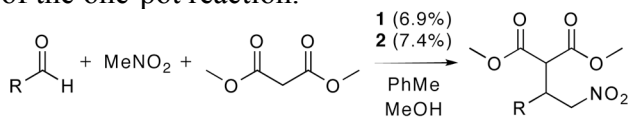

7

Entry	R	Product	Yield (%)
1	Ph	**7a**	80
2	4-Me—Ph	**7b**	94
3	4-MeO—Ph	**7c**	89
4	4-Br—Ph	**7d**	43
5	4-Cl—Ph	**7e**	48
6	4-CN—Ph	**7f**	<5
7	4-NO_2—Ph	**7g**	<5
8	$CH(Me)_2$	**7h**	71
9	$CH_2CH(Me)_2$	**7i**	65

To gain information about the mechanism of the overall tandem reaction, we carried out kinetic studies to identify the rate-determining step. Changing the catalyst concentration in the reaction between 3-methylbutyraldehyde (**8**), nitromethane, and dimethyl malonate revealed that the reaction is first order in nickel catalyst **2** (Figure 4.3), indicating that the Michael addition of dimethyl malonate to the nitroalkene is the rate-determining step.

The kinetic data shown in Figure 4.3 reveal that the rate of the tandem reaction depends on the concentration of nickel catalyst **2**. It is therefore instructive to determine whether the rate-determining step is at all retarded by the interaction between the two catalysts.

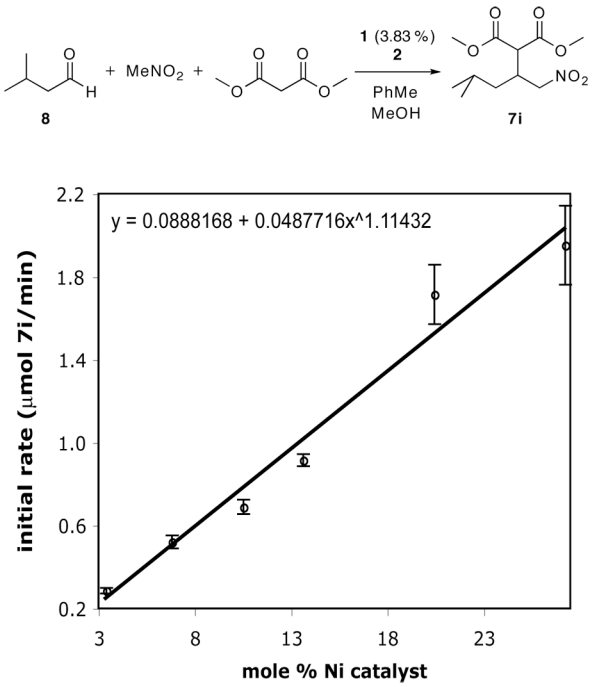

Figure 4.3. Kinetic studies on the tandem reaction of 3-methylbutyraldehyde, nitromethane, and dimethyl malonate.

We began our investigation by comparing the rates of the Michael addition in the absence and presence of the microencapsulated catalyst. One complicating factor, however, is that the catalytic amines within the μcaps irreversibly react with nitroalkenes, decreasing the amount of starting material available for reaction. Using the Michael addition between trans-β-nitrostyrene (**5**) and dimethyl malonate as a model, we approached this problem in two ways. The first approach was to "normalize" the data from the μcap-containing reaction in order to account for the loss of starting material (Figure 4.4a). Product yields were calculated using the formula (mol of **7a**)/(mol of **5** + mol of **7a**). It should be noted that these calculations correct only for decreased product formation due to nitroalkene-μcap interaction; any product suppression due to catalyst interaction should still be apparent. Both reactions attain an adjusted yield of 90% after 10 h, indicating that the presence of the μcaps does not

depress the rate of the Michael addition. Indeed, they instead appear to provide rate enhancement as the μcap-containing reaction reached its final yield after only 4 h.

To demonstrate that the apparent rate enhancement is not merely an artifact of data correction, we acylated the reactive amines in order to prevent their reaction with **5**. The data shown in Figure 4.4b confirms the rate enhancement in the presence of microcapsules. Our initial explanation of these results is based on previous studies reporting the acceleration of Michael additions by ureas and thioureas.[20] Since the capsule walls are composed of polyurea, we suggested that this was the reason that we observe the same phenomenon in our system, and proposed the transition state for the tandem reaction in Figure 4.5. Later, however, we determined that the urea groups are not responsible for the observed rate enhancement. This work will be discussed in Chapter 5. Upon further investigation into this rate enhancement, the reaction proved to be first order in the concentration of acylated microcapsules (Figure 4.6). This finding indicates that the presence of the μcaps accelerates the Michael addition and ultimately the overall one-pot reaction. In addition, this rate enhancement does not appear to be accompanied by any degradation in yield, suggesting that the interaction of the two catalysts is not detrimental.

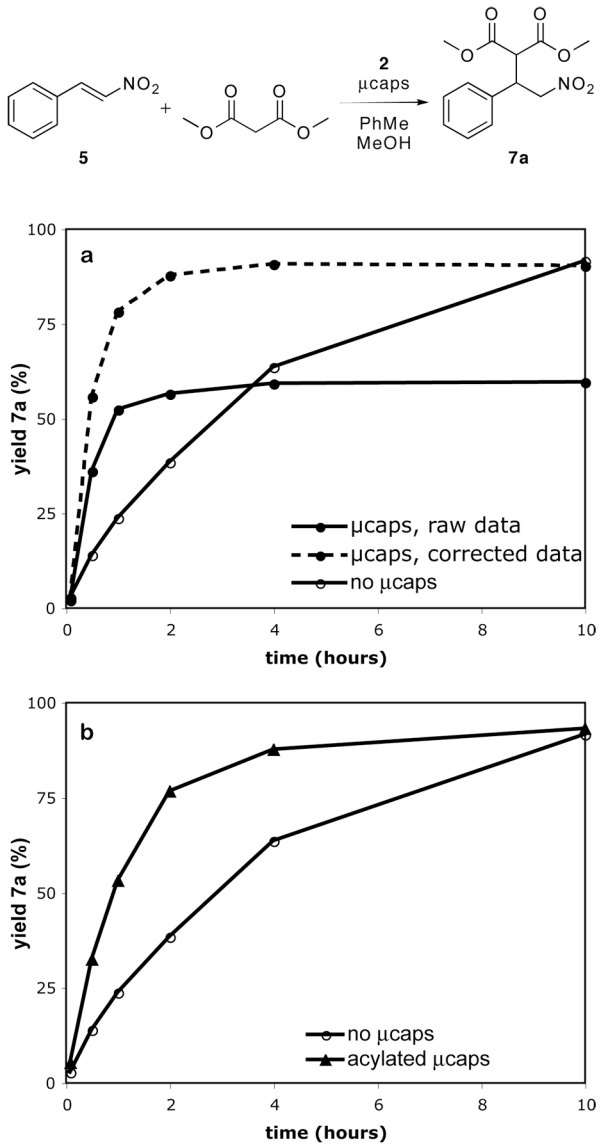

Figure 4.4. µcap-accelerated Michael addition between benzaldehyde (**4**) and dimethyl malonate in the presence of untreated µcaps (a) and in the presence of acylated µcaps (b).

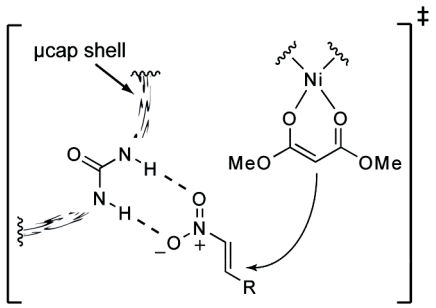

Figure 4.5. Proposed transition state for the tandem reaction.

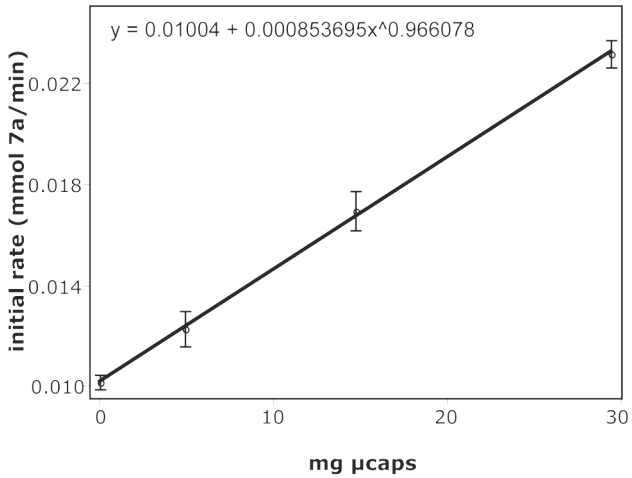

Figure 4.6. Order plot for the Michael addition between benzaldehyde (**4**) and dimethyl malonate in the presence of acylated µcaps. Rate is plotted as a function of nickel catalyst **2**.

Enantioselective Synthesis of Pregabalin. An attractive feature of our two-step one-pot reaction is that it not only incorporates an innovative technique for site-isolation but also produces synthetically useful products when an enantioselective version of **2** is used. The Michael adducts that are created are precursors to γ-amino acids, allowing access to γ-amino butyric acid (GABA) analogs. Pregabalin is one such analog that is approved for the treatment of both epilepsy and neuropathic pain. We imagined a synthesis of pregabalin where our two-catalyst system forms the pregabalin backbone efficiently and enantioselectively. The desirability of performing these reactions in tandem rather than sequentially is evident when one considers the difficulty of isolating of the nitroalkene intermediate. An efficient nitroalkene-forming reaction between 3-methylbutyraldehyde (**8**) and nitromethane has only been reported once[21] and in our hands often yields a significant amount of byproducts. However, we demonstrated that with our one-pot reaction there is no need for nitroalkene isolation and the byproducts are avoided.

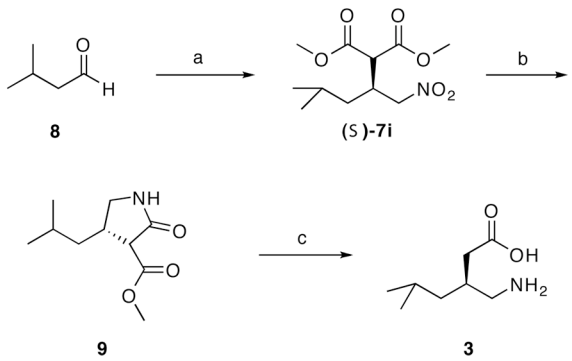

Scheme 4.5. Synthesis of pregabalin (**3**). Reagents and conditions: (a) nitromethane, dimethyl malonate, **1**, **2**, toluene, methanol, room temperature, 48 h, 94%, 72% ee. (b) Raney Ni, H_2 (45 psi), EtOH, room temperature, 18 h, 96%. (c) 5 M HCl, 115 °C, 18 h, 95%, 72% ee.

The total synthesis of pregabalin is depicted in Scheme 4.5. Using 3-methylbutyraldehyde (**8**) as the starting material and an enantioselective version of nickel catalyst **2**, the tandem reaction produced the corresponding Michael adduct (S)-**7i** in 94% yield and 72% ee. It should be noted that this tandem catalysis system efficiently suppressed the yield of the undesired dinitro byproduct to less than 5%. Overnight hydrogenation of (S)-**7i** with Raney Ni gave nearly quantitative conversion to the ring-closed product **9**. Subsequent acid hydrolysis and decarboxylation proceeded in 95% yield of the HCl salt of pregabalin (**3**), which retains an ee of 72%. It has been reported that enantiomeric enrichment of pregabalin can be achieved by recrystallization for cases in which the ee is at least 85% of the *S*-enantiomer.[22] Treatment of the 72% ee HCl salt with base followed by a single recrystallization from isopropyl alchol/water afforded a product with 91.5% ee. Our successful enrichment demonstrates the viability of obtaining an enantiomerically pure product without the need for a resolution step, which would bring the overall yield of this synthesis to 74% of enantiomerically pure material.

Conclusion

We developed and evaluated a two-step reaction that is capable of converting both aromatic and aliphatic aldehydes to their corresponding Michael adducts in a single reaction vessel. The two-catalyst system was made possible by microencapsulation of PEI in order to two otherwise incompatible catalysts compatible. Kinetic studies indicated that the presence of the microcapsule shell of catalyst **1** enhanced the rate of the reaction promoted by catalyst **2**. Therefore, the microcapsules not only make the reaction possible by imparting compatibility, but they also serve a second function by enhancing the rate-determining step. Using this tandem reaction we achieved a three-step total synthesis of pregabalin in 74% overall yield, demonstrating the applicability of this system to creating synthetically interesting compounds. By obtaining a better understanding of this complex multicomponent system, we continue to make progress toward the development of similar tandem reactions.

Afterword

This work provided us with much information about our multicatalyst system. For example, we noticed interesting phase separation behavior upon swelling the capsules in multiple solvents, and Muris Kobašlija went on to explore this phenomenon in more detail. However, as chemistry always does, our results led to even more questions, such as the origin of the rate enhancement of the Michael addition. We sought to explain this observation, and the results are discussed in Chapter 5.

Experimental Section

General Considerations

Celite 545 (Acros), 4-cyanobenzaldehyde (Acros, 98%), isobutyraldehyde (Acros, 99+%), isovaleraldehyde (Acros, 98%), 4-nitrobenzaldehyde (Acros, 99%), *p*-tolualdehyde (Acros, 99+%), trifluoroacetic anhyhdride (Acros, 99+%), valeraldehyde (Acros, 98%), (±)-*trans*-1,2-diaminocyclohexane (Aldrich, 98%), mesitylene (Aldrich, 98%), *trans*-β-nitrostyrene (Aldrich, 99%), polyisobutylene (Aldrich, MW 400, 000), Raney Ni (Aldrich, pH 10, 50% solution in water), tolylene 2,4-diisocyanate (Aldrich, technical grade, 80%), (1*S*,2*S*)-(+)-1,2-diaminocyclohexane (Alfa Aesar, 98%), chloroform (J. T. Baker), hydrochloric acid (J. T. Baker, 36.5-38%), nitromethane (J. T. Baker, 99%), acetic anhydride (Mallinckrodt), cyclohexane (Mallinckrodt), methanol (Mallinckrodt), toluene (Mallinckrodt), ethanol (Pharmaco-AAPER, 200 proof), branched poly(ethyleneimine) (Polysciences, Inc., 10,000 MW), *p*-anisaldehyde (Sigma), and Span 85 (Sigma) were used as received. Dimethyl malonate (Acros, 97%) and benzaldehyde (Aldrich, 99.5%) were washed with saturated $NaHCO_3$, distilled, and dried over Na_2SO_4 prior to use. 4-Bromobenzaldehyde (Aldrich, 99%) and 4-chlorobenzaldehyde (Aldrich, 97%) were recrystallized from 95% EtOH prior to use. Reactions were rocked on a Thermolyne Speci-Mix test tube rocker. Hydrogenations were performed in a PARR hydrogenation apparatus 3911EA. For ^{19}F elemental analysis, μcaps acylated with trifluoroacetic anhydride were sent to Robertson Microlit Laboratories for analysis (www.robertson-microlit.com). For ^{16}O elemental analysis, μcaps were sent to Elemental Analysis, Inc. for analysis (elementalanalysis.com). Gas chromatographic (GC) analyses were performed using a Varian CP-3800 GC equipped with a Varian CP-8400 autosampler, a flame ionization detector (FID) and a Varian CP-Sil 5CB column (length = 15 m, inner diameter = 0.25 mm, and film thickness = 0.25 μm. The

temperature program for GC analysis held the temperature constant at 80 ºC, heated samples from 80 to 200 ºC at 17 ºC/min, and held at 200 ºC for 2 min. Inlet and detector temperatures were set constant at 220 and 250 ºC, respectively. Mesitylene was used as an internal standard to calculate reaction conversion. High Performance Liquid Chromatography (HPLC) analyses were performed using a Hewlett-Packard Series II 1090 Liquid Chromatograph equipped with an autosampler HP 79846A, a solvent delivery system HP 79835A and a diode-array detector HP 79883A. ^{1}H NMR and ^{13}C NMR spectra were recorded on a Varian Inova-400 (400 MHz) spectrometer and are reported in ppm using solvent as an internal standard ($CDCl_3$ at 7.26 ppm). Data are reported as s = singlet, d = doublet, t = triplet, quin = quintet, m = multiplet. Optical microscopy images were obtained on an inverted Leica DMIL with a mounted Sony DSC-F717 digital camera and ebq100 UV source.

Synthesis of Microencapsulated Poly(ethyleneimine) Catalyst (1). The catalyst was prepared as described in the Experimental Section of Chapter 3.

Determination of Catalyst Loading. Primary amine loading for the microcapsule catalyst was determined via labeling with fluorine and a subsequent fluorine elemental analysis. To microcapsule catalyst (100 mg), loaded in a syringe equipped with a frit, methanol (5 mL) was added to swell them. After 5 minutes the excess methanol was removed and the solution containing trifluoroacetic anhydride (1 mL) in methanol (5 mL) was drawn into the syringe. The mixture was rocked at room temperature overnight. Fluorine labeled microcapsules were extensively washed with methanol, dried under stream of N_2 and sent for fluorine elemental analysis. To ensure that all the active sites were acylated, the microcapsules were checked for the activity in

nitroalkene formation. As expected for fully acylated microcapsules, showed no activity. Elemental analysis revealed a fluorine loading of 26.54 mass %.

$$\frac{0.2654 \text{ g F}}{1 \text{ g µcaps}} \bullet \frac{1 \text{ mol F}}{19 \text{ g F}} \bullet \frac{1 \text{ mol “N”}}{3 \text{ mol F}} \bullet \frac{1000 \text{ mmol “N”}}{1 \text{ mol “N”}} = 4.66 \text{ mmol “N”/g}$$

where “N” is any amine that is capable of being trifluoroacylated (1^o and 2^o amines). Since the primary, secondary, and tertiary amines of PEI statistically exist in a 1:2:1 ratio, the loading of 1^o amines in the microencapsulated catalyst is approximately 1.55 mmol/g.

The 1^o amine loading of 10,000 MW PEI was calculated based on the assumption that the primary, secondary, and tertiary amines exist in a 1:2:1 ratio, as stated by the vendor. The 1^o amine loading was calculated to be 5.81 mmol/g.

The urea loading of the microencapsulated catalyst was determined by oxygen elemental analysis after the µcaps were dried under vacuum. Results indicated that the oxygen loading was 9.03 mass %.

$$\frac{0.0903 \text{ g O}}{1 \text{ g µcaps}} \bullet \frac{1 \text{ mol O}}{16 \text{ g O}} \bullet \frac{1000 \text{ mmol O}}{1 \text{ mol O}} = 5.64 \text{ mmol O/g}$$

The oxygen content of the acylated µcaps (see Section *3.4*) was found to be 15.83 mass %.

$$\frac{0.1583 \text{ g O}}{1 \text{ g µcaps}} \bullet \frac{1 \text{ mol O}}{16 \text{ g O}} \bullet \frac{1000 \text{ mmol O}}{1 \text{ mol O}} = 9.89 \text{ mmol O/g}$$

Assuming that 5.64 mmol O/g is due to urea groups, there are 4.26 mmol O/g due to the acylation of 1^o and 2^o amines, consistent with the findings above.

Ni(II)–bis[(±)-*trans* -N,N'-Dibenzylcyclohexane-1,2-diamine]Br_2 (2). Prepared according to the method of Evans et al.[12] and as described in the Experimental Section of Chapter 3 using (±)-*trans*-1,2-diaminocyclohexane or (1*S*-2*S*)-(+)-diaminocyclohexane as the starting material.

General Procedure for µcap-Catalyzed Reaction Solvent Study. Either free PEI (7.9 mg, 4.6 mole % 1^oamines) or encapsulated PEI (**1**, 30 mg, 4.6 mole % 1^o amines) was placed in a 4 mL glass vessel. Solvent (1 mL) was added, and the vessel was sealed and allowed to stand at 297 K overnight. For the 1:3 ethanol:toluene mixture, the caps were swollen in 0.25 mL ethanol for 10 minutes before the addition of 0.75 mL toluene. Benzaldehyde (**4**, 101.6 µL, 1 mmol), nitromethane (0.54 mL, 10 mmol), and mesitylene (13.9 µL, 0.1 mmol) were added. The vessel was sealed and the reaction was rocked at 297 K on a rocker. Reaction conversion was monitored by withdrawing aliquots from the reaction at different time intervals, diluting with methylene chloride, and analyzing by GC with reference to mesitylene.

***trans*-β-Nitrostyrene (5)**. The title compound can be commercially obtained from Aldrich for comparison purposes. ^{1}H NMR (400 MHz, $CDCl_3$) δ 7.90 (d, J = 13.65 Hz, 1H), 7.53 (d, J = 13.65 Hz, 1H), 7.48-7.35 (m, 5H); ^{13}C NMR (400 MHz, $CDCl_3$) δ 139.1, 137.1, 132.2, 130.1, 129.4, 129.3.

1,3-dinitro-2-phenyl-propane (6). The title compound can be purified by column chromatography (20%EtOAc/hexanes) to give a brown oil. ^{1}H NMR (400 MHz, $CDCl_3$) δ 7.36-7.29 (m, 3H), 7.2-7.17 (m, 2H), 4.76-4.65 (m, 4H), 4.3-4.22 (quin, J = 7.21 Hz, 1H); ^{13}C NMR (400 MHz, $CDCl_3$) δ 134.5, 129.7, 129.2, 127.6, 76.9, 41.9.

General Procedure for Tandem Reaction. Microencapsulated PEI catalyst (**1**, 15 mg, 6.9 mol %) was swollen in 0.5 mL methanol in a 4 mL glass vessel before use. Nickel catalyst (**2**, 60 mg, 7.4 mol %), aldehyde (1 mmol), nitromethane (0.54 mL, 10 mmol), dimethyl malonate (114.3 μL, 1 mmol), and toluene (1 mL) were added to the vessel, which was sealed with a screw cap. The reaction was rocked at room temperature on a rocker for 24 hours. The volatile components were removed under reduced pressure and the crude product was purified by column chromatography.

Methyl-2-carbomethoxy-4-nitro-3-phenyl-butyrate (7a). The title compound can be purified by column chromatography (20% EtOAc/hexanes) to give a white solid. ^{1}H NMR (400 MHz, $CDCl_3$) δ 7.33-7.26 (m, 3H), 7.24-7.21 (m, 3H), 4.95-4.84 (m, 2H), 4.24 (dt, J = 5.1 Hz, 9.0 Hz, 1H), 3.86 (d, J = 9.16, 1H), 3.75 (s, 1H), 3.54 (s, 1H); ^{13}C NMR (400 MHz, $CDCl_3$) δ 168.1, 167.5, 136.4, 129.3, 128.7, 128.1, 77.6, 54.9, 53.3, 53.1, 43.2.

Methyl-2-carbomethoxy-4-nitro-3-(4-methylphenyl)butyrate (7b). The title compound can be purified by column chromatography (20% EtOAc/hexanes) to give a white solid. ^{1}HNMR (400 MHz, $CDCl_3$) δ 7.16-7.10 (m, 4H), 4.93-4.86 (dd, 2H), 4.24-4.18 (m, 1H), 3.87-3.84 (d, 1H), 3.79 (s, 3H), 3.60 (s, 3H), 2.33 (s, 3H); ^{13}CNMR (400 MHz, $CDCl_3$) δ 168.1, 167.5, 138.3, 133.2, 129.9, 127.9, 77.7, 55.0, 53.2, 53.2, 53.0, 42.8, 21.3.

Methyl-2-carbomethoxy-4-nitro-3-(4-methoxyphenyl)butyrate (7c). The title compound can be purified by column chromatography (20% EtOAc/hexanes) to give a white solid. ^{1}HNMR (400 MHz, $CDCl_3$) δ 7.18-7.15 (d, 2H), 6.83-6.80 (d, 2H), 4.90-4.83 (dd, 2H), 4.23-4.17 (m, 1H), 3.83-3.81 (d, 1H), 3.80 (s, 3H), 3.79 (s, 3H), 3.59 (s,

3H); ^{13}CNMR (400 MHz, $CDCl_3$) δ 168.1, 167.5, 159.7, 129.2, 128.1, 114.6, 77.9, 55.4, 55.1, 53.2, 53.1, 42.5, 12.1.

Methyl-2-carbomethoxy-4-nitro-3-(4-bromophenyl)butyrate (7d). The title compound can be purified by column chromatography (20% EtOAc/hexanes) to give a colorless oil. ^{1}HNMR (400 MHz, $CDCl_3$) δ 7.48-7.44 (d, 2H), 7.16-7.12 (d, 2H), 4.97-4.82 (m, 2H), 4.28-4.20 (dt, 1H), 3.86-3.82 (d, 1H), 3.78 (s, 3H), 3.60 (s, 3H); ^{13}CNMR (400 MHz, $CDCl_3$) δ 167.8, 167.2, 135.4, 132.4, 129.8, 122.7, 77.3, 54.6, 53.3, 53.2, 42.6.

Methyl-2-carbomethoxy-4-nitro-3-(4-chlorophenyl)butyrate (7e). The title compound can be purified by column chromatography (20% EtOAc/hexanes) to give a colorless oil. ^{1}HNMR (400 MHz, $CDCl_3$) δ 7.36-7.32 (d, 2H), 7.20-7.16 (d, 2H), 4.96-4.88 (m, 2H), 4.26-4.20 (m, 1H), 3.83-3.80 (d, 1H), 3.77 (s, 3H), 3.60 (s, 3H); ^{13}CNMR (400 MHz, $CDCl_3$) δ 167.8, 167.3, 134.9, 143.5, 129.6, 129.4, 77.4, 54.6, 53.3, 53.1, 42.5.

Methyl-2-carbomethoxy-3-(nitromethyl)-4-methylpentanoate (7h). The title compound can be purified by column chromatography (20% EtOAc/hexanes) to give a colorless oil. ^{1}HNMR (400 MHz, $CDCl_3$) δ 4.78-4.72 (dd, 1H), 4.62-4.57 (dd, 1h), 3.79 (s, 3H), 3.76 (s, 3H), 3.74-3.70 (d, 1H), 2.97-2.94 (m, 1H), 1.90-1.91(m, 1H), 0.98-0.94 (m, 6H); ^{13}CNMR (400 MHz, $CDCl_3$) δ 169.0, 168.8, 75.6, 53.2, 53.0, 51.5, 42.8, 29.8, 20.0, 19.4.

Methyl-2-carbomethoxy-3-(nitromethyl)-5-methylhexanoate (7i). The title compound can be purified by column chromatography (20% EtOAc/hexanes) to give a

colorless oil. ^{1}HNMR (400 MHz, $CDCl_3$) 4.70-4.63 (dd, 1H), 4.53-4.46 (dd, 1H), 3.77 (s, 3H), 3.76 (s, 3H), 3.63-3.61 (d, 1H), 2.98-2.92 (m, 1H), 1.67-1.61 (m, 1H), 1.31-1.26 (m, 2H), 0.91-0.87 (m, 6H); ^{13}CNMR (400 MHz, $CDCl_3$) δ 168.6, 168.4, 76.9, 53.1, 52.9, 52.5, 39.1, 35.1, 25.3, 22.6, 22.4.

Stepwise Synthesis of Pregabalin (3)

(*S*)-Methyl-2-carbomethoxy-3-(nitromethyl)-4-methylpentanoate (*S*-7i). Microencapsulated PEI catalyst (**1**, 250 mg, 11.5 mol %) was swollen in 5 mL methanol in a 50 mL glass vessel before use. *S*-Nickel catalyst (*S*-**2**, 550 mg, 6.8 mol %), 3-methylbutyraldehyde (**8**, 1.63 mL, 15 mmol), nitromethane (5.4 mL, 0.1 mol), dimethyl malonate (1.14 mL, 10 mmol), and toluene (25 mL) were added to the vessel, which was sealed with a screw cap. The reaction was rocked at room temperature on a rocker for 48 hours. The μcaps were filtered off by vacuum filtration. The volatile components were removed under reduced pressure and the product was purified by column chromatography (20% EtOAc/hexanes) to give 2.46 g (94%) of a colorless oil. Spectral data is given above. Enantiomeric excess was determined by HPLC with a Chiralcel OD-H column (94:6 hexanes:isopropanol, 1.0 mL/min 215 nm; minor enantiomer t_r = 6.5 min, major enantiomer t_r = 11.3 min; 72% ee.

Methyl 4-isobutyl-2-oxopyrrolidine-3-carboxylate (9). A solution of **(*S*)-7i** (1.05 g, 5.26 mmol) and 10 mL EtOH was added to a hydrogenation bottle containing Raney Ni (0.85 mg, water wet) at room temperature under N_2. The flask was evacuated and refilled with hydrogen three times and the reaction was shaken on a Parr hydrogenation apparatus at room temperature and 45 psi for 18 hours. Upon completion, the reaction mixture was filtered through Celite 545 and washed with

EtOH. The volatile components were removed under reduced pressure and the product was purified by column chromatography (4% MeOH/$CHCl_3$) to give 770 mg (96%) of a colorless oil that solidified upon standing. ^{1}HNMR (400 MHz, $CDCl_3$) δ 7.6 (s, 1H), 3.72 (s, 3H), 3.48-3.42 (t, 1H), 3.05-3.02 (d, 1H), 2.91-2.86 (m, 2H), 1.50-1.44 (m, 1H), 1.38-1.25 (m, 2H), 0.83-0.78 (m, 6H); ^{13}CNMR (400 MHz, $CDCl_3$) δ 174.0, 170.6, 55.0, 52.8, 47.1, 43.3, 37.5, 26.1, 22.7, 22.7.

(S)-3-Aminomethyl-5-methyl-hexanoic acid (Pregabalin) hydrochloride **(3)**. **9** (80 mg, 0.4 mmol) and 5M HCl_{aq} (3 mL) were heated at 125 °C for 18 hours. Upon cooling, the mixture was extracted with EtOAC (4 x 10 mL). The aqueous layer was stirred with activated charcoal at 70 °C and filtered through Celite. The volatile components were removed under reduced pressure to give 75 mg (95%) as a white solid. ^{1}HNMR (400 MHz, CD_3OD) δ 2.95-2.92 (d, 2H), 2.41-2.37-2.28 (d, 2H), 2.21-2.16 (m, 1H), 1.68-1.61 (m, 1H), 1.24-1.20 (t, 2H), 0.96-0.89 (dd, 6H); ^{13}CNMR (400 MHz, CD_3OD) δ 175.8, 44.5, 41.9, 37.1, 32.5, 26.1, 23.2, 22.4. For the purposes of analysis, the product was converted to the zwitterion by the addition of NaOH so that pH = 7.5-8.5 and then recrystallized from isopropanol/water. The amine was Boc-protected and the acid converted to the methyl amide as follows: Boc-protection was achieved by stirring the zwitterion in the presence of di-*tert*-butyl dicarbonate, and $NaHCO_3$ in a 1:1 mixture of THF:water.[23] Amide formation was achieved by treatment with methyl amine in the presence of *N*-methylmorpholine and isobutyl chloroformate in THF.[18] Enantiomeric excess was determined by HPLC with a Chiralcel OD-H column (95:5 hexanes:isopropanol, 0.7 mL/min, 215 nm); minor enantiomer t_r = 4.4 min, major enantiomer = 7.8 min; 91.5% ee.

Condensed Synthesis of Pregabalin (3)

(*S*)-Methyl-2-carbomethoxy-3-(nitromethyl)-4-methylpentanoate (*S*-7i). Microencapsulated PEI catalyst (**1**, 250 mg, 11.5 mol %) was swollen in 5 mL methanol in a 50 mL glass vessel before use. *S*-Nickel catalyst (*S*-**2**, 550 mg, 6.8 mol %), 3-methylbutyraldehyde (**8**, 1.63 mL, 15 mmol), nitromethane (5.4 mL, 0.1 mol), dimethyl malonate (1.14 mL, 10 mmol), and toluene (25 mL) were added to the vessel, which was sealed with a screw cap. The reaction was rocked at room temperature on a rocker for 48 hours. The μcaps were filtered off by vacuum filtration, 1 mL PEI was added to the filtrate, and the mixture was stirred until all of the nickel had been chelated, indicated by a color change from green to yellow. The mixture was filtered through celite, the volatile compounds were removed under reduced pressure, and the crude product was carried directly to the next step. The remainder of the synthesis was performed as described above to afford 1.68 g (85.7%) of (*S*)-3-aminomethyl-5-methyl-hexanoic acid (pregabalin) hydrochloride (**3**). Spectral data is given above.

Supporting Information

Experimental methods and kinetic studies are located in Appendix 2.

REFERENCES

1. Hall, N. *Science* **1994**, *266*, 32.

2. Tietze, L. F. *Chem. Rev.* **1996**, *96*, 115.

3. Wasilke, J.-C.; Obrey, S. J.; Baker, R. T.; Bazan, G. C. *Chem. Rev.* **2005**, *105*, 1001.

4. Cohen, B. J.; Kraus, M. J.; Patchornik, A. *J. Am. Chem. Soc.* **1981**, *103*, 7620.

5. Gelman, F.; Blum, J.; Avnir, D. *J. Am. Chem. Soc.* **2000**, *122*, 11999.

6. Gelman, F.; Blum, J.; Avnir, D. *Angew. Chem. Int. Ed.* **2001**, *40*, 3647.

7. Gelman, F.; Blum, J.; Avnir, D. *New J. Chem.* **2003**, *27*, 205.

8. Helms, B.; Guillaudeu, S. J.; Xie, Y.; McMurdo, M.; Hawker, C. J.; Fréchet, J. M. J. *Angew. Chem., Int. Ed.* **2005**, *44*, 3684.

9. Phan, N. T. S.; Gil, C. S.; Nguyen, J. V.; Zhang, Z. J.; Jones, C. W. *Angew. Chem., Int. Ed.* **2006**, *45*, 2209.

10. Motokura, K.; Fujita, N.; Mori, K.; Mizugaki, T.; Ebitani, K.; Kaneda, K. *J. Am. Chem. Soc.* **2005**, *127*, 9674.

11. Poe, S. L.; Kobašlija, M.; McQuade, D. T. *J. Am. Chem. Soc.* **2006**, *128*, 15586.

12. Evans, D. A.; Seidel, D. *J. Am. Chem. Soc.* **2005**, *127*, 9958.

13. For a detailed characterization of oil-in-oil microcapsules, see Kobašlija, M.; McQuade, D. T. *Macromolecules* **2006**, *39*, 6371.

14. We define catalytic amines as the primary amines of PEI.

15. See Supporting Information for full range of solvents.

16. Kobašlija, M.; Bogdan, A. R.; Poe, S. L.; McQuade, D. T. *J. Polym. Sci. Pol. Chem.* **2008**, *46*, 2309.

17. Tamura, R.; Sato, M.; Oda, D. *J. Org. Chem.* **1986**, *51*, 4368.

18. Demicheli, G.; Maggi, R.; Mazzacani, A.; Righi, P.; Sartori, G.; Bigi, F. *Tetrahedron Lett.* **2001**, *42*, 2401.

19. Santerre, G. M.; Hansrote, C. J.; Crowell, T. L. *J. Am. Chem. Soc.* **1958**, *80*, 1254.

20. Okino, T.; Hoashi, Y.; Furukawa, T.; Xu, X.; Takemoto, Y. *J. Am. Chem. Soc.* **2005**, *127*, 119.

21. Kantam, M. L.; Sreekanth, P. *Catal. Lett.* **1999**, *57*, 227.

22. Bao, J.; Beylin, V. G.; Greene, D.; Hoge, G. S.; Kissel, W.; Marlatt, M. E.; Pflum, D. A.; Wu, H.-P. U.S. Patent Application 2005/0228190 A1, **2005**.

23. Shendage, D. M.; Fröhlich, R.; Haufe, G. *Org. Lett.* **2004**, *6*, 3675.

Chapter 5

Exploration of Rate Enhancement in a Nickel-Catalyzed Michael Addition

Preface

The multicatalyst system discussed in Chapters 3 and 4 provided us with an unexpected result: the microencapsulated amine catalyst for the first step of the reaction provided rate enhancement for the second reaction as well. Though we initially attributed this phenomenon to the ureas in the microcapsule shell, we later discovered that it was, in fact, due to the amines. This chapter discusses our investigation of the observed rate enhancement and its impact on the selectivity of the reaction.

Abstract

The rate of the Michael addition between *trans*-β-nitrostyrene and dimethyl malonate was found to be enhanced in the presence of a polyurea-encapsulated polymeric amine. This rate enhancement was determined to be due to the encapsulated amine groups, and it was discovered that the amine and the nickel-based Michael addition catalyst form a catalyst complex. Kinetic models and experiments suggest that the complex is composed of a 2:1 amine-to-nickel ratio and that the reaction is half-order in complex. The effects of the amine on the selectivity of the Michael reaction is discussed.

Introduction

Chemists have long realized the advantage of using multiple catalysts in a single process.[1] Early examples are found predominantly in the field of polymer synthesis, most notably in reactions such as Ziegler-Natta chain transfer

polymerization.[2] Defined here as co-catalysis, these multicatalyst systems require the presence of a second species to activate or regenerate the catalytic species. The continued desire for more efficient and selective chemistry has led to the application of new types of multicatalyst systems to small molecule synthesis. Tandem catalysis, for example, involves the performance of two reactions in the same flask, each catalyzed by a different catalyst. Dual catalysis, on the other hand, involves the presence of a species that increases the rate of a single reaction, but unlike co-catalysis, the presence of the additive is not required for catalysis to proceed. The value of placing catalysts together is therefore multifold; this strategy can result in more reactions per vessel, as in tandem catalysis, or in single reactions with faster rates or more selective outcomes, as in dual or co-catalysis.

These early ideas are being extended to small molecule synthesis, where the use of a second species to activate either the catalyst or substrate has resulted in faster or more selective reactions. In a 1999 review, Shibasaki et al. outlined cases in which amines, *N*-oxides, alcohols, phosphine oxides, and ionic species enhanced the yields and enantioselectivities of transition metal-based reactions.[3] Miller et al. continued by demonstrating that a non-transition metal dual amine system effectively promoted asymmetric Baylis-Hillman reactions.[4] More recently, Yamamoto reviewed systems where dual Brønsted and Lewis acid catalysts are used to effectively promote new and faster reactions.[5] This growing field of work highlights the advantages of combining two catalysts in a single reaction and shows promise for the development of faster and more selective chemistry.

In Chapters 3 and 4, we discussed a multicatalyst system that enantioselectively forms a Michael adduct from an aldehyde, a nitroalkane, and a malonate ester (Scheme 5.1). The first step of this tandem reaction employs microencapsulated poly(ethyleneimine) (PEI) as a catalyst for nitroalkene formation,

while the second step involves a nickel-mediated Michael addition. Furthermore, we showed that in addition to catalyzing the first step, the microencapsulated catalyst enhanced the rate of the second step as well. Determining the origin of this rate enhancement, as well as understanding the interactions between the microencapsulated catalyst and the nickel catalyst, would be beneficial for designing other dual catalytic systems. In this work, we investigate the origin of rate enhancement and examine the kinetics of this dual catalysis in order to better understand our system.

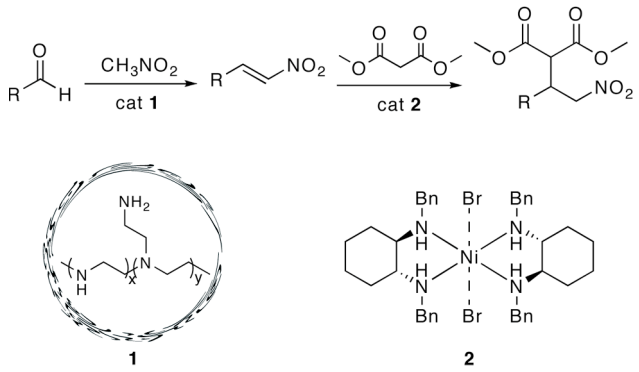

Scheme 1. Dual catalyst system catalyzed by an encapsulated amine (**1**) and a nickel-based catalyst (**2**).

Results and Discussion

In order to investigate the rate enhancement for the Michael addition discussed in Chapter 4, we examined a series of polymeric and small-molecule ureas. The polyurea shell of the microencapsulated catalyst **1** is represented in Figure 5.1. We looked at diphenyl urea (**4**) and ethyl phenyl urea (**5**) as simple urea analogs, as well as a polymeric urea (**6**) formed by the condensation of poly(methylene (polyphenyl) isocyanate) (PMPPI) and tetraethylenepentamine (TEPA). When tested in the Michael addition between *trans*-β-nitrostyrene and dimethyl malonate (DMM), however, no rate enhancement was observed in the presence of any of these ureas.

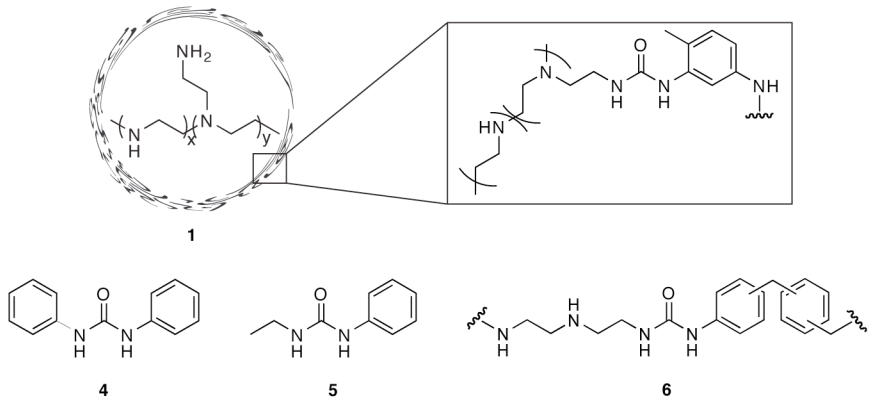

Figure 5.1. Small-molecule and polymeric ureas.

We then prepared more direct analogs of the polyurea shell of **1** in order to determine the origin of the observed rate enhancement. A polymeric version (**7**) was prepared by the condensation of free PEI with phenyl isocyanate, while a small molecule analog (**8**) was synthesized from *N,N*-dimethylethylenediamine and phenyl isocyanate (Figure 5.2). Both **7** and **8** increased the rate of the Michael addition, indicating that these analogs do contain the feature responsible for the rate enhancement observed in the presence of the microencapsulated catalyst.

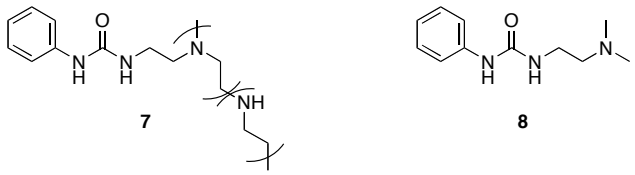

Figure 5.2. Small-molecule and polymeric analogs of the polyurea shell of **1**.

While precedent exists for the unique activity of bifunctional ureas,[6-9] we could not rule out the possibility that the observed rate enhancement is due to the amine alone. To isolate the effects of the amine and the urea, we investigated the amide versions of the urea analogs shown in Figure 5.2, as well as simple small molecule amines (Figure 5.3). The rate enhancement provided by each of these amines indicated, along with the observation that none of the ureas shown in Figure 5.1

affected the rate of the Michael indicated that the amine, not the urea, is responsible for the rate enhancement.

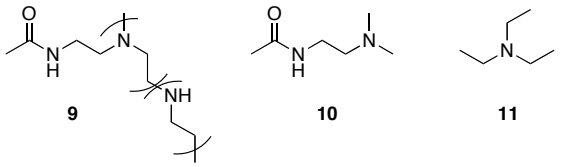

Figure 5.3. Small-molecule and polymeric amines.

Having determined that the increased rates provided by **1** were due to amines rather than ureas, we next sought to establish the specific origin of the rate enhancement, as both the microcapsule shell and the encapsulated PEI contain tertiary amines that may be capable of providing the observed rate enhancement. Because we showed in Chapter 3 that nickel catalyst **2** is able to function in the presence of PEI, it is possible that the rate enhancement is imparted by the encapsulated amines rather than the shell itself. An interesting observation is that although rate enhancement of the Michael addition is observed in the presence of swollen acylated μcaps (Figure 5.4), no enhancement is observed if the μcaps are not swollen. An explanation consistent with shell amine-enhancement is that the geometry of the crenated shell does not allow access to the amines of the capsule wall. However, an alternate explanation is that the reagents and catalyst for the Michael addition cannot access the encapsulated PEI if the capsules are not swollen. This is consistent with the observation that nitroalkene formation does not occur in the presence of unswollen μcaps because the catalytic amines are not accessible. Though both of these explanations are plausible, the absence of rate enhancement with amine-containing μcaps **6** suggests that the shell amines of both **6** and **1** may both be incapable of accelerating the reaction. Though further experiments are necessary to conclusively

demonstrate that the rate enhancement is due to the amines of the encapsulated PEI rather than the shell itself, preliminary evidence suggests that this is the case.

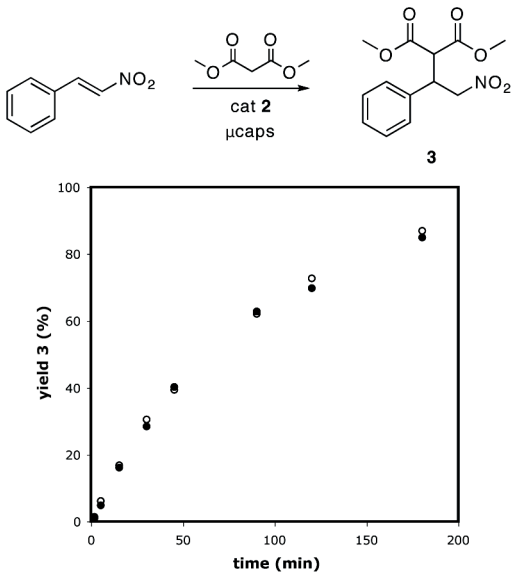

Figure 5.4. Michael addition in the presence (●) and absence (○) of unswollen acylated microcapsules.

Kinetic Studies. In order to gain more insight into the role of amine in the Michael addition, we carried out kinetic studies. Because much of this work was done before the discovery that the rate enhancement is due to the amine rather than the urea, the data here is presented here using bifunctional urea **8** but will be referred to as "amine **8**." For cases in which the experiments presented below were repeated using amine **11** in place of **8**, the results were consistent with each other, indicating that this substitution is valid. Instead of finding the reaction to be first order in both **8** and **2** as we expected from the data shown in Chapter 4, however, we found that the reaction was not first order in either. Instead, although at low concentrations of **8**, the reaction appeared to be first order in amine, the order plot loses linearity at higher concentrations (Figure 5.5).

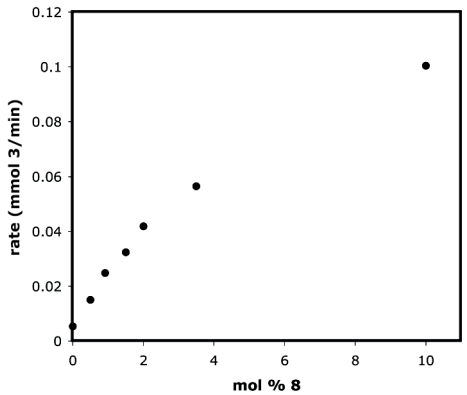

Figure 5.5. Order in amine **8**, 2% nickel catalyst **2**.

The order plot for nickel catalyst **2** produced unexpected results as well. With no amine present, the data indicated that the Michael addition was first order in **2**, which is consistent with previously reported results.[10] However, in the presence of amine **8**, the reaction was no longer first order in **2**. For a variety of concentrations of **8** (Figure 5.6 and Supporting Information), the order plots for **2** exhibited curvature. When fitted to a $y = mx^b$ plot, these plots did not produce consistent results for the order in **2**, making it unlikely that the reaction is half or other partial order in **2**.

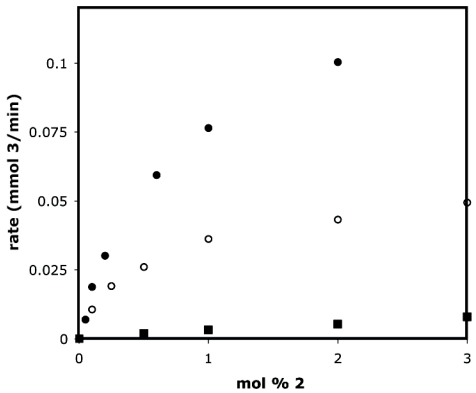

Figure 5.6. Order in nickel catalyst **2**, 10% (●), 3.5 % (○), and 0 % (■) amine **8**.

Unable to fit the data for either **8** or **2** to any particular order, we wondered if the two catalysts were not acting independently, but instead forming a complex that itself catalyzed the Michael addition. To address this possibility, we created a model

to see whether we could predict our experimental results theoretically. In creating the model, we made the following assumptions. The reaction can proceed *via* two different pathways: one catalyzed by the complex, and one catalyzed by nickel catalyst **2** (Eq. 5.1). Assigning the rate constants k_1 and k_2, respectively, the rate of formation of **3** can be written as

$$d[\mathbf{3}]/dt = k_1[\mathbf{2{\bullet}8}][NS][DMM] + k_2[\mathbf{2}][NS][DMM] \qquad \text{(Equation 5.1)}$$

where "**2•8**" refers to the complex, "NS" to *trans*-β-nitrostyrene, and "DMM" to dimethyl malonate. Because we are interested only in the initial rate of the reaction, the rate expression can be simplified to Equation 5.2.

$$d[\mathbf{3}]/dt = k_1[\mathbf{2{\bullet}8}] + k_2[\mathbf{2}] \qquad \text{(Equation 5.2)}$$

A second assumption is that the free catalysts **2** and **8** are in equilibrium with catalyst complex **2•8**. Assuming that **2** and **8** form the complex in a 1:1 ratio, the equilibrium expression can be written as follows.

$$K_{eq} = \frac{[\mathbf{2{\bullet}8}]}{[\mathbf{2}][\mathbf{8}]} \qquad \text{(Equation 5.3)}$$

At equilibrium,

$$K_{eq} = \frac{[x]}{[\mathbf{2}_o\text{-}x][\mathbf{8}_o\text{-}x]} \qquad \text{(Equation 5.4)}$$

where x represents the amount of complex **2•8** formed from **2** and **8**. Equation 5.4 can be solved in terms of x (see Supporting Information). By choosing appropriate values

for k_1, k_2, and K_{eq}, Equations 5.2 and 5.4 can be used to create order plots for the Michael addition.

In assigning the rate constants for the model, we assumed that $k_1 > k_2$ due to the rate enhancement that is observed in the presence of amine **8**. K_{eq}, on the other hand, was chosen arbitrarily, as we had no insight into where the equilibrium lay. Figure 5.7 shows the results of models for which $K_{eq} = 0.01$ (a and b) and $K_{eq} = 5$ (c and d). For both cases, $k_1 = 5$ and $k_2 = 0.1$. It is evident that only the first graph for order in amine (Figure 5.7a) produces data that is similar to the experimental results. However, since the corresponding order in nickel graph (Figure 5.7b) is not consistent with our observations, it is unlikely that the model is valid.

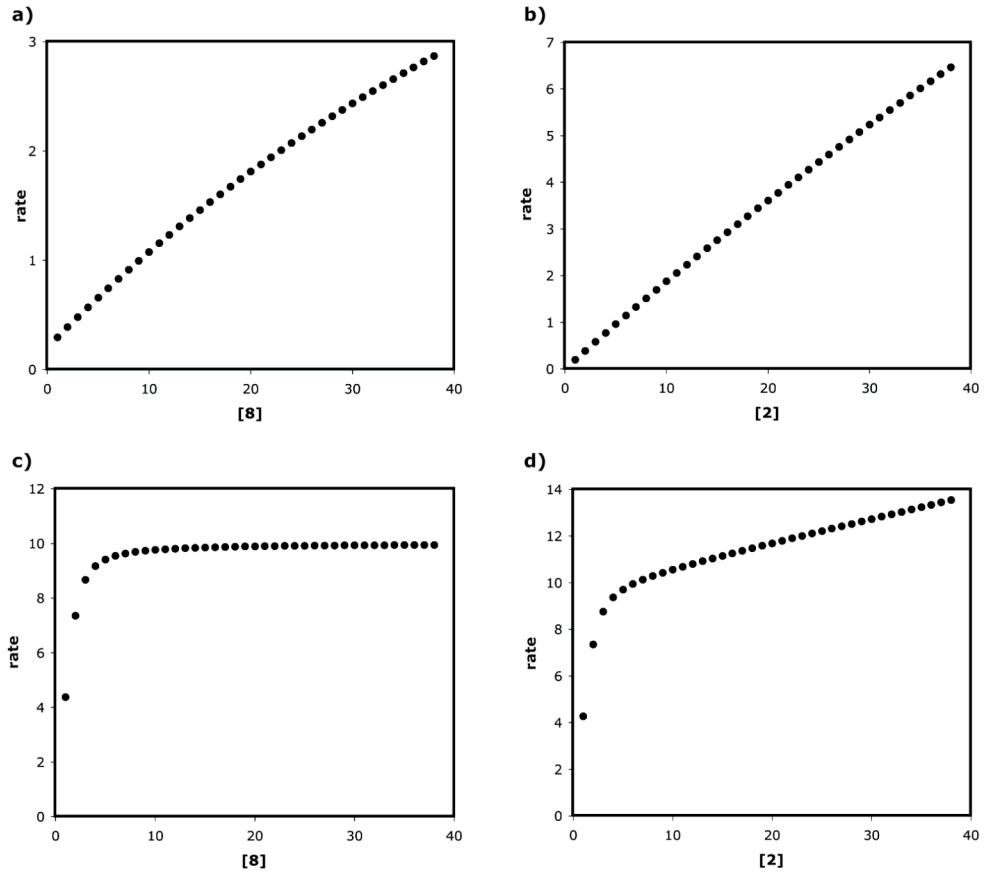

Figure 5.7. Order plots constructed from Equations 5.2 and 5.4, $k_1 = 5.0$, $k_2 = 0.1$. (a) order in amine, nickel = 3, $K_{eq} = 0.01$; (b) order in nickel, amine = 3.5, $K_{eq} = 0.01$; (c) order in amine, nickel = 3, $K_{eq} = 5.0$; (d) order in nickel, amine = 3.5, $K_{eq} = 5.0$.

The discrepancies between our experimental and theoretical results prompted us to reexamine the assumptions we made in our model. The most likely explanation for why our data did not fit our model is that we did not understand the nature of the catalyst complex, i.e., the ratio of nickel catalyst to amine was not 1:1. Faced with this possibility, we attempted to determine the stoichiometry of the complex in a number of ways. Co-crystallization of the nickel catalyst with amine **8** (or amine **11**) did not result in crystallization of the complex. In addition, ^{1}H NMR observation of the nickel and amine at various ratios were unhelpful, as they did not reveal any evidence of a catalyst complex. Unable to isolate and characterize the complex, we turned to the method of continuous variation to construct a Job plot. Often used to determine binding stoichiometry, the method of continuous variation monitors the change in a chosen response when the ratio of two interacting components are varied while keeping their total concentration constant.[11-12] The maximum on the response curve indicates the binding stoichiometry of the two components. We constructed a Job plot using nickel catalyst **2** and amine **8** in hopes that it would give us information about the stoichiometry of the catalyst complex. Keeping the total catalyst concentration constant at 2 mol %, we varied the ratio of **2**:**8** and monitored the rate of reaction. The Job plot shown in Figure 5.8 is representative of the results of experiments carried out over a range of total reaction concentrations (see Supporting Information), and it indicates that the ratio of amine-to-nickel catalyst is 2:1 rather than 1:1.

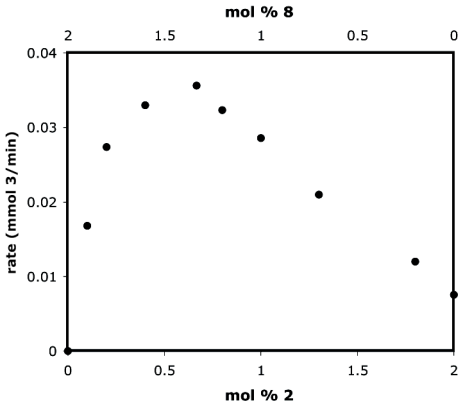

Figure 5.8. Job plot, 2% total catalyst concentration.

With more insight into the nature of the catalyst complex **2•8**, we revised our model as follows. Instead of assuming a 1:1 catalyst ratio, Equation 5.5 is the equilibrium expression for an amine-to-nickel ratio of 2:1.

$$K_{eq} = \frac{[\mathbf{2}\bullet\mathbf{8}]}{[\mathbf{2}][\mathbf{8}]^2} \qquad \text{(Equation 5.5)}$$

At equilibrium,

$$K_{eq} = \frac{[x]}{[\mathbf{2}_o\text{-}x][\mathbf{8}_o\text{-}2x]^2} \qquad \text{(Equation 5.6)}$$

which can again be solved for x (see Supporting Information).

When we used these modified equations in our rate model, we again found that the results did not correspond well with our experimental data (Figure 5.9). For this model, the amine and nickel appeared second order and first order, respectively. On the other hand, the experimental results resembled to first and partial order. These observations suggested that rather than being first order in complex, the reaction might be half-order in complex, with the corresponding rate expression shown in Equation 5.7.

$$d[\mathbf{3}]/dt = k_1[\mathbf{2}\bullet\mathbf{8}]^{0.5} + k_2[\mathbf{2}] \qquad \text{(Equation 5.7)}$$

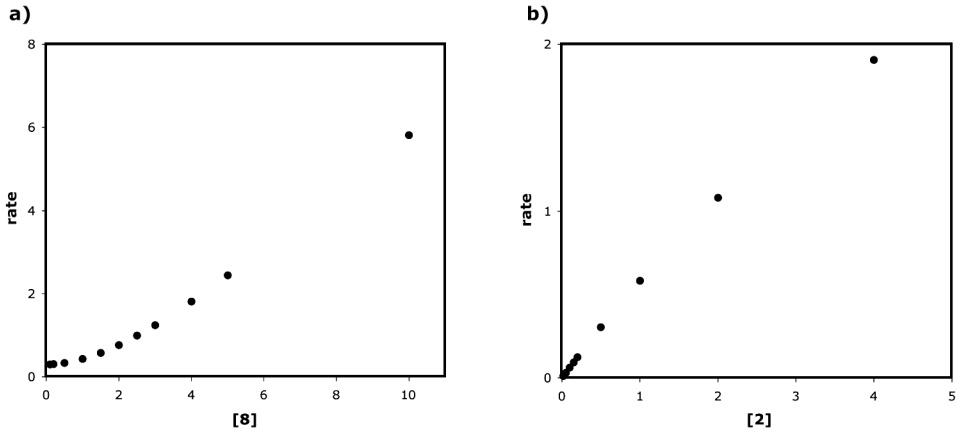

Figure 5.9. Order plots constructed from Equations 5.2 and 5.6, k_1 = 5.0, k_2 = 0.1, K_{eq} = 0.01. (a) order in amine, nickel = 3; (b) order in nickel, amine = 3.5. See Experimental Section for reaction conditions.

When the reaction was modeled as half order in catalyst complex, we found that the theoretical results that we obtained matched our experimental results quite well. The order plot for amine appears to be first order at low amine concentrations but lower order at high concentrations (Figure 5.10a), while the order plot for the nickel catalyst exhibits the same curvature that is seen in Figure 5.6 (Figure 5.10b). These results suggested that the data we obtained from our Job plots was valid, and that the catalyst complex consists of amine and nickel catalyst in a 2:1 ratio.

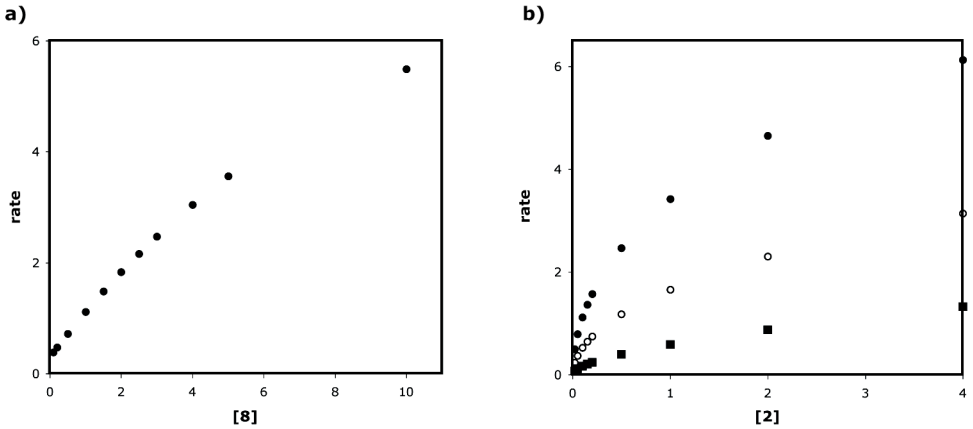

Figure 5.10. Order plots constructed from Equations 5.6 and 5.7, k_1 = 5.0, k_2 = 0.1, K_{eq} = 0.01. (a) Order in amine, nickel = 3; (b) order in nickel, amine = 10 (●), 3.5 (○), 1 (■).

To verify our model, experimentally, we constructed an order plot for the catalyst complex by varying the catalyst concentrations while keeping them in a 2:1 ratio. Although it is not possible to know the absolute amount of complex in solution without knowing the equilibrium constant, its concentration will vary in proportion to its individual constituents. Depending on the values of K_{eq}, and the relative values of k_1 and k_2, we expected to obtain an order in complex between 0.5 and 1.0, since the observed rate will be the result of the half-order complex-catalyzed pathway and the first order nickel-catalyzed pathway. Furthermore, the order in complex should be closer to 0.5 than 1.0, since the reaction is dominated by the complex-catalyzed pathway. Indeed, Figure 5.11 shows that the apparent order in complex is 0.59, consistent with our expected results.

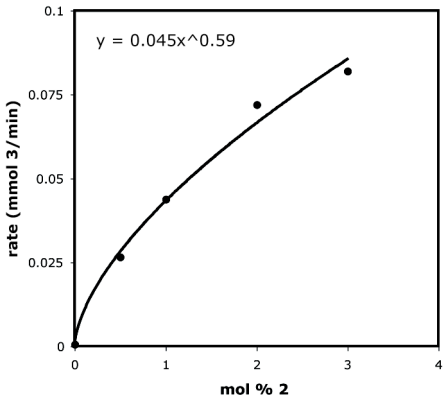

Figure 5.11. Michael addition order in catalyst complex, amine-to-nickel ratio of 2:1.

Our theoretical and experimental results indicate that the Michael addition is catalyzed by a 2:1 amine-to-nickel complex and that the reaction is half order in this complex. However, the physical meaning of these results is currently unknown. More experiments are necessary to determine why this reaction is half-order in complex, but the results discussed above provide us with preliminary evidence that is crucial to better understanding this dual catalyst system.

Selectivity Studies. With a better understanding of the interaction between the nickel catalyst and amine, we turned our focus toward the impact of the amine on the selectivity of the Michael addition. Since the catalyst complex is in equilibrium with its individual components, increasing the initial concentration of either one of the components would result in the increase in complex concentration. Since the nickel catalyst synthesis is relatively resource- and time-consuming, the ability to increase the rate of the reaction by the addition of an inexpensive, commercially available amine is appealing. However, we noticed that the enantioselectivity of the one-pot reaction in the synthesis of pregabalin was lower than the selectivity of the Michael addition reported by Evans et al.[10] and wondered how the selectivity changed in response to the presence of various amounts of amine. Figure 5.12 shows the ee of product **3** when the nickel catalyst loading was kept constant and the amine loading was varied. The closed open and closed circles represent nickel catalyst loadings of 0.5 and 2.0%, respectively, indicating that change in selectivity is a result of amine-to-nickel ratio rather than overall catalyst concentration. The addition of more amine results in a faster reaction due to in increased concentration of catalyst complex, but it also leads to reduced selectivity.

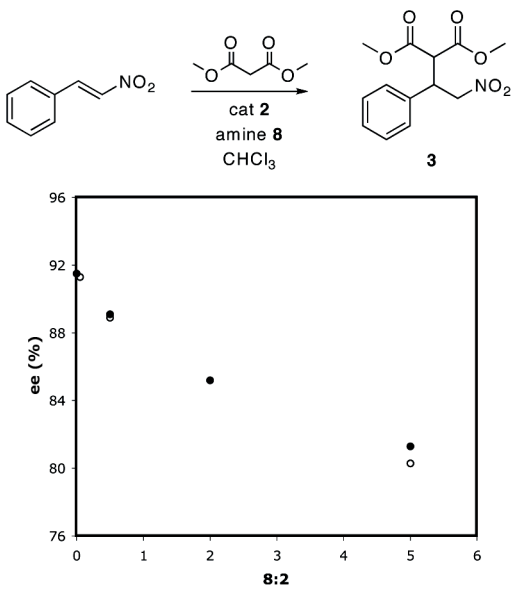

Figure 5.12. Selectivity of the Michael addition with various amine loadings at 0.5 mol % (●) and 2 mol % (○) nickel catalyst **2**.

In an attempt to recover the selectivity that is lost due to increased amine loadings, we performed the Michael addition at lower temperatures at a variety of amine-to-nickel ratios. Surprisingly, we found that for all cases in which the amine was present, when the temperatures were lowered, the selectivies decreased (Figure 5.13). On the other hand, when the reactions were performed at elevated temperatures, the selectivities initially increased before decreasing when the temperatures were increased further. This effect was observed in both chloroform and toluene, though the specific response to the change in temperature varied between the two solvents. This unexpected result may be due to a preferential increase of the rate of the nickel-catalyzed pathway over the complex-catalyzed pathway elevated temperatures, resulting in catalysis *via* the more selective route. This hypothesis could be verified by constructing an order plot for the nickel-catalyzed reaction at increased temperatures.

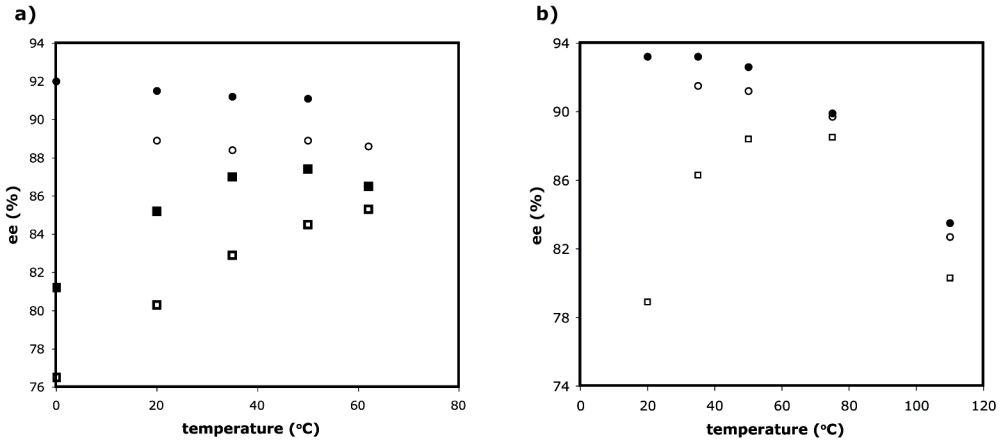

Figure 5.13. Selectivity of the Michael addition with 2 mol % **2** at various temperatures in chloroform (a) and toluene (b). **8**:**2** = 0 (●), 0.5 (○), 2.0 (■), 5.0 (□).

The increased selectivities at elevated temperatures in the presence of the amine suggested that we could perform the reaction at reduced catalyst loadings while still obtaining reasonable reaction rates. By raising the temperature, we expected to obtain higher rates and selectivities compared to room temperature in the presence of the amine. Indeed, the selectivites for the Michael addition performed at 50 ^{o}C with 0.2 mol % nickel catalyst **2** were virtually the same in the absence and presence of 0.1 mol % amine **11** (92.6% and 92.3%, respectively). However, at these low loadings, the rate enhancement imparted by the amine was minimal (Figure 5.14), exhibiting a k_{rel} of only 1.77 and reducing the reaction time by merely one hour. Although under these conditions, the amine does provide modest rate enhancement while maintaining good enantioselectivities, the effects of the amine additive are as not as beneficial as we initially thought.

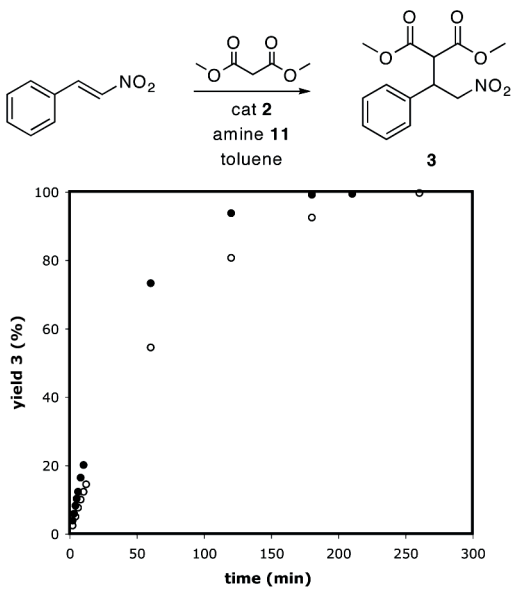

Figure 5.14. Michael addition at 50 ^{o}C, 0.2 mol % nickel catalyst loading, 0.1% (●) and 0% (○) amine **11**.

Conclusion

We have shown that the rate enhancement provided by our microencapsulated amine catalyst is due to the encapsulated amines rather than the polyurea shell. Kinetic studies suggested that rather than acting independently, the two catalysts form a complex in a 2:1 amine-to-nickel reaction. Furthermore, this dual-catalyst system behaves unexpectedly in response to temperature changes, providing increased selectivity at elevated temperatures. Although these results taken together showed promise for performing rapid Michael additions at reduced catalyst loadings, in practice, the low amine loadings required for high selectivities were not able to effect considerable rate enhancement. However, the discoveries that we made have provided us with a better understanding this dual-catalytic system, and will aid us as we continue to explore multicatalyst reaction.

Afterword

This work concludes a four-year project that began the day I joined the McQuade group and was asked to develop a multicatalyst system for the synthesis of pregabalin. Not surprisingly, this project, while resulting in a successful multicatalyst reaction, led us in unexpected directions, including the investigation of the phase behavior inside the microcapsules (Muris Kobašlija) as well as the work discussed in this chapter. It also prompted us to look at ureas as potential partners in multicatalyst systems. The results of this work are discussed in Chapter 6.

Experimental Section

General Considerations

All reagents were used without purification unless otherwise noted. Ethyl phenyl urea was recrystallized from ethyl acetate, *trans*-β-nitrosobenzene was recrystallized from ethanol, and dimethyl malonate was distilled under vacuum prior to use. Gas chromatographic (GC) analyses were performed using a Varian CP-3800 GC equipped with a Varian CP-8400 autosampler, a flame ionization detector (FID) and a Varian CP-Sil 5CB column (length = 15 m, inner diameter = 0.25 mm, and film thickness = 0.25 μm. The temperature program for GC analysis held the temperature constant at 80 ºC, heated samples from 80 to 200 ºC at 17 ºC/min, and held at 200 ºC for 2 min. Inlet and detector temperatures were set constant at 220 and 250 ºC, respectively. Mesitylene was used as an internal standard to calculate reaction conversion. Alternatively, GC analyses were performed using an Agilent 7890A GC equipped with an Agilent 7683B autosampler, a flame ionization detector (FID), and a J&W Scientific 19091J-413 column (length = 30 m, inner diameter = 320 μm, and film thickness = 250 μm). The temperature program for GC analysis held the temperature constant at 80 ^{o}C for 1 min, heated samples from 80 to 200 ^{o}C at 25

^{o}C/min and held at 200 ^{o}C for 1.5 min. Inlet and detector temperatures were set constant at 250 and 300 ^{o}C, respectively. ^{1}H NMR and ^{13}C NMR spectra were recorded on a Varian Inova-400 (400 MHz) spectrometer and are reported in ppm using solvent as an internal standard ($CDCl_3$ at 7.26 ppm). Data are reported as s = singlet, d = doublet, t = triplet, quin = quintet, m = multiplet. High performance liquid chromatography (HPLC) was performed using a Varian Pro Star chromatograph using a CHIRALPAK IA column (250 mm x 4.6 mm) and CHIRALPAK IA guard column (1 cm x 0.4 cm). All chromatograms were obtained using a wavelength of 254 nm.

Synthesis of Microencapsulated Poly(ethyleneimine) Catalyst (1). The catalyst was prepared as described in the Experimental Section of Chapter 3.

Synthesis of PMPPI caps (4). All compounds were deoxygenated prior to encapsulation. To a 250 mL Erlenmeyer flask was added an aqueous solution of poly(vinyl alcohol) (150 mL, 0.5% w/w in DI H_2O, M_w = 89,000-98,000, 99+% hydrolyzed). The organic phase, consisting of $CHCl_3$ (17 mL) and poly(methylene (polyphenyl) isocyanate) (3 mL, 1 equiv isocyanate, 30% incorporation) was dispersed in the aqueous phase using an IKA Ultra-Turrax T25 homogenizer at 6500 rpm for 2 min. The resulting emulsion was stirred gently. After stirring for 5 minutes, a second aqueous phase consisting of tetraethylenepentamine (100 μL, 0.17 equiv) in a solution of poly(vinyl alcohol) (20 mL) was added to the emulsion via syringe. The emulsion was allowed to stir gently overnight. The resulting microcapsules were isolated by centrifugation and washed with DI H_2O (2 x 200 mL), EtOH (2 x 200 mL), and Et_2O (1 x 100 mL). The microcapsules were dispersed in Et_2O (100 mL), transferred to a 250 mL round-bottom flask, concentrated by rotary evaporation, and dried under vacuum to yield a free-flowing powder.

Preparation of 5. PEI (MW = 10,000, 1 g, 5.81 mmol 1^o amines) was dissolved in $CHCl_3$ (10 mL). Phenyl isocyanate (0.63 mL, 5.81 mmol) was added at slowly, resulting in the formation of a white precipitate. The reaction was stirred for 15 min and the polymer was washed with $CHCl_3$ and dried under vacuum to provide the polymeric urea **5**.

1-(2-(dimethylamino)ethyl)-3-phenylurea (6). Phenyl isocyanate (1.08 mL, 10 mmol, 1 eq) was added dropwise to a solution of *N*,*N*-dimethylethylenediamine (1.1 mL,10 mmol, 1 eq) in $CHCl_3$ (10 mL) at room temperature and the reaction was stirred for 30 min. The solvent was removed *in vacuo* and the product was recrystallized from EtOAc to afford white crystals (1.8 g, 87%). ^{1}H NMR (300 MHz, $CDCl_3$) δ 7.35 (d, 2H), 7.22 (t, 2H), 6.97 (t, 1H), 6.36 (t, 1H), 3.30 (q, 2H), 2.42 (t, 2H), 2.12 (s, 3H); ^{13}C NMR (75 MHz, $CDCl_3$) δ 157.8, 139.9, 129.2, 122.7, 120.0, 60.1, 45.5, 38.7.

Preparation of 7. PEI (MW = 750,000, 50 wt% solution in water, 1.9 g, 5.52 mmol 1^o amines) was dissolved in MeOH (10 mL). The solution was cooled to -78 ^{o}C and acetyl chloride (0.78 mL, 11.0 mmol) was added dropwise. The reaction was removed from the cold bath and was stirred at room temperature for 16 h. The solvent was removed *in vacuo* and the acylated polymer was dialyzed against H_2O (pH = 11) for 8 h, and H_2O (pH = 7) (2 x 8 h). The solvent was removed *in vacuo* to provide the acylated polymer **7**.

***N*-(2-(dimethylamino)ethyl)ethanamide (8).** Acetyl chloride (1.4 mL, 20 mmol, 2 eq) was added dropwise to a solution of *N*,*N*-dimethylethylenediamine (1.1 mL,10

mmol, 1 eq) in $CHCl_3$ (5 mL) at -78 ^oC and the reaction was stirred for 2 h at -78 to 25 ^oC. The solvent was removed *in vacuo* and the product was chromatographed (silica gel, 96:4 $CHCl_3$:MeOH) to afford a light yellow oil (1.2 g, 92%). ^1H NMR (300 MHz, $CDCl_3$) δ 6.41 (br, 1H), 3.22 (m, 2H), 2.32 (t, 2H), 2.16 (s, 6H), 1.94 (s, 3H); ^{13}C NMR (75 MHz, $CDCl_3$) δ 170.3, 57.9, 45.1, 36.9, 32.2.

General procedure for determination of rate enhancement. To *trans*-β-nitrostyrene (149.2 mg, 1 mmol), nickel catalyst **2** (16.2 mg, 0.02 mmol), and mesitylene (13.9 μL, 0.1 mmol) in solvent (1 mL) was added the appropriate polymer, urea, or amine. Dimethyl malonate (137.1 μL, 1.2 mmol) was added and the reaction was stirred at room temperature. Reaction conversion was monitored by withdrawing aliquots from the reaction at different time intervals, diluting with methylene chloride, and analyzing by GC with reference to mesitylene. See Supporting Information for full conditions and results.

Acylation of encapsulated amines. To microcapsule catalyst **1** (100 mg), loaded in a syringe equipped with a frit, methanol (5 mL) was added to swell them. After 5 minutes the excess methanol was removed and the solution containing acetic anhydride (1 mL) in methanol (5 mL) was drawn into the syringe. The mixture was rocked at room temperature overnight. The acylated microcapsules were extensively washed with methanol and dried *in vacuo*.

Michael addition in the presence of acylated microcapsules. To *trans*-β-nitrostyrene (149.2 mg, 1 mmol), nickel catalyst **2** (16.2 mg, 0.02 mmol), acylated microcapsules (15 mg), and mesitylene (13.9 μL, 0.1 mmol) in toluene (1 mL) was added dimethyl malonate (137.1 μL, 1.2 mmol) and the reaction was stirred at room

temperature. Reaction conversion was monitored by withdrawing aliquots from the reaction at different time intervals, diluting with methylene chloride, and analyzing by GC with reference to mesitylene.

General procedure for kinetic studies. To *trans*-β-nitrostyrene (149.2 mg, 1 mmol), mesitylene (13.9 mL, 0.1 mmol), and the appropriate amounts of nickel catalyst **2** and amine **8** in chloroform was added dimethyl malonate (137.1 μL, 1.2 mmol) and the reaction was stirred at room temperature. Reaction conversion was monitored by withdrawing aliquots from the reaction at different time intervals, diluting with methylene chloride, and analyzing by GC with reference to mesitylene. See Supporting Information for full conditions and results.

Supporting Information

Experimental details, kinetic studies, and rate models are located in Appendix 3.

REFERENCES

1. Wasilke, J.-C.; Obrey, S. J.; Baker, R. T.; Bazan, G. C. *Chem. Rev.* **2005**, *105*, 1001.

2. Corradini, P.; Guerra, G.; Cavallo, L. *Acc. Chem. Res.* **2004**, *37*, 231.

3. Vogl, E. M.; Groeger, H.; Shibasaki, M. *Angew. Chem. Int. Ed.* **1999**, *38*, 1570.

4. Aroyan, C. E.; Vasbinder, M. M.; Miller, S. J. *Org. Lett.* **2005**, *7*, 3849.

5. Yamamoto, H.; Futatsugi, K. *Angew. Chem. Int. Ed.* **2005**, *44*, 1924.

6. Taylor, M. S.; Jacobsen, E. N. *Angew. Chem. Int. Ed.* **2006**, *45*, 1520.

7. Connon, S. J. *Chem. Eur. J.* **2006**, *12*, 5418.

8. Schreiner, P. R.; Wittkop, A. *Org. Lett.* **2002**, *4*, 217.

9. Okino, T.; Hoashi, Y.; Furukawa, T.; Xu, X.; Takemoto, Y. *J. Am. Chem. Soc.* **2005**, *127*, 119.

10. Evans, D. A.; Seidel, D. *J. Am. Chem. Soc.* **2005**, *127*, 9958.

11. Huang, C. Y.; *Method Enzymol.* **1982**, *87*, 509.

12. Huang, C. Y.; Zhou, R.; Yang, D. C. H.; Chock, P. B. *Biophys. Chem.* **2003**, *100*, 143.

Chapter 6

Using Bifunctional Ureas to Increase the Rate of Proline-Catalyzed α-Aminoxylations

Preface

Before we discovered the rate enhancement for the Michael addition was provided by the amine and not the urea, my adviser asked me to find a proline-catalyzed reaction that would potentially benefit from electrophile activation. In the last few days before packing up the lab and moving it to Tallahassee, I stumbled across the α-aminoxylation of aldehydes, as it was one of the few proline-catalyzed reactions for which we had all of the reagents on hand. Rate enhancement was indeed observed in the presence of our bifunctional urea, and further investigation upon arriving at Florida State University led to even more unexpected results.

Abstract[*]

The rate of the proline-catalyzed α-aminoxylation of aldehydes is significantly increased in the presence of a bifunctional urea. Structure-activity relationship data indicates that both an amine and urea are crucial for rate enhancement. The evidence presented herein suggests that this rate enhancement originates from hydrogen bonding interaction between the bifunctional urea and an oxazolidinone intermediate to increase the rate of enamine formation. Proline derivatives that are incapable of forming oxazolidinones exhibit no rate enhancement in the presence of the bifunctional urea. The rate enhancement is general for a variety of aldehydes, and the faster reactions do not reduce yields or selectivities.

---

[*] Reproduced with permission from: Poe, S. L.; Bogdan, A. R.; Mason, B. P.; Steinbacher, J. L.; Opalka, S. M.; McQuade, D. T. *J. Org. Chem.* **2008**, *submitted*.

Introduction

The field of organocatalysis is comprised of many catalyst classes that enable an expanding range of selective transformations.[1-3] Though amine-based catalysts were some of the first organocatalysts to be explored, interest in them remains strong because they offer enamine, iminium ion, and SOMO mechanisms that provide a wide range of highly enantioselective reactions.[4,5] Proline alone, one of the most widely-used organocatalysts, catalyzes transformations ranging from aldol condensations and Mannich reactions to Diels-Alder reactions, and many proline derivatives are also effective catalysts.[6-9] Though proline catalysis is quite versatile, limitations exist, including the need for high catalyst loadings and excess reagents, slow reaction rates, complex reaction kinetic profiles, and the use of unfavorable solvents.[10,11] These obstacles limit the application of proline-based catalysis, and a new strategy is required to exploit its full potential in both academic and industrial settings.

In the past five years, the proline-catalyzed α-aminoxylation of aldehydes and ketones with nitrosobenzene has received attention because it provides an effective route to α-hydroxy carbonyl species.[12-18] Initially reported in 2003 by the groups of both Zhong and MacMillan, this reaction was believed to proceed through a mechanism consistent with standard enamine catalysis, involving the formation of an enamine in a pre-equilibrium step followed by reaction with nitrosobenzene. However, subsequent work has revealed that α-aminoxylation exhibits unusual kinetic behavior that is not observed in typical proline catalysis. Detailed studies by Blackmond and coworkers have shown that this reaction displays autoinduction that cannot be attributed to simple proline dissolution.[19-23] Instead, they propose a model in which a product-proline complex is formed and converted directly to the enamine, allowing for a faster pathway that circumvents free proline. In addition, independent work by Seebach et al. has addressed the oxazolidinone species that have been

observed in proline-catalyzed reactions, and has shown evidence for their role as productive intermediates in enamine formation.[24] Taking this into account, we provide a modified version of the catalytic cycle put forth by Blackmond, which is proposed to proceed via rate-limiting enamine formation before entering a faster catalytic cycle in which exchange between the product-proline complex **D** and the enamine **B** becomes rate determining (Scheme 6.1).[22,23]

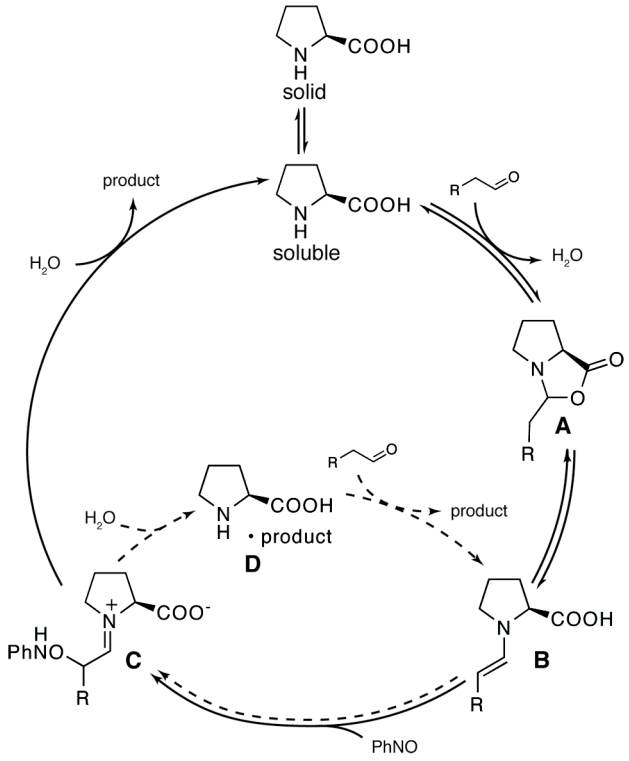

Scheme 6.1. A Blackmond et al.-inspired catalytic cycle for the α-aminoxylation of aldehydes. Observed autoinduction is justified by the emergence of an alternate pathway (dashed lines) that is mediated by the product-proline complex **D**.

Although the α-aminoxylation of aldehydes is much more rapid than other proline-catalyzed reactions, it does suffer from drawbacks such as byproduct formation and generally high catalyst loadings.[10,11] Accelerating the rate-limiting enamine formation would result in a faster overall reaction and potentially mitigate or eliminate such problems. Furthermore, the reported optimal solvents for the α-

aminoxylation of aldehydes are chloroform and DMSO, which are environmentally unfavorable. A faster reaction would enable the use of greener solvents that might otherwise provide a slow or unproductive reaction. In addition, perturbation of any of the steps along this complex reaction pathway may help to elucidate some of its mechanistic features. Inspired by the recent work that has successfully used additives such as amines, water, and diols to improve the proline-catalyzed aldol reaction,[25] we sought to identify an additive that could provide similar enhancements for the α-aminoxylation. If successful, it is possible that the rate enhancement might be extended to other proline-catalyzed reactions as well. We initially explored the use of bifunctional ureas in the α-aminoxylation of aldehydes due to the wide body of recent work suggesting that ureas activate carbonyl species by lowering the LUMO of the electrophile.[26-29] In addition to the potential for activating the aldehyde toward attack by proline, it has been shown that ureas with tethered Lewis bases can aid deprotonation, which would further enhance the formation of the activated enamine species.[30-32] Herein, we demonstrate that a bifunctional urea significantly increases the rate of α-aminoxylation while maintaining high yields and enantioselectivities, and we discuss the origin of the observed rate enhancement.

Results and Discussion

Rate Enhancement and Structure-Activity Relationship Study.

Bifunctional urea **1** was prepared from phenyl isocyanate and *N,N*-dimethylethylenediamine to obtain a compound consisting of both a urea and a tertiary amine. We examined the α-aminoxylation of hexanal in chloroform, shown by MacMillan[12] to produce high yields and enantioselectivities, as well as in ethyl acetate, a solvent that is more environmentally benign but that has not yet been shown to be a suitable solvent for this reaction.[33] As seen in Table 6.1 (entries 1, 3 and 4, 6),

the presence of urea **1** significantly increases the rate of α-aminoxylation in both solvents. The effect of **1** is especially pronounced when the reaction is performed in ethyl acetate; though product **5a** was undetectable after 40 minutes for the proline-only case, the presence of urea **1** results in a yield of over 80% in the same amount of time. The acceleration that we observe for both solvents suggests that **1** enhances the rate-determining enamine formation.

To investigate the origin of the observed rate enhancement, we performed a structure-activity relationship study with a series of ureas, amines, and amides (Figure 6.1). When examined individually, each of these functional groups provided only modest rate enhancement (Table 6.1, entries 7-9). Furthermore, the combination 1-ethyl-3-phenylurea (**2**) and *N,N*-dimethylethylamine (**3**, Table 6.1, entry 10) does not reproduce the rate enhancement that is observed with **1**, strongly suggesting that the proximity of the urea and amine is significant. Interestingly, although thioureas have been shown to be more effective hydrogen bond donors than their urea counterparts,[34] the thiourea analog of **1** resulted in a slightly slower reaction than **1** (see Supporting Information).

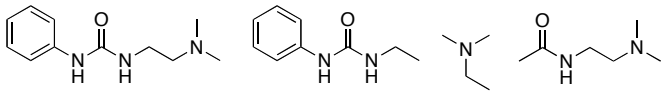

Figure 6.1. Additives used in the α-aminoxylation of hexanal.

Table 6.1. α-Aminoxylation of hexanal with nitrosobenzene in the presence of various additives.

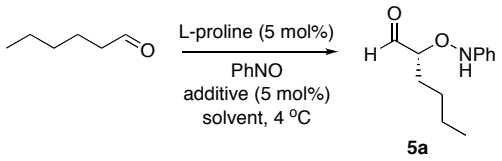

5a

Entry	Additive	Solvent	Time (min)	Yield **5a** (%)[a]	ee (%)
1	no additive	$CHCl_3$	5	5	99
2	**1**, no proline	$CHCl_3$	5	NR	-
3	**1**	$CHCl_3$	5	96	99
4	no additive	EtOAc	40	<1	98
5	**1**, no proline	EtOAc	40	NR	-
6	**1**	EtOAc	40	81	98
7	**2**	EtOAc	40	3	98
8	**3**	EtOAc	40	2	>99
9	**4**	EtOAc	40	2	>99
10	**2** + **3**	EtOAc	40	7	>99

[a]Yields based on calibrated GC data.

Scope. To show that the rate enhancement provided by bifunctional urea **1** does not come at the cost of degraded yields and enantioselectivities, we performed the α-aminoxylation on a range of aldehydes in ethyl acetate (Table 6.2).[35] The excellent to moderate yields and excellent enantioselectivities that were obtained with the proline-urea system are similar to those observed by others using proline only. Because the presence of urea increases the rate but does not alter yields or selectivities of this reaction, we suggest that it serves only to facilitate enamine formation and does not impact the selectivity-determining step. If the urea did influence the selectivity-determining step we would expect changes in the enantioselectivity and alterations in *O*- and *N*-selectivity.

Table 6.2. α-Aminoxylation of aldehydes with nitrosobenzene.

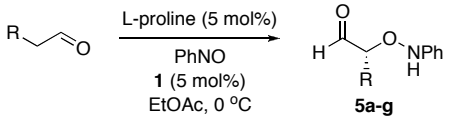

Entry	R	Product	Time (h)	Yield[a] (%)	ee (%)
1	nBu	**5a**	2	96	99
2	Me	**5b**	3	90	98
3	iPr	**5c**	3.5	97	99
4	nhex	**5d**	5	84	99
5	CH_2Ph	**5e**	3.5	84	>99
6	Ph	**5f**	2	55	99
7	$CH_2CH{=}CH_2$	**5g**	2.5	75	99

[a]Due to the instability of the aldehyde, *O*-addition products were reduced to their corresponding 2-aminoxy alcohols prior to isolation.

Catalyst Loading. The increased reaction rates we observed with urea **1** prompted us to investigate the potential for decreased catalyst loadings. The solubility of proline in many organic solvents is low, and the conditions at the beginning of the reaction are saturating in proline. However, the α-aminoxylation reaction becomes homogeneous as the reaction proceeds, indicating that proline becomes soluble as the reaction progresses.[36] We looked at catalyst loadings of 0.5, 1.0, and 2.5 mol %, where [proline] = [urea], and compared the results with the proline-only controls. As expected, the rates of both the proline-only and proline-urea cases changed in response to changes in catalyst loading (Figure 6.2). In addition, all cases displayed significant rate enhancement when the urea was present, with the 2.5% and 1% catalyst loadings resulting in yields of 97% and 91%, respectively. As the loadings were progressively lowered and the reactions became slower, yields suffered as the oxidant began to decompose faster than it reacted with the enamine (Figure 6.2c). It should, however, be noted that none of the proline-only cases achieved yields above 50% due to this decomposition, highlighting the value of urea **1** in these reactions. The results seen in

Figures 6.2a and 6.2b suggest the potential for additives such as **1** to enable reactions with even lower catalyst loadings, especially those that do not suffer from decomposition or byproduct formation.

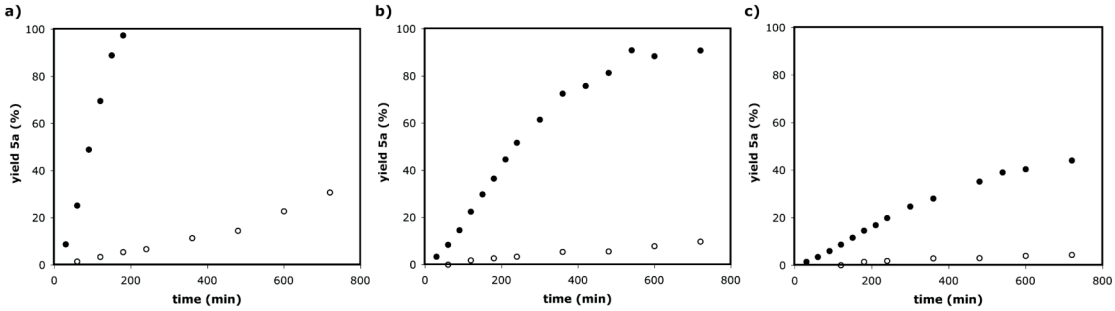

Figure 6.2. Reaction profiles for the α-aminoxylation of hexanal with a) 2.5% proline, b) 1% proline, and c) 0.5% proline. Urea concentration varies as follows: [urea] = [proline] (●), no urea (○).

Extension to the Mannich Reaction. As suggested above, accelerating the rate of enamine formation may have implications for other proline-catalyzed reactions involving rate-determining enamine formation. When urea **1** was employed in the Mannich reaction between benzaldehyde *N*-Boc imine and propionaldehyde, a faster reaction was observed in comparison to the proline-only case while the yields and selectivities of product **6** were left unchanged (Scheme 6.2). A structure-activity relationship revealed that as for the α-aminoxylation, using urea **2** or amine **3** individually in place of **1** did not provide as great an enhancement, but in this case, the combination of **2** and **3** were able to reproduce the enhancement provided by **1** (see Supporting Information). The reasons for this difference are currently unknown, but in any case, because urea **1** provides rate enhancement in this reaction as well as in the α-aminoxylation, it is possible that the increase in the rate of enamine formation may be general for other proline-catalyzed reactions.

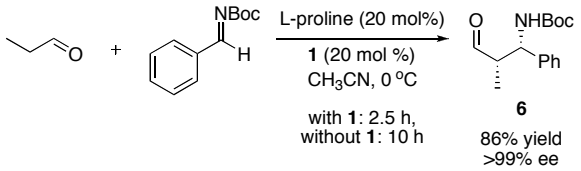

Scheme 6.2. Proline-catalyzed Mannich reaction between propionaldehyde and benzaldehyde *N*-Boc imine.

Solubility Studies. We considered the possibility that the observed rate enhancement may be due to an increased solubility of proline in the presence of **1** rather than faster enamine formation. Indeed, Hayashi has shown that a more soluble proline derivative displays greater catalytic activity than proline in the α-aminoxylation of carbonyl species.[10,37-40] However, when proline and **1** were placed in ethyl acetate, no appreciable dissolution was observed after 48 hours, and there was no distinguishable difference in dissolution between the proline-urea case and the proline-only control. We addressed this issue more quantitatively with a ^{1}H NMR experiment in which we assessed the solubility of proline in $CDCl_3$ by comparison against an internal standard (see Supporting Information). Again, there was no difference in the extent of proline dissolution for the urea and non-urea cases; the observed solubility in both cases was approximately 0.0045 M, in agreement with previously reported results.[22] These findings suggest that urea **1** does not directly solubilize proline but instead provides rate enhancement through a different mechanism.

Further evidence against the role of urea **1** in proline dissolution is provided by the persistence of rate enhancement by urea **1** even when catalyst dissolution cannot be a factor in the rate of α-aminoxylation. When oxazolidinone **7** (intermediate **A** in Scheme 6.1) was prepared from proline and hexanal and used as the catalyst, a significantly faster reaction is observed in the presence of **1** (Figure 6.3). It is interesting to note that as does the proline-only case, the reaction using oxazolidinone **7** alone exhibits autoinduction—although to a lesser extent—but that the addition of

urea **1** eliminates this phenomenon completely (Figure 6.3, inset). The mechanistic implications of this observation are discussed below. Furthermore, rate enhancement by urea **1** is also observed when an insoluble solid-supported proline is used in place of free proline.[41] Because catalyst dissolution does not play a role in either of these reactions, it cannot be the reason for the rate enhancement imparted by **1**.

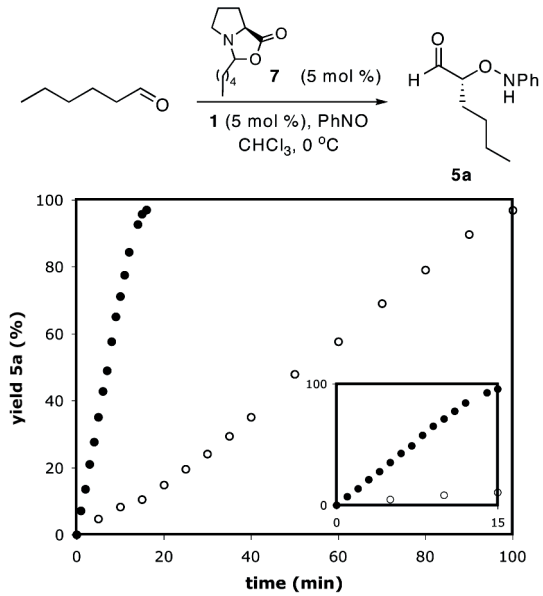

Figure 6.3. Oxazolidinone **7**-catalyzed α-aminoxylation of hexanal: with 1 (●) and without **1** (○).

Origin of Rate Enhancement. While exploring the use of proline derivatives in this reaction, we observed that the presence of urea **1** did not enhance the rate of α-aminoxylation when pyrrolidine-tetrazole **8** was used as the catalyst (Figure 6.4).[42]

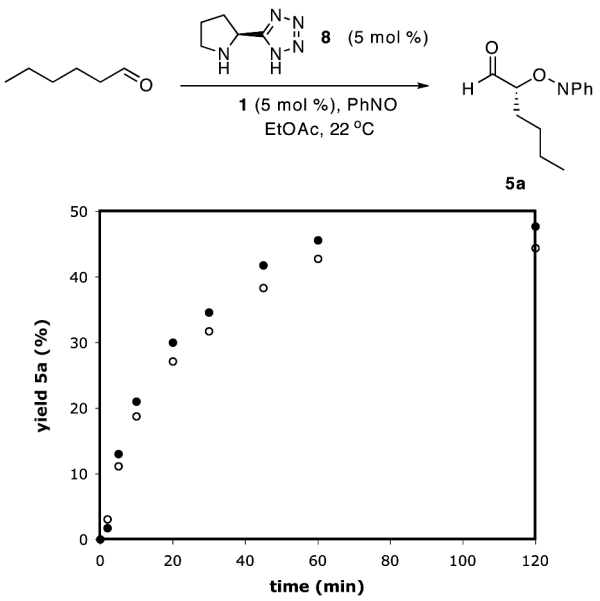

Figure 6.4. Pyrrolidine-tetrazole-catalyzed α-aminoxylation of hexanal: with **1** (●) and without **1** (○).

The absence of rate enhancement in this case is not consistent with a scenario involving the electrophile activation that has been implicated in other cases of urea catalysis,[26-29] because aldehyde activation by the urea would be expected to provide rate enhancement independent of pyrrolidine structure. A similar argument can be made against the activation of nitrosobenzene. Instead, this observation strongly suggests that the urea promotes enamine formation through a different mechanism. If oxazolidinones are indeed productive intermediates in the α-aminoxylation pathway, the rate enhancement that we observe may be due to interaction between the oxazolidinone and urea **1**. Specifically, this hydrogen bonding could enhance the oxazolidinone carboxylate's ability to act as a leaving group, resulting in faster enamine formation (Figure 6.5).

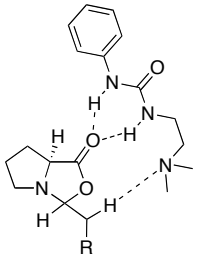

Figure 6.5. Proposed interaction between bifunctional urea **1** and oxazolidinone intermediate.

The results shown in Figure 6.4 also support our hypothesis; since the pyrrolidine-tetrazole cannot form an oxazolidinone species,[43] the urea cannot provide rate enhancement through the proposed mechanism. On the other hand, when carboxylate-containing siloxyproline **9**[44] was employed as the catalyst, rate enhancement was again observed upon the addition of urea **1** (Figure 6.6), again implicating the role of the oxazolidinone in the origin of rate enhancement.

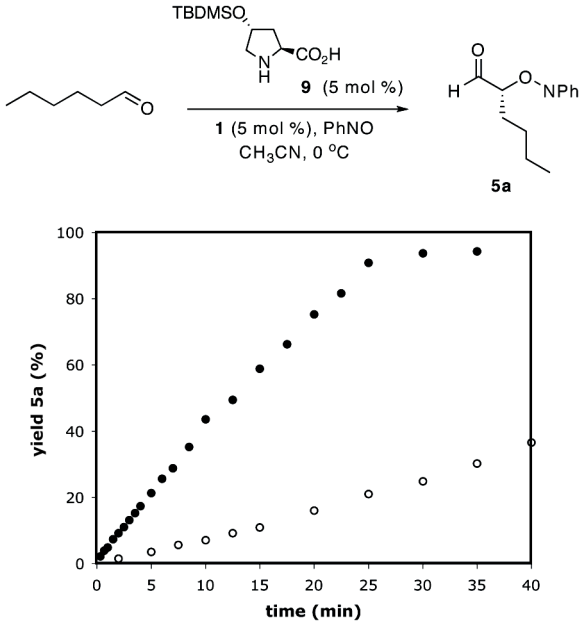

Figure 6.6. Soluble proline **9**-catalyzed α-aminoxylation of hexanal: with **1** (●) and without **1** (○).

To further explore this hypothesis, we looked at the influence the amine tether has on the rate of α-aminoxylation. Increasing the tether by one methylene resulted in

a reaction that was twice as fast as with urea **1**, while altering the conformation with a 2,2-dimethylpropyl tether decreased the rate of reaction (see Supporting Information). Further studies to probe these interactions are in progress, but these preliminary results suggest that the position and accessibility of the amine play an important role in the observed rate enhancement.

The results presented above certainly do not preclude the possibility for the participation of urea **1** in a step other than enamine formation. It is plausible that **1** instead accelerates a different step such as the proposed exchange between the product-proline complex and the enamine. However, the observation of rate enhancement in the proline-catalyzed Mannich reaction, which does not exhibit autoinduction, strongly suggests that the urea is involved in a step that takes place prior to entering the autoinductive pathway. Based on this, we propose the catalytic cycle shown in Scheme 6.3, which is consistent with our results as well as those presented by others. Because we observe the same behavior regardless of whether we start with free proline or with oxazolidinone **A** (water was not observed by ^{1}H NMR), we can simplify the pathway by eliminating both free proline and the water that is liberated from its condensation with the aldehyde.

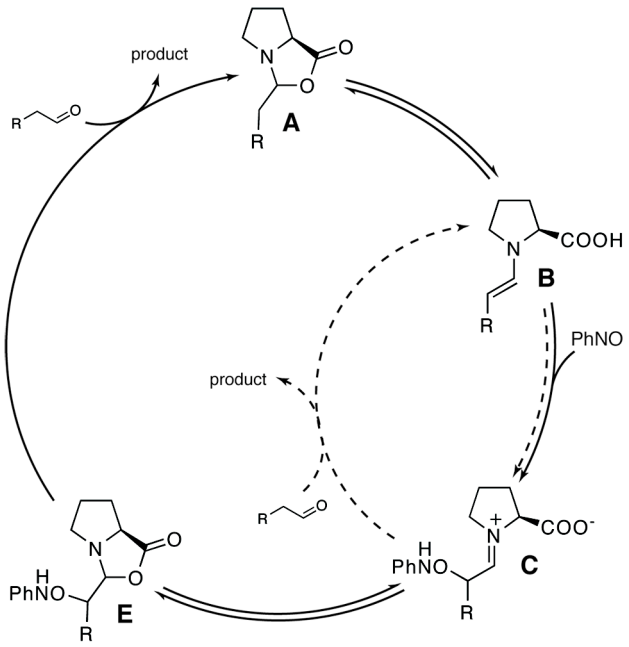

Scheme 6.3. Proposed catalytic cycle for the α-aminoxylation of aldehydes based on the rate enhancement provided by urea **1**. The cycle contains an autoinductive pathway (dashed lines, without urea **1**) and a non-autoinductive pathway (solid lines, with urea **1**).

Like Blackmond, we suggest the existence of two possible pathways in the α-aminoxylation catalytic cycle, with one (inner pathway) involving the transformation of a proline-product complex directly to the enamine. However, because no water is present to effect the release of product by hydrolysis, we propose that this complex is actually the iminium species **C** that is generated by the addition of nitrosobenzene to enamine **B**. Conversion of **C** to **B** with the concomitant release of product may proceed by the mechanism shown in Scheme 6.4. Though 2+2 cycloadditions are thermally unfavored for the formation of carbocycles, 2+2 cyclizations involving carbonyls are known.[45] In addition, preliminary calculations for such a transformation indicate a favorable ΔG° (see Supporting Information). Such a mechanism could explain why autoinduction is observed in some proline-catalyzed reactions but not in others, since the properties of the added electrophile should play a role in determining whether this exchange is possible. In cases for which it is not possible, reactions such

as the Mannich would operate only through the outer pathway, where autoinduction is not possible.

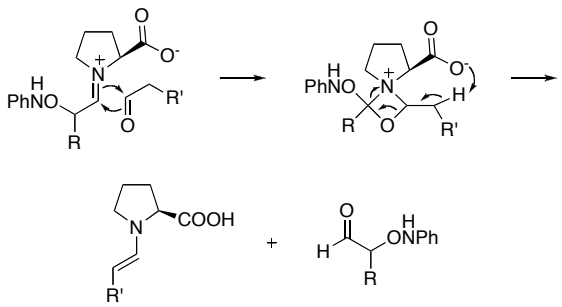

Scheme 6.4. Proposed mechanism for the iminium-enamine exchange in the α-aminoxylation autoinductive pathway.

In the context of this model, the explanation for the autoinduction that is observed in the proline-only case is the same as that previously proposed by Blackmond: the reaction proceeds slowly in the beginning due to slow enamine formation from the starting oxazolidinone **A** but becomes faster as the enamine is generated more rapidly through the inner cycle. On the other hand, when urea **1** is present, we propose that enamine formation is accelerated enough to allow the outer pathway to dominate. For this model to be valid, both the transformation from oxazolidinone **A** to enamine **B** as well as the oxazolidinone exchange between **E** and **A** along the outer pathway must be faster (when the urea is present) than the iminium-enamine conversion along the inner pathway. If not, the inner pathway would be expected to dominate and the autoinduction would persist. It is plausible that the transformation from **E** to **A** is fast, as oxazolidinone exchange has been shown to occur freely,[22,43] and we propose that urea **1** accelerates the transformation from oxazolidinone **A** to enamine **B** enough so that the change from the inner to the outer pathway can occur.

Evidence to support our proposed model is seen in the oxazolidinone **7**-catalyzed α-aminoxylation, for which the presence of urea **1** eliminates the

autoinduction that is seen in the proline-only case. **1** appears to sufficiently enhance the rate of enamine formation so that the outer pathway dominates, making the autoinductive inner pathway unimportant. An argument can be made that the urea sufficiently accelerates the reaction that the exchange between iminium **C** and enamine **B** becomes rate-limiting, as has been proposed for the outer pathway.[23] This would indeed eliminate autoinduction while allowing the reaction to proceed through the inner pathway. However, this would also result in the proline-only and proline-urea cases exhibiting the same rate. Even at its fastest, the proline-only reaction does not achieve the same rate as the proline-urea reaction, indicating that the latter proceeds *via* a different pathway. Also consistent with the model presented in Scheme 3 are the unchanged selectivities that we observe when urea **1** is present: since selectivity is determined during a step that is common to both pathways, the enantioselectivity should be the same regardless of which pathway is operative.

Conclusion

In summary, we have reported that the proline-catalyzed α-aminoxylation of aldehydes is enhanced by the presence of bifunctional urea **1**, which exhibits high reaction rates in a more benign solvent while still providing high enantioselectivities and yields. Our results suggest that **1** promotes enamine formation by interacting with the oxazolidinone intermediate, supporting the role of the oxazolidinone as a productive catalytic species. Our observation that urea **1** removes the autoinductive behavior typically seen in proline-catalyzed α-aminoxylations has allowed us to provide a model that is consistent with both the proline-only and proline-urea cases. We propose that the enhanced enamine formation that we observe will allow for the acceleration of other existing reactions as well as the realization of new reaction pathways.

Afterword

Though we were expecting the observed rate enhancement to be due to urea-aldehyde interaction, the urea-oxazolidinone interaction that our results suggest provided us with an even richer system to study. Though this project was based on the mistaken assumption that the bifunctional urea provided rate enhancement for the Michael addition discussed in Chpaters 3-5, our seemingly random choice of a follow-up reaction serendipitously led to some interesting findings. Our exploration of this system led to a greater understanding of the role of the oxazolidinone intermediate, as well an explanation of the autoinductive pathway that is present in the α-aminoxylation catalytic cycle.

Experimental Section

General Considerations

All reagents were used without purification unless otherwise noted. Nitrosobenzene was recrystallized from ethanol prior to use. Ethyl phenyl urea was recrystallized from ethyl acetate prior to use. Propionaldehyde, hexanal, and octanal were vacuum distilled prior to use. Reactions were rocked on a Thermolyne Speci-Mix test tube rocker where indicated. Gas chromatographic (GC) analyses were performed using an Agilent 7890A GC equipped with an Agilent 7683B autosampler, a flame ionization detector (FID), and a J&W Scientific 19091J-413 column (length = 30 m, inner diameter = 320 μm, and film thickness = 250 μm). The temperature program for GC analysis held the temperature constant at 80 ^{o}C for 1 min, heated samples from 80 to 200 ^{o}C at 25 ^{o}C/min and held at 200 ^{o}C for 1.5 min. Inlet and detector temperatures were set constant at 250 and 300 ^{o}C, respectively. Mesitylene was used as an internal standard to calculate reaction conversion. ^{1}H NMR and ^{13}C NMR spectra were recorded in $CDCl_3$ on Varian Mercury 300MHz operating at

300.070 MHz and 75.452 MHz, respectively, using the residual solvent peak as reference. Data are reported as s = singlet, d = doublet, t = triplet, m = multiplet, q = quadruplet. High performance liquid chromatography (HPLC) was performed using a Varian Pro Star chromatograph using a CHIRALPAK IA column (250 mm x 4.6 mm) and CHIRALPAK IA guard column (1 cm x 0.4 cm). Retention times for *R* and *S* isomers were determined by using (DL)-proline instead of (L)-proline in the general procedure. All chromatograms were obtained using a wavelength of 254 nm.

1-(2-(dimethylamino)ethyl)-3-phenylurea (1). Prepared as described in the Experimental Section of Chapter 5.

***N*-(2-(dimethylamino)ethyl)ethanamide (4).** Prepared as described in the Experimental Section of Chapter 5.

General Procedure for α-Aminoxylation of Hexanal with Additives 1-4. A solution of additive (0.05 mmol, 0.05 eq) in 1 mL solvent was added to (L)-proline (5.8 mg, 0.05 mmol, 0.05 eq) in a 1 dram screw cap vial. The vial was sonicated for 1 min and held at 4 ^{o}C for 15 min. 1 mL of a stock solution of nitrosobenzene (1 M), hexanal (3 M), and mesitylene (0.1 M) was added and the reaction was rocked at 4 ^{o}C. Reaction conversion was monitored by withdrawing aliquots from the reaction, diluting into ethyl acetate, and analyzing by GC with reference to mesitylene. Yields at 40 minutes were determined using calibrated GC results.

General Procedure for α-Aminoxylation of Aldehydes. Nitrosobenzene (214 mg, 2.0 mmol, 1.0 eq), (L)-proline (11.6 mg, 0.1 mmol, 0.05 eq) and urea **1** (20.8 mg, 0.1 mmol, 0.05 eq) were added to a 2 dram screw cap vial equipped with a stir bar. Ethyl

acetate (4 mL) was added to the vial, upon which the reaction mixture turned green. The reaction mixture was submerged in an ice bath and stirred for 15 min. The appropriate aldehyde (6.0 mmol, 3.0 eq) was added to the reaction mixture in one portion at 0 ˚C. The reaction mixture was continuously stirred at 0 ˚C until the reaction color changed from green to yellow and the reaction was determined to be complete by GC. The reaction was transferred to a suspension of sodium borohydride (300 mg, 8.0 mmol, 4.0 eq) in ethanol (10 mL) at 0 ˚C. An additional 5 mL of ethanol was used to rinse the reaction vessel and added to the sodium borohydride suspension. After 20 min, the reaction mixture was poured into a separatory funnel containing 25 mL saturated aqueous $NaHCO_3$ and the aqueous phase extracted with EtOAc (3 x 20 mL). The combined organic extracts were dried with $MgSO_4$, filtered, concentrated *in vacuo*, and dried under vacuum. The resulting residue was purified using column chromatography to afford the desired compounds. Enantioselectivities were determined using chiral HPLC analysis.

(*R*)-2-(*N*-Phenyl-aminooxy)-hexan-1-ol (5a). Prepared according to the general procedure using hexanal (750 μL, 6.0 mmol, 3.0 eq) for 2 h to afford the title compound as a yellow oil (400 mg, 96 % yield, 99 % ee) after column chromatography (silica gel, 4:1 hexanes/EtOAc, R_f = 0.18). ^{1}H NMR (300 MHz, $CDCl_3$) δ 7.28 (m, 2H), 6.99 (m, 2H), 3.95 (m, 1H), 3.81 (m, 2H), 2.50 (bs, 1H), 1.68 (m, 1H), 1.40 (m, 6H), 0.93 (t, 3H); ^{13}C NMR (75 MHz, $CDCl_3$) δ 148.7, 129.0, 122.1, 114.6, 84.0, 64.7, 29.7, 28.0, 22.9, 14.0. The enantiomeric ratio was determined by HPLC using a CHIRALPAK IA and IA guard column (5 % IPA/hexanes, 1 mL/min); (*S*) isomer t_r= 15.0 min and (*R*) isomer t_r= 17.6 min.

(*R*)-2-(*N*-Phenyl-aminooxy)-propan-1-ol (5b). Prepared according to the general procedure using propionaldehyde (437 μL, 6.0 mmol, 3.0 eq) for 3 h to afford the title compound as a yellow oil (300 mg, 90 % yield, 98 % ee) after column chromatography (silica gel, 4:1 hexanes/EtOAc, R_f = 0.09). ^{1}H NMR (300 MHz, $CDCl_3$) δ 7.28 (m, 2H), 7.00 (m, 3H), 4.13 (m, 1H), 3.76 (m, 2H), 1.26 (d, 3H); ^{13}C NMR (75 MHz, $CDCl_3$) δ 148.8, 131.1, 129.1, 122.1, 80.2, 65.8, 15.5. The enantiomeric ratio was determined by HPLC using a CHIRALPAK IA and IA guard column (5 % IPA/hexanes, 1 mL/min); (*S*) isomer t_r= 20.2 min and (*R*) isomer t_r= 22.0 min.

(*R*)-3-methyl-2-(*N*-Phenyl-aminooxy)-butan-1-ol (5c). Prepared according to the general procedure using isovaleraldehyde (650 μL, 6.0 mmol, 3.0 eq) for 3.5 h to afford the title compound as a yellow oil (380 mg, 97 % yield, 99 % ee) after column chromatography (silica gel, 4:1 hexanes/EtOAc, R_f = 0.18). ^{1}H NMR (300 MHz, $CDCl_3$) δ 7.28 (m, 2H), 7.03 (bs, 1H), 7.01 (m, 3H), 3.88 (m, 2H), 3.75 (m, 1H), 2.84 (bs, 1H), 2.04 (m, 1H), 1.04 (dd, 6H); ^{13}C NMR (75 MHz, $CDCl_3$) δ 148.6, 129.1, 122.5, 115.1, 88.7, 63.4, 28.8, 18.9, 18.7. The enantiomeric ratio was determined by HPLC using a CHIRALPAK IA and IA guard column (5 % IPA/hexanes, 1 mL/min); (*S*) isomer t_r= 13.4 min and (*R*) isomer t_r= 15.4 min.

(*R*)-2-(*N*-Phenyl-aminooxy)-octan-1-ol (5d). Prepared according to the general procedure using octanal (940 μL, 6.0 mmol, 3.0 eq) for 5 h to afford the title compound as a yellow oil (400 mg, 84 % yield, 99 % ee) after column chromatography (silica gel, 4:1 hexanes/EtOAc, R_f = 0.14). ^{1}H NMR (300 MHz, $CDCl_3$) δ 7.28 (m, 2H), 7.00 (m, 4H), 3.95 (m, 1H), 3.78 (m, 2H), 2.62 (bs, 1H), 1.48 (m, 10H), 0.91 (t, 3H); ^{13}C NMR (75 MHz, $CDCl_3$) δ 148.7, 129.0, 122.2, 114.8, 84.1, 64.8, 31.8, 30.1, 29.3, 25.9, 22.7, 14.2. The enantiomeric ratio was determined by HPLC using a

CHIRALPAK IA and IA guard column (5 % IPA/hexanes, 1 mL/min); (*S*) isomer t_r= 13.9 min and (*R*) isomer t_r= 16.0 min.

(*R*)-3-phenyl-2-(*N*-Phenyl-aminooxy)-propan-1-ol (5e). Prepared according to the general procedure using 3-phenylpropionaldehyde (793 μL, 6.0 mmol, 3.0 eq) for 3.5 h to afford the title compound as a yellow oil (410 mg, 84 % yield, >99 % ee) after column chromatography (silica gel, 4:1 hexanes/EtOAc, R_f= 0.09). ^{1}H NMR (300 MHz, $CDCl_3$) δ 7.18 (m, 7H), 6.97 (bs, 1H), 6.86 (t, 1H), 6.78 (d, 2H), 4.08 (m 1H), 3.78 (m, 1H), 3.66 (m, 1H), 3.02 (dd, 1H), 2.80 (dd, 1H), 2.38 (bs, 1H); ^{13}C NMR (75 MHz, $CDCl_3$) δ 148.5, 138.0, 129.6, 1291, 128.6, 126.6, 122.3, 114.7, 85.2, 64.0, 36.6. The enantiomeric ratio was determined by HPLC using a CHIRALPAK IA and IA guard column (5 % IPA/hexanes, 1 mL/min); (*S*) isomer t_r= 25.8 min and (*R*) isomer t_r= 31.2 min.

(*R*)-2-phenyl-2-(*N*-Phenyl-aminooxy)-ethan-1-ol (5f). Prepared according to the general procedure using phenylacetaldehyde (766 μL, 6.0 mmol, 3.0 eq) for 2 h to afford the title compound as a yellow oil (250 mg, 55 % yield, 99 % ee) after column chromatography (silica gel, 4:1 hexanes/EtOAc, R_f= 0.20). ^{1}H NMR (300 MHz, $CDCl_3$) δ 7.30 (m, 7H), 7.00 (m, 4H), 5.03 (dd, 1H), 3.98 (m, 1H), 3.86 (m, 1H), 2.58 (bs, 1H); ^{13}C NMR (75 MHz, $CDCl_3$) δ 148.1, 138.0, 129.1, 128.7, 128.6, 127.2, 122.5, 115.0, 86.6, 66.1. The enantiomeric ratio was determined by HPLC using a CHIRALPAK IA and IA guard column (5 % IPA/hexanes, 1 mL/min); (*S*) isomer t_r= 25.9 min and (*R*) isomer t_r= 28.9 min.

(*R*)-2-(*N*-Phenyl-aminooxy)-pent-4-en-1-ol (5g). Prepared according to the general procedure using 4-pentenal (621 μL, 6.0 mmol, 3.0 eq) for 2.5 h to afford the title

compound as a yellow oil (290 mg, 75 % yield, 99 % ee) after column chromatography (silica gel, 4:1 hexanes/EtOAc, R_f = 0.14). ^{1}H NMR (300 MHz, $CDCl_3$) δ 7.28 (m, 2H), 7.05 (s, 1H), 7.00 (m, 3H), 5.89 (m, 1H), 5.14 (dt, 2H), 4.04 (m, 1H), 3.89 (m, 2H), 2.94 (m, 1H), 2.38 (m, 2H); ^{13}C NMR (75 MHz, $CDCl_3$) δ 148.6, 134.2, 129.2, 122.6, 117.9, 114.9, 83.5, 64.6, 34.8. The enantiomeric ratio was determined by HPLC using a CHIRALPAK IA and IA guard column (5 % IPA/hexanes, 1 mL/min); (*S*) isomer t_r= 20.2 min and (*R*) isomer t_r= 23.1 min.

Benzaldehyde *N*-Boc Imine. Prepared according to the method of Wenzel et al.[46] *tert*-Butyl carbamate (1.0 g, 8.6 mmol) and benzenesulfinic acid sodium salt (2.8 g, 17 mmol) were suspended in a solution of MeOH and water (1:2, 25 mL). Benzaldehyde (1.3 mL, 12.8 mmol) was added in one portion, followed by formic acid (88%, 7.1 mL), and the reaction was stirred at room temperature for 2 days. The resulting white product was isolated by filtration, washed with water, and dried under vacuum to give *N*-(*tert*-butoxycarbonyl)-α-(phenylsulfonyl)benzylamine as a white solid (2.77 g, 93.9% yield): ^{1}H NMR (300 MHz, $CDCl_3$): δ 7.92 (d, 2H), 7.63 (t, 1H), 7.57 (t, 2H), 7.42 (m, 5H), 5.93 (bd, 1H), 5.76 (bd, 1H), 1.24 (s, 9H). K_2CO_3 (4.1 g, 29.8 mmol) and Na_2SO_4 (4.96 g) were placed in a round bottom flask containing a stir bar. The solids were placed under vacuum and flame-dried. Once cool, *N*-(*tert*-butoxycarbonyl)-α-(phenylsulfonyl)benzylamine (1.72 g, 5 mmol) was added under a stream of N_2, followed by THF (46 mL). The reaction was stirred at reflux under an atmosphere of N_2 for 16 h. The reaction was cooled and the solids were removed by filtration. The filtrate was concentrated and dried under vacuum to give benzaldehyde *N*-Boc imine as a colorless oil (1.02 g, quant): ^{1}H NMR ($CDCl_3$, 300 MHz); δ 8.89 (s, 1H), 7.92 (d, 2H), 7.58 (t, 1H), 7.49 (t, 2H), 1.61 (s, 9H).

General Procedure for Mannich Reaction Between Propionladehyde and *N*-Boc Imine. Adapted from the method of Yang et al.[47] A solution of additive (0.05 mmol, 0.05 eq) in 1 mL solvent was added to (L)-proline (5.8 mg, 0.05 mmol, 0.05 eq) in a 1 dram screw cap vial. The vial was sonicated for 1 min and stirred at 0 ^{o}C for 15 min. 1 mL of a stock solution of benzaldehyde *N*-Boc imine (1.0 M) and mesitylene (0.1 M) was added, followed by propionaldehyde (72.2 μL, 4 mmol, 4 eq) and the reaction was stirred at 0 ^{o}C. Reaction conversion was monitored by withdrawing aliquots from the reaction, diluting into dichloromethane, and analyzing by GC with reference to mesitylene.

***tert*-Butyl (2*S*)-2-methyl-3-oxo-1-phenylpropylcarbamate (6).** Prepared according to the procedure described above. After the reaction was complete, it was quenched into water and extracted with ether (3x). The combined organic layers were dried over Na_2SO_4, filtered, and concentrated. HPLC analysis was performed prior to recrystallization from hexanes and ether. ^{1}H NMR (300 MHz, $CDCl_3$) δ 9.71 (s, 1H), 7.38-7.23 (m, 5H), 5.09 (m, 2H), 2.91 (m, 1H), 1.42 (s, 9H), 1.05 (d, 3H); ^{13}C NMR (75 MHz, $CDCl_3$) δ 203.2, 155.3, 129.0, 127.8, 126.8, 80.3, 54.9, 51.8, 28.5, 9.4. The enantiomeric ratio was determined by HPLC using a CHIRALPAK IA and IA guard column (10 % IPA/hexanes, 1 mL/min); t_r= 8.2 min and 9.8 min.

Preparation of Oxazolidinone 7. Preparation of oxazolidinone **7** was modified from the literature.[21] Hexanal (123 μL, 1 mmol) and proline (115.2 mg, 1 mmol) and 4 Å molecular sieves (139 mg) were stirred in $CDCl_3$ (5 mL) under an environment of N_2 for 14 hours. Catalyst concentration was assessed by ^{1}H NMR using mesitylene as an internal standard. Typical concentrations were 0.02-0.05 M.

α-Aminoxylation of Hexanal with Oxazolidinone 7. Urea **1** (10.4 mg, 0.05 mmol, 0.05 eq), $CHCl_3$ (volume varied depending on concentration of oxazolidinone **7**) and 4 Å molecular sieves (35 mg) were stirred at 0 °C for 10 min. Propionaldehyde (370 μL, 3 mmol, 3 eq) was added, followed by a stock solution (1 mL) of nitrosobenzene (1 M) and mesitylene (0.1 M) in $CHCl_3$. Oxazolidinone **7** in $CDCl_3$ (volume varied depending on concentration) was added, and reaction conversion was monitored by withdrawing aliquots from the reaction at different time intervals, diluting into ethyl acetate, and analyzing by GC with reference to mesitylene. The control reaction was performed in the same way but without urea **1**.

α-Aminoxylation of Hexanal with Pyrrolidine Tetrazole 8. Pyrrolidine-tetrazole **8** (7.0 mg, 0.05 mmol), urea **1** (10.4 mg, 0.05 mmol) and EtOAc (1 mL) were sonicated in a 1 dram screw cap vial for 1 min. A stock solution (1 mL) of hexanal (3 M), nitrosobenzene (1 M), and mesitylene (0.1 M) in EtOAc was added and the reaction was rocked at 22 °C. Reaction conversion was monitored by withdrawing aliquots from the reaction at different time intervals, diluting into ethyl acetate, and analyzing by GC with reference to mesitylene. The control reaction was performed in the same way but without urea **1**.

Preparation of (4*R*)-4-(*t*-butyldimethylsilyloxy)-L-proline (9). Siloxyproline **9** was prepared as reported in the literature.[11,44] *N*-Cbz-hydroxy-L-proline (1.5 g, 5.7 mmol), benzyl bromide (0.67 mL, 5.7 mmol), K_2CO_3 (781 mg, 5.7 mmol), and NaI (84.7 mg, 0.57 mmol) were stirred in DMF (5 mL) at room temperature for 16 h. The reaction was quenched by slow addition of saturated LiBr (5 mL) and acidified with 1 M HCl. The product was extracted with CH_2Cl_2 (3 x 20 mL), dried over Na_2SO_4, and concentrated. The remaining DMF was removed by vacuum distillation and the

product was purified by column chromatography (silica, 95:5 $CHCl_3$:MeOH) to give (4*R*)-*N*-Cbz-4-hydroxy-L-proline benzyl ester (2.01 g, quant): ^{1}H NMR: δ 7.39-7.22 (m, 10H), 5.22-5.15 (m, 2H), 5.07-4.99 (m, 2H), 4.61-4.44 (m, 2H), 3.77-3.25 (m, 3H), 2.39-2.23 (m, 1H), 2.18-2.07 (m, 1H). (4*R*)-*N*-Cbz-4-hydroxy-L-proline benzyl ester (1.96 g, 5.5 mmol), TBDMSCl (1 g, 6.6 mmol), and imidazole (450 mg, 6.6 mmol) were stirred in DMF (25 mL) at room temperature for 16 h. The solvent was removed by vacuum distillation and the resulting white solid was taken up in H_2O (25 mL). The product was extracted with $CHCl_3$ (3 x 25 mL), dried over Na_2SO_4, and concentrated. The product was purified by column chromatography (silica, 95:5 $CHCl_3$:MeOH) to give (4*R*)-*N*-Cbz-4-(*t*-butyldimethylsilyloxy)-L-proline benzyl ester (2.12 g, 82% yield): ^{1}H NMR ($CDCl_3$, 300 MHz): δ 7.39-7.21 (m, 10H), 5.22-4.96 (m, 4H), 4.60-4.41 (m, 2H), 3.72-3.63 (m, 1H), 3.55-3.42 (m, 1H), 2.26-2.17 (m, 1H), 2.10-2.00 (m, 1H), 0.83 (s, 9H), 0.03 (s, 6H). (4*R*)-*N*-Cbz-4-(*t*-butyldimethylsilyloxy)-L-proline benzyl ester (1.98 g, 4.2 mmol), Pd/C (palladium, 10 wt% (dry basis) on activated carbon, wet, Degussa type E101 NE/W, 1 g), and MeOH (20 mL) were stirred under a balloon of H_2 for 4 h. The Pd/C was filtered off over Celite and the product was concentrated to give crude product. The product was dissolved in a small amount of MeOH and triturated with EtOAc to give (4*R*)-4-(*t*-butyldimethylsilyloxy)-L-proline as a white solid: ^{1}H NMR (CD_3OD, 300 MHz): δ 4.63 (m, 1H), 4.51 (dd, 1H), 3.50 (dd, 1H), 3.26 (m, 1H), 2.39 (m, 1H), 2.23 (m, 1H), 0.92 (s, 1H), 0.17 (s, 3H), 0.16 (s, 3H); ^{13}C NMR (CD_3OD, 75 MHz): δ 171.6, 72.7, 59.9, 55.7, 39.6, 26.3, 19.0, -4.7, -4.8.

α-Aminoxylation of Hexanal with Siloxyproline 9. Siloxyproline **9** (12.3 mg, 0.05 mmol, 0.05 eq), urea **1** (10.4 mg, 0.05 mmol, 0.05 eq), and acetonitrile (1 mL) were placed in a 1 dram screw cap and stirred at 0 ^{o}C for 15 min. A stock solution (1 mL)

of nitrosobenzene (1 M) and mesitylene (0.1 M) in acetonitrile was added, followed by hexanal (370 μL, 3 mmol, 3 eq) and the reaction was stirred at 0 ^{o}C. Reaction conversion was monitored by withdrawing aliquots from the reaction at different time intervals, diluting into ethyl acetate, and analyzing by GC with reference to mesitylene. The control reaction was performed in the same way but without urea **1**.

Supporting Information

Experimental details, ^{1}H NMR studies, and calculations are located in Appendix 4.

REFERENCES

1. Pellissier, H. *Tetrahedron* **2007**, *63*, 9267

2. Guillena, G.; Nájera, C.; Ramón, D. J. *Tetrahedron—Asymmetry*, **2007**, *18*, 2249.

3. List, B. *Acc. Chem. Res.* **2004**, *37*, 548.

4. List, B. *Tetrahedron* **2002**, *58*, 5573.

5. Bertelsen, S., Nielsen, M.; Jørgensen, K. A. *Angew. Chem. Int. Ed.* **2007**, *46*, 7356.

6. Ting, A.; Schaus, S. E. *Eur. J. Org. Chem.* **2007**, 5797.

7. List, B.; Lerner, R. A.; Barbas, C. F. *J. Am. Chem. Soc.* **2000**, *122*, 2395.

8. Wang, W.; Wang, J.; Li, H.; Liao, L. *Tetrahedron Lett*. **2004**, *45* 7235.

9. Notz, W.; Tanaka, F.; Barbas, C. F. *Acc. Chem. Res.* **2004**, *37*, 580.

10. Hayashi, Y.; Yamaguchi, J.; Sumiya, T.; Hibino, K.; Shoji, M. *J. Org. Chem.* **2004**, *69*, 5966.

11. Hayashi, Y.; Yamaguchi, J.; Hibino, K.; Sumiya, T.; Urushima, T.; Shoji, M.; Hashizume, D.; Koshino, H. *Adv. Synth. Catal.* **2004**, *346*, 1435.

12. Brown, S. P.; Brochu, M. P.; Sinz, C. J.; MacMillan, D. W. C. *J. Am. Chem. Soc.* **2003**, *125*, 10808.

13. Zhong, G. *Angew. Chem.* **2003**, *115*, 4379; *Angew. Chem. Int. Ed.* **2003**, *42*, 4247.

14. Hayashi, Y.; Yamaguchi, J.; Hibino, K.; Shoji, M. *Tetrahedron Lett.* **2003**, *44*, 8293.

15. List, B.; Hoang, L.; Martin, H. J. *P. Natl. Acad. Sci. U.S.A.* **2004**, *101*, 5839.

16. Córdova, A.; Sundén, H.; Bøegvig, A.; Johansson, M.; Himo, F. *Chem. Eur. J.* **2004**, *10*, 3673.

17. Hayashi, Y.; Yamaguchi, J.; Sumiya, T.; Shoji, M. *Angew. Chem.* **2004**, *116*, 1132; *Angew. Chem. Int. Ed.* **2004**, *43*, 1112.

18. Bøegvig, A.; Sundén, H.; Córdova, A. *Angew. Chem.* **2004**, *116*, 1129; *Angew. Chem. Int. Ed.* **2004**, *43*, 1109.

19. Both the α-aminoxylation and α-amination of aldehydes have been found to exhibit autoinduction. See references 20-23.

20. Mathew, S. P.; Iwamura, H.; Blackmond, D. G. *Angew. Chem.* **2004**, *116*, 3379; *Angew. Chem. Int. Ed*, **2004**, *43*, 3317.

21. Iwamura, H.; Mathew, S. P.; Blackmond, D. G. *J. Am. Chem. Soc.* **2004**, *126*, 11770.

22. Iwamura, H.; Wells, D. H., Jr.; Mathew, S. P.; Klussmann, M.; Armstrong, A.; Blackmond, D. G. *J. Am. Chem. Soc*. **2004**, *126*, 16312.

23. Mathew, S. P.; Klussmann, M.; Iwamura, H.; Wells, D. H.; Armstrong, A.; Blackmond, D. G. *Chem. Commun.* **2006**, 4291.

24. Seebach, D.; Beck, A. K.; Badine, D. M.; Limbach, M.; Eschenmoser, A.; Treasurywala, A. M.; Hobi, R.; Prikoszovich, W.; Linder, B. *Helv. Chim. Acta* **2007**, *90*, 425.

25. Zhou, Y.; Shan, Z. *J. Org. Chem.* **2006**, *71*, 9510; Pihko, P. M.; Laurikainen, K. M.; Usano, A.; Nyberg, A. I. J. A. Kaavi, *Tetrahedron* **2006**, *62*, 317.

26. Taylor, M. S.; Jacobsen, E. N. *Angew. Chem. Int. Ed.* **2006**, *45*, 1520.

27. Connon, S. J. *Chem. Eur. J.* **2006**, *12*, 5418.

28. Schreiner, P. R.; Wittkop, A. *Org. Lett.* **2002**, *4*, 217.

29. Schreiner, P. R. *Chem. Soc. Rev.* **2003**, *32*, 289.

30. Okino, T.; Hoashi, Y.; Takemoto, Y. *J. Am. Chem. Soc.* **2003**, *125*, 12672.

31. Berkessel, A.; Cleemann, F.; Mukherjee, S.; Müller, T. N.; Lex, J. *Angew. Chem.* **2005**, *117*, 817; *Angew. Chem. Int. Ed*. **2005**, *44*, 807.

32. Fuerst, D. E.; Jacobsen, E. N. *J. Am. Chem. Soc.* **2005**, *127*, 8964.

33. Rate enhancement in the presence of urea was observed in the following solvents: $CHCl_3$, EtOAc, DMSO, THF, toluene, acetonitrile, and DMF. We did not encounter a case in which no rate enhancement was observed.

34. Bordwell, F. G.; Algrim, D. J.; Harrelson, J. A. Jr. *J. Am. Chem. Soc.* **1988**, *110*, 5903.

35. We also observed rate enhancement in the α-aminoxylation of ketones.

36. Interestingly, although proline fully dissolved during the course of the proline-only reactions, solid proline was still present even after 24 hour in the proline-urea reactions.

37. Aratake, S.; Itoh, T.; Okano, T.; Nagae, N.; Sumiya, T.; Shoji, M.; Hayashi, Y. *Chem. Eur. J.* **2007**, *13*, 10246.

38. Enders, D.; Chow, S. *Eur. J. Org. Chem.* **2006**, 4578.

39. Hong, B.-C.; Wu, M.-F.; Tseng, H.-C.; Huang, G.-F.; Su, C.-F,; Liao, J.-H. *J. Org. Chem.* **2007**, *72*, 8459.

40. Zhang, D.; Yuan, C. *Tetrahedron* **2008**, *64*, 2480.

41. Unpublished results.

42. Momiyama, N.; Torii, H.; Saito, S.; Yamamoto, H. *P. Natl. Acad. Sci. USA* **2004**, *101*, 5374.

43. Isart, C.; Burés, J.; Villarasa, J. *Tetrahedron Lett.* **2008**, *49*, 5414.

44. **7** was prepared from *N*-Cbz-hydroxy-(L)-proline according to published procedures; see reference 11 and Ohtake, H.; Imada, Y.; Murahashi, S.-I. *Bull. Chem. Soc. Jpn.* **1999**, *72*, 2737.

45. Richter, R.; Tucker, B.; Ulrich, H. *J. Org. Chem.* **1983**, *48*, 1694.

46. Wenzel, A. G.; Jacobsen, E. N. *J. Am. Chem. Soc.* **2002** *124*, 12964.

47. Yang, J. W.; Stadler, M.; List, B. *Angew. Chem. Int. Ed.* **2007**, *46*, 609.

APPENDIX 1

Supporting Information for Chapter 3

*Micrographs of microencapsulated catalyst **1***

Figure A1.1. SEM micrograph of crenated polyurea microcapsules.

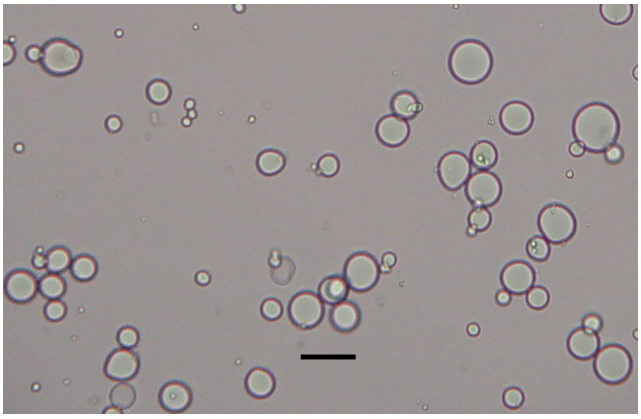

Figure A1.2. Optical micrograph of swollen capsules in methanol. The scale bar is 50 µm.

*Preliminary evidence for trans-β-Nitrostyrene (**4**) binding to the μcaps*

In order to account for the lost material in cases where conversion of benzaldehyde was not quantitative we did a *trans*-β-nitrostyrene (**4**) binding experiment to the μcaps. Based on literature reports of nitroalkenes reacting in a Michael-type reaction with primary and secondary amines[1-4], we hypothesized that the μcaps were removing nitrostyrene from our reaction mixture in a similar fashion. Briefly, μcaps (30 mg) swollen in methanol (0.1 mL) were dispersed in toluene (0.5 mL) and *trans*-β-nitrostyrene, **4** (150 mg, 1 mmol) was added to the mixture followed by mesitylene (13.7 μL, internal standard). Nitrostyrene concentration was followed over time with GC.

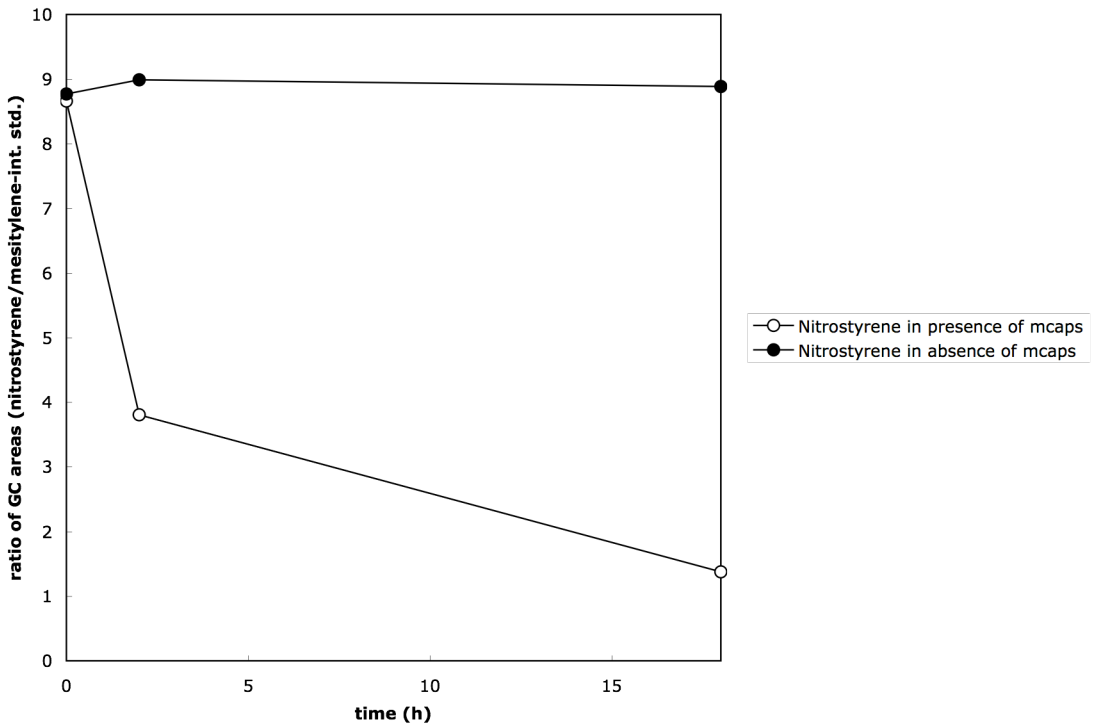

Figure A1.3. Components of the monitored mixture: nitrostyrene, toluene, μcaps swollen in methanol (-○-), and control mixture of nitrostyrene, toluene, and methanol (-●-).

As it can be seen from the Figure A1.3 *trans*-β-nitrostyrene (**4**) is removed from the reaction mixture with μcaps through an unproductive pathway. This is avoided if nitrostyrene is promptly directed to the Michael adduct (**6**) with the second catalyst (**2**). We are currently investigating the details of the unproductive pathways.

UV-Vis studies

In order to quantify how much of the nickel catalyst (**2**) is being degraded by μcap catalyst (**1**), UV-Vis absorbance of the nickel catalyst was monitored over time in the presence and in the absence of the μcaps. To nickel catalyst (**2**, 60 mg), dissolved in toluene (1 mL), μcap catalyst (**1**, 15 mg) slurry in methanol (0.5 mL) was added. Absorbance at 394 and 656 nm was followed over time. The control experiment consisted of measuring absorbance at the same wavelengths of the nickel catalyst solution without the μcap catalyst present. Percent nickel catalyst was normalized to the relative absorbance at time zero. Percentages were averaged over the two wavelengths. Results, shown in the Figure A1.4, suggest that the μcaps degrade nearly 20% of the initial nickel catalyst within 40 hours. On the other hand, the control also shows 10% degradation. Therefore, μcap catalyst is responsible of less than 10% degradation of the nickel catalyst during the course of the one pot reaction.

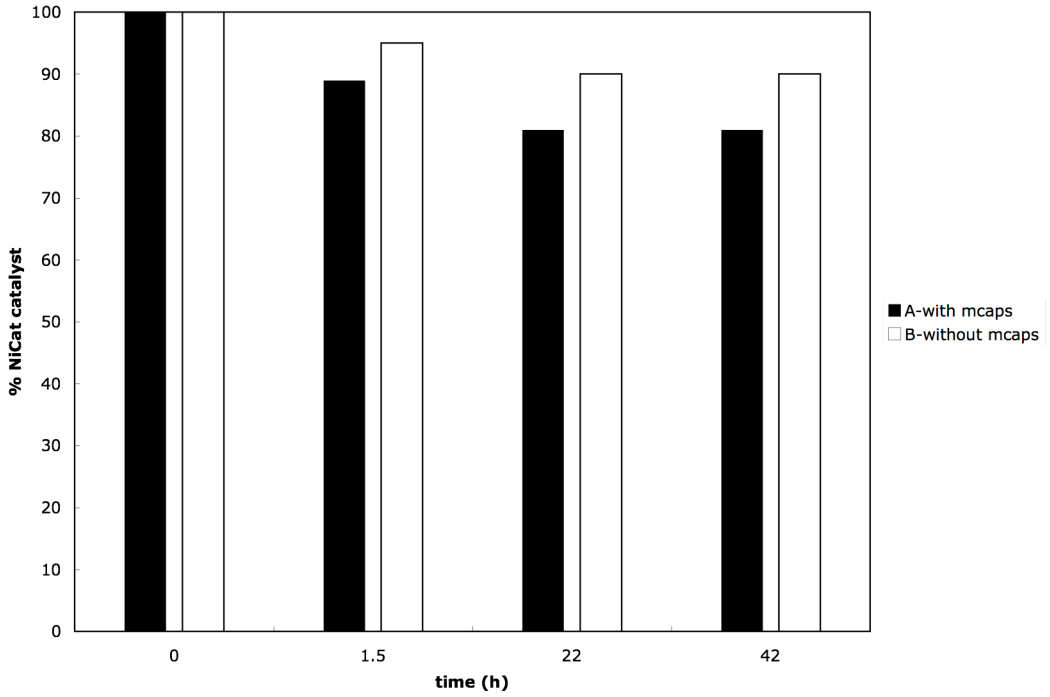

Figure A1.4. Percent nickel catalyst degradation as a function of time: A) in the presence of μcaps, and B) in the absence of μcaps.

Qualitative assessment of nickel catalyst interaction with μcaps and free PEI

To nickel catalyst (**2**, 60 mg) dissolved in toluene (1 mL), either μcap catalyst (**1**, 30 mg) or, as a control, free PEI (30 mg) was added. Color change was captured with a digital camera and displayed below.

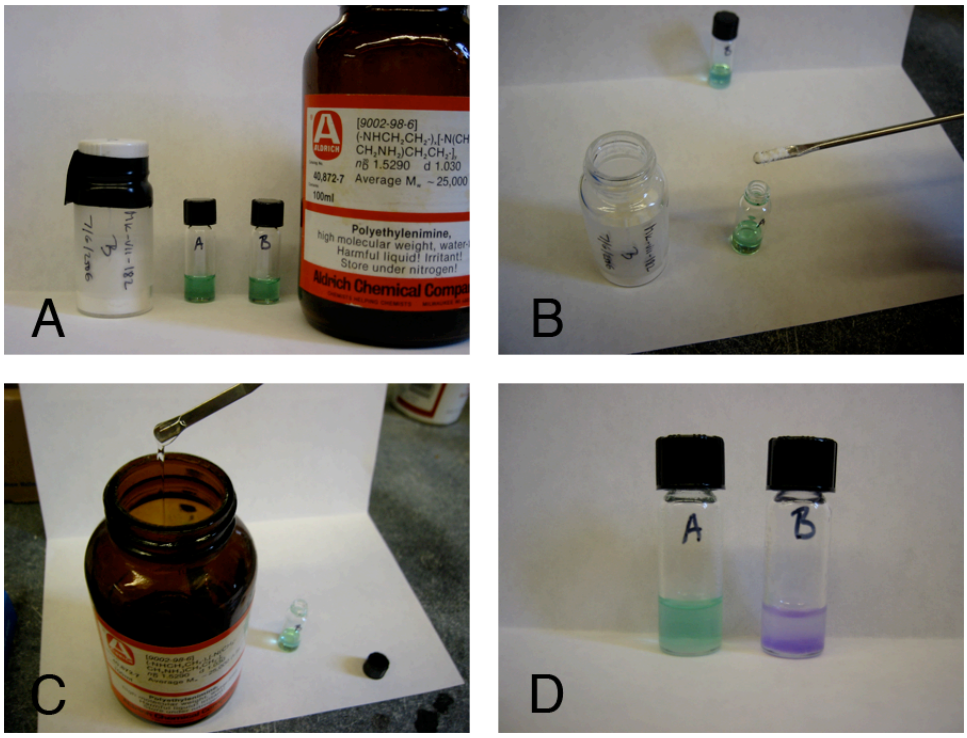

Figure A1.5. Qualitative assessment of nickel catalyst interaction with μcaps and free PEI: μcaps, two solutions of nickel catalyst, and free PEI (A), μcaps being added to the nickel catalyst solution (B), free PEI being added to the nickel catalyst solution (C), and comparison of nickel catalyst solutions with μcaps and free PEI added (D).

*Michael addition in the presence and absence of microencapsulated PEI (**1**)*

The Michael addition between *trans*-β-nitrostyrene (**4**) and dimethyl malonate was performed in the presence and absence of microencapsulated PEI (**1**) in order to determine if the presence of the μcaps decreases the catalytic activity of the nickel catalyst (**2**). In order to prevent the binding of *trans*-β-nitrostyrene to the μcaps, the primary amines of the μcaps were acylated with acetic anhydride. The Michael additions were performed as followed: to either a vial containing 30 mg acylated μcaps swollen in 0.5 mL MeOH, a vial containing 30 mg of untreated μcaps swollen in 0.5 mL MeOH, or a vial containing 0.5 mL MeOH was added *trans*-β-nitrostyrene

(**4**) (149.2 mg, 1 mmol), nickel catalyst **2** (16.2 mg, 2.0 mol%), and toluene (1 mL). The vial was sealed with a screw cap and he reaction was rocked at room temperature on a rocker. Reaction conversion was monitored by withdrawing aliquots from the reaction at different time intervals, diluting with methylene chloride, and analyzing by GC with reference to mesitylene.

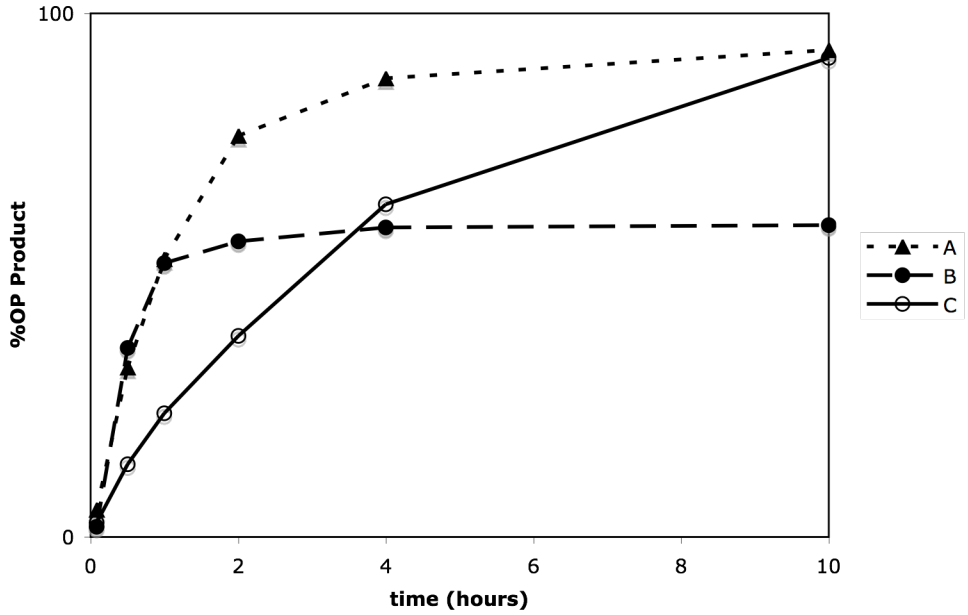

Figure A1.6. Uncorrected data from the Michael addition between *trans*-β-nitrostyrene (**4**) and dimethyl malonate in the presence of acylated μcaps (A), in the presence of untreated μcaps (B), and in the absence of μcaps (C).

It can be seen that in both cases where μcaps are present (Figure A1.6, A and B), there is an initial rate enhancement compared to the control (Figure A1.6, C). The reaction with acylated μcaps (Figure A1.6, A) maintains this rate enhancement throughout the entire reaction while the reaction with untreated μcaps levels off after 60% conversion. This is due to **4** binding irreversibly to the μcaps and being rendered unavailable for conversion to **6**. This effect can be corrected for by reporting the

normalized yield of **6**: (moles of **6**)/(moles of **4** + moles of **6**). These results are shown in Figure A1.7.

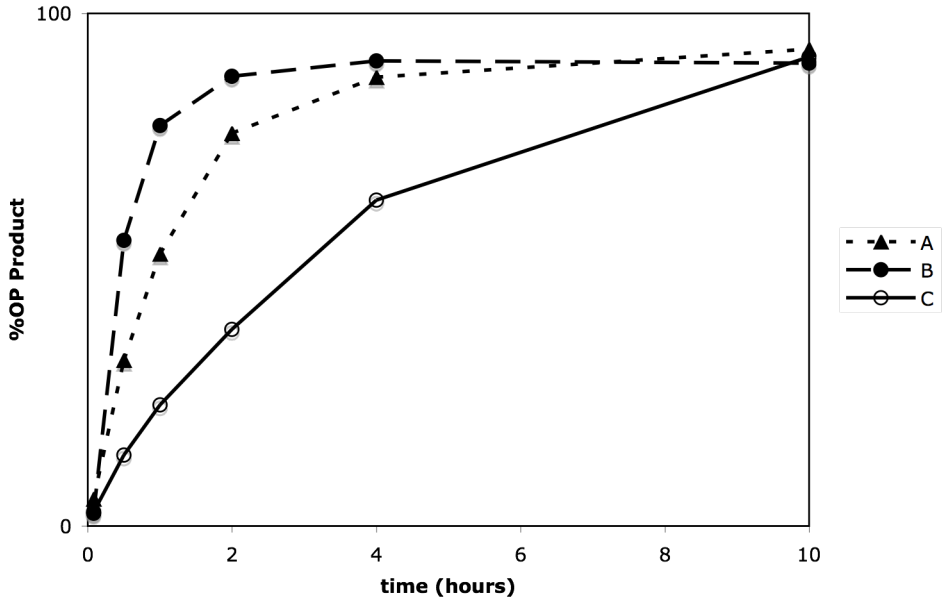

Figure A1.7. Corrected data from the Michael addition between *trans*-β-nitrostyrene (**4**) and dimethyl malonate in the presence of acylated μcaps (A), in the presence of untreated μcaps (B), and in the absence of μcaps (C). Data from cases A and C have not been modified. Data from case B has been standardized to account for the irreversible binding of starting material to μcaps.

When the results for the untreated μcaps are corrected, it can be seen that acylated (Figure A1.7, A) and untreated (Figure A1.7, B) μcaps demonstrate similar rate enhancement. More importantly, μcap presence does not decrease the overall yield, as all three cases remain stable at 90% yield of **6** past the 10 hour point. If the nickel catalyst were able to interact with the encapsulated PEI, we would expect to see a dramatic decrease in yield of **6**, as is observed in the control experiments. Negligible (0-5%) yield of **6** is obtained in control experiments (not shown) employing μcaps alone, μcaps in the presence of PEI, or no catalyst.

REFERENCES

1. Bernasconi, C. F; Renfrow, R. A.; Tia, P. R. *J. Am. Chem. Soc.* **1986**, *108*, 4541.

2. Lough, C. E.; Currie, D. J. *Can. J. Chem.* **1966**, *44*, 1563.

3. Mouhtaram, M.; Jung, L.; Stambach, J. F. *Tetrahedron* **1993**, *49*, 1391.

4. Worrall, D. E. *J. Am. Chem. Soc.* **1927**, *49*, 1598.

APPENDIX 2

Supporting Information for Chapter 4

Microcapsule-catalyzed reaction in different solvents

General Procedure: Either free PEI (15 mg, 13.8 mole %) or encapsulated PEI (**1**, 30 mg, 26.4 mole %) was placed in a 4 mL glass vessel. Solvent (1 mL) was added, and the vessel was sealed and allowed to stand at room temperature overnight. Benzaldehyde (**4**, 101.6 µL, 1 mmol), nitromethane (0.54 mL, 10 mmol), and mesitylene (13.9 µL, 0.1 mmol) were added. The vessel was sealed and the reaction was rocked at room temperature on a rocker. Reaction conversion was monitored by withdrawing aliquots from the reaction at different time intervals, diluting with methylene chloride, and analyzing by GC with reference to mesitylene.

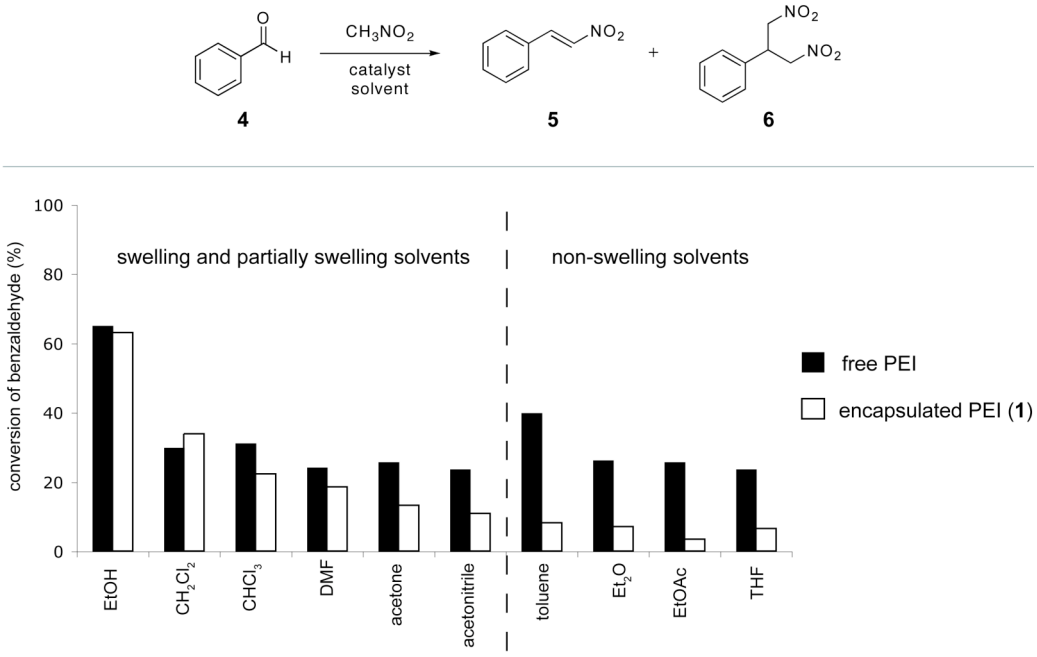

Figure A2.1. Conversion of benzaldehyde (**4**) after 6 hours for the amine-catalyzed reaction between benzaldehyde and nitromethane. Catalysts for the reaction were free PEI (black, 4.6 mol %) and encapsulated PEI (white, 4.6 mol %).

Evidence against nitroalcohol intermediate

2-nitro-1-phenylethanol. The title compound was prepared according to the following procedure: Benzaldehyde (**4**, 0.48 mL, 4.7 mmol), nitromethane (0.5 mL, 9.2 mmol), triethylamine (6 drops), and EtOH (0.54 mL) were stirred at room temperature for 18 hours. The volatile components were removed under reduced pressure and the crude product was purified by column chromatography (20% EtOAc/hexanes). ^{1}HNMR (400 MHz, $CDCl_3$) δ 7.46-7.41 (m, 5H), 5.52-5.48 (dd, 1H), 4.66-4.62 (dd, 1H), 4.58-4.53 (dd, 1H), 3.86 (s, 1H); ^{13}CNMR (400 MHz, $CDCl_3$) δ 138.4, 129.2, 129.1, 126.2, 81.4, 71.2.

Microencapsulated PEI catalyst (**1**, 25 mg, 11.5 mol %) was swollen in 1 mL methanol in a 4 mL glass vessel before use. 2-nitro-1-phenylethanol (167 mg, 1 mmol) and mesitylene were added to the vessel, which was sealed and rocked at room temperature on a rocker. Reaction conversion was monitored by withdrawing aliquots from the reaction at different time intervals, diluting with methylene chloride, and analyzing by GC with reference to mesitylene. No *trans*-β-nitrostyrene (**5**) formation was observed over the course of the reaction.

Kinetic studies for tandem reaction

Microencapsulated PEI catalyst (**1**, 25 mg, 3.83 mol %) was swollen in 0.5 mL methanol in a 4 mL glass vessel before use. Nickel catalyst **2**, aldehyde **8** (108.2 μL, 1 mmol), nitromethane (0.54 mL, 10 mmol), dimethyl malonate (114.3 μL, 1 mmol), and toluene (1 mL) were added to the vessel, which was sealed with a screw cap. The

reaction was rocked at room temperature on a rocker. Reaction conversion was monitored by withdrawing aliquots from the reaction at different time intervals, diluting with methylene chloride, and analyzing by GC with reference to mesitylene.

Data Summary:

mg Ni cat	mole % Ni cat	rate (μmol **7i**/min)	std dev
27.5	3.4	0.305	0.037
55	6.8	0.520	0.031
85	10.5	0.689	0.035
110	13.6	0.915	0.029
165	20.4	1.714	0.143
220	27.2	1.952	0.190

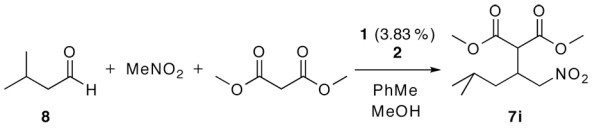

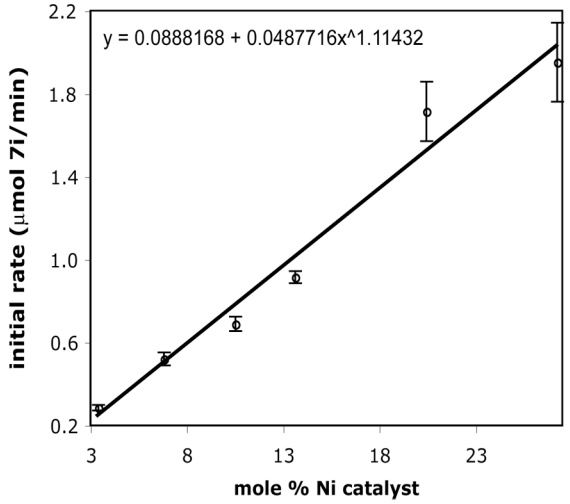

Kinetic studies for Michael addition

The 1^{o} and 2^{o} amines of microencapsulated catalyst **1** were acylated in the following manner: methanol (2.5 mL) was added to microcapsule catalyst (500 mg)

loaded in a syringe equipped with a frit. Acetic anhydride (3 mL) was drawn into the syringe and the mixture was rocked at room temperature overnight. The μcaps were washed with methanol and dried under vacuum before use.

Acylated μcaps were swollen in 0.5 mL methanol in a 4 mL glass vessel before use. Nickel catalyst (**2**, 16.2 mg, 2 mol %), *trans*-β-nitrostyrene (**5**, 149.2 mg, 1 mmol), dimethyl malonate (137 μL, 1.2 mmol), and toluene (0.5 mL) were added to the vessel, which was sealed with a screw cap. The reaction was rocked at 297 K on a rocker. Reaction conversion was monitored by withdrawing aliquots from the reaction at different time intervals, diluting with methylene chloride, and analyzing by GC with reference to mesitylene.

Data Summary:

mg μcaps	mg μcaps	Rate (mmol **7a**/min)	std dev
0	0	0.0101	0.0003
5	5	0.0122	0.0007
15	15	0.0169	0.0008
30	30	0.0231	0.0005

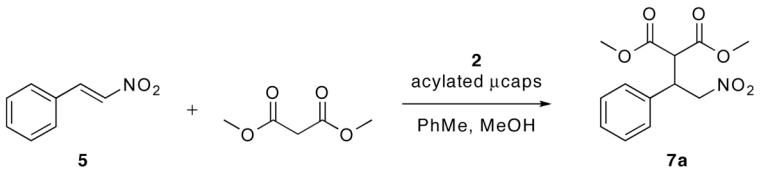

5 **7a**

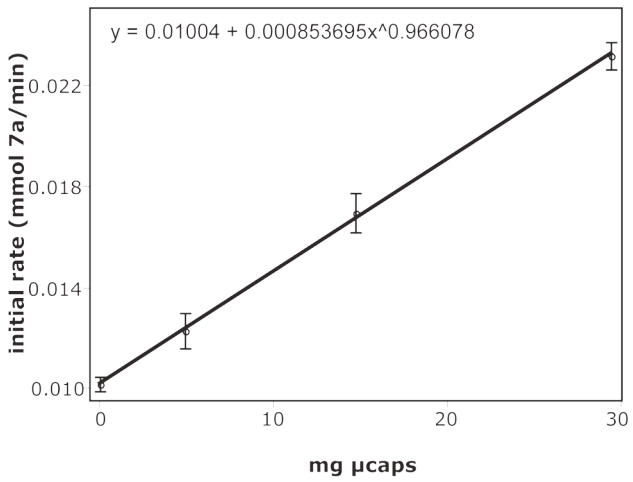

APPENDIX 3

Supporting Information for Chapter 5

Examination of additives for rate enhancement in the Michael Addition

General Procedure: To *trans*-β-nitrostyrene (149.2 mg, 1 mmol), nickel catalyst **2** (16.2 mg, 0.02 mmol), and mesitylene (13.9 μL, 0.1 mmol) in solvent (1 mL) was added the appropriate polymer, urea, or amine. Dimethyl malonate (137.1 μL, 1.2 mmol) was added and the reaction was stirred at room temperature. Reaction conversion was monitored by withdrawing aliquots from the reaction at different time intervals, diluting with methylene chloride, and analyzing by GC with reference to mesitylene.

Table A3.1 Michael addition in the presence of urea and amine additives.

Additive	Amount	Mol %	Solvent	k_{rel}[a]
4	31.2 mg	14.7	toluene	1.01
5	24.1 mg	14.7	toluene	0.94
6	15.0 mg	—	THF	0.81
7	15.0 mg	—	$CHCl_3$	1.64
8	15.2 mg	7.3	$CHCl_3$	2.66
9	17.0 mg	—	$CHCl_3$	1.54
11	7.0 μL	5.0	$CHCl_3$	2.07

[a] k_{rel} values are reported relative to the control reaction with no additive in the same respective solvent.

Michael addition: Order in amine

General Procedure: *trans*-β-Nitrostyrene (149.2 mg, 1 mmol), and mesitylene (13.9 mL, 0.1 mmol) were dissolved in $CHCl_3$. The amount of nickel catalyst **2** was held constant while the amount of amine **8** was varied (Table A3.2). Dimethyl

malonate (137.1 μL, 1.2 mmol) was added and the reaction was stirred at room temperature. Reaction conversion was monitored by withdrawing aliquots from the reaction at different time intervals, diluting with methylene chloride, and analyzing by GC with reference to mesitylene.

Table A3.2. Variation of nickel catalyst **2**.

% Nickel catalyst **2**	mg nickel catalyst **2**
0.5	4.05
1.0	8.1
2.0	16.2
3.0	24.3

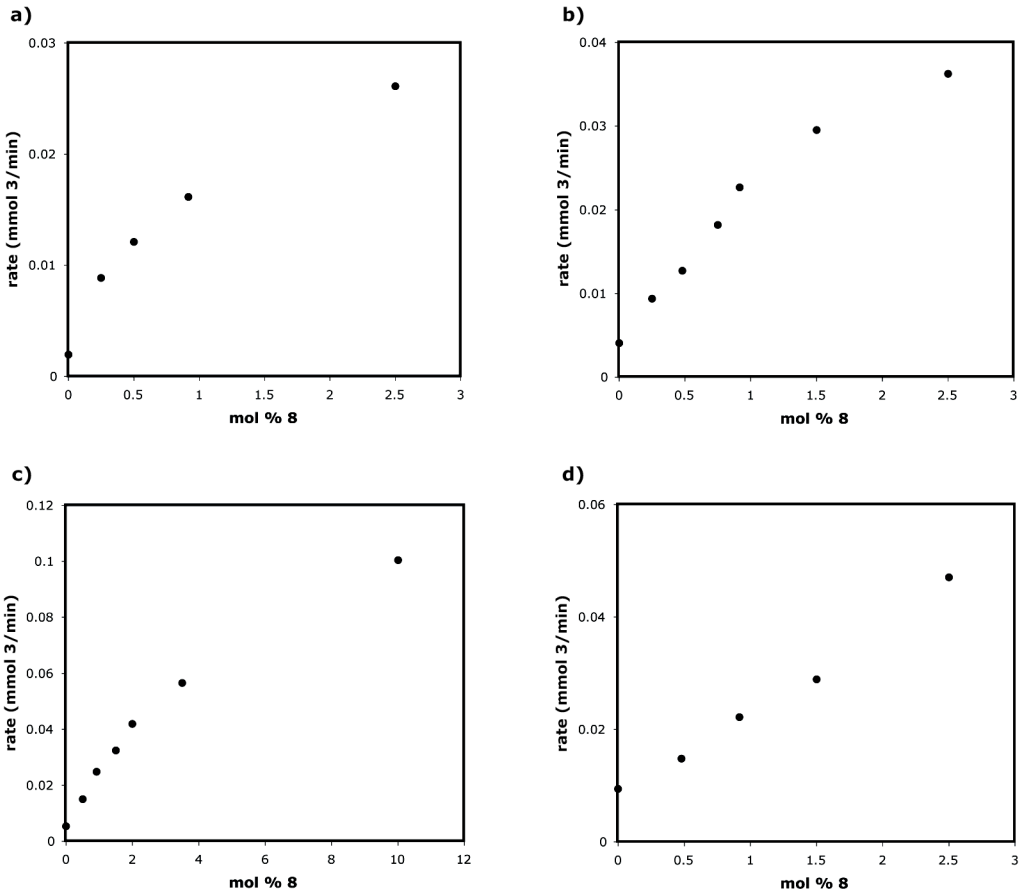

Figure A3.1. Order in amine **8** at nickel catalyst loadings of 0.5% (a), 1.0% (b), 2.0% (c), and 3.0% (d).

Michael addition: Order in amine

General Procedure: *trans*-β-Nitrostyrene (149.2 mg, 1 mmol), and mesitylene (13.9 mL, 0.1 mmol) were dissolved in $CHCl_3$. The amount of amine **8** was held constant while the amount of nickel catalyst **2** was varied (Table A3.3). Dimethyl malonate (137.1 μL, 1.2 mmol) was added and the reaction was stirred at room temperature. Reaction conversion was monitored by withdrawing aliquots from the reaction at different time intervals, diluting with methylene chloride, and analyzing by GC with reference to mesitylene.

Table A3.3. Variation of amine **8**.

% amine **8**	mg amine **8**
0	0
0.92	1.9
2.5	5.2
3.5	7.3
10	20.7

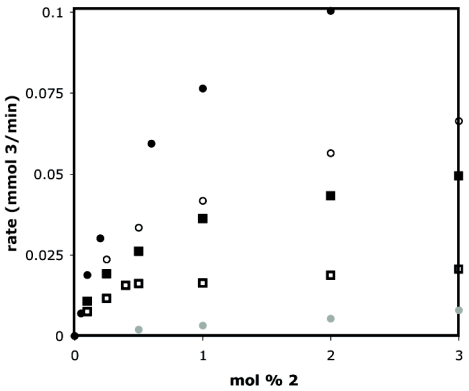

Figure A3.2. Order in nickel for amine loadings of 10% (●), 3.5% (○), 2.5% (■), 0.92% (□), and 0% (●).

Method of continuous variation

General Procedure: *trans*-β-Nitrostyrene (149.2 mg, 1 mmol), and mesitylene (13.9 mL, 0.1 mmol) were dissolved in $CHCl_3$ (amount varies). The total amount of amine **8** and nickel catalyst **2** was held constant while their ratio was varied. Dimethyl malonate (137.1 μL, 1.2 mmol) was added and the reaction was stirred at room temperature. Reaction conversion was monitored by withdrawing aliquots from the reaction at different time intervals, diluting with methylene chloride, and analyzing by GC with reference to mesitylene.

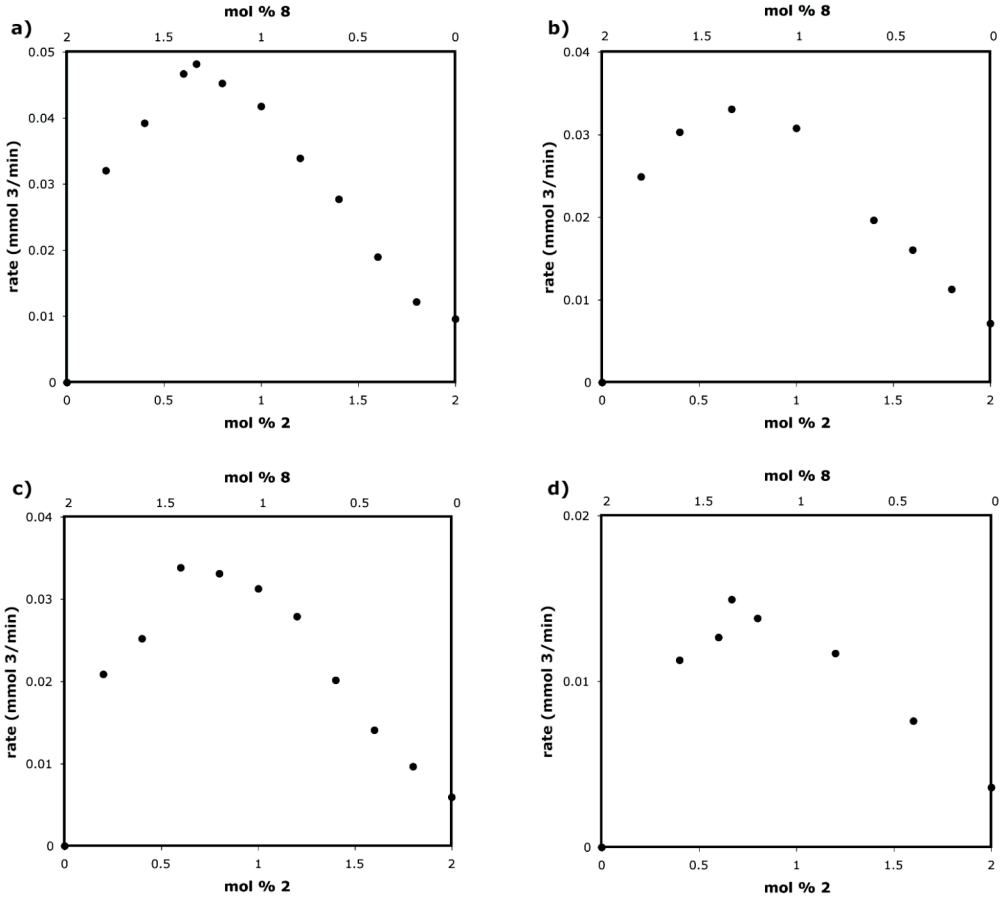

Figure A3.3. Job plots, 2% total catalyst concentration for total solvent volumes of 0.2 mL (a), 0.5 mL (b), 1.0 (c), and 2.5 mL (d).

The general procedure was repeated using triethylamine (**11**) instead of amine **8** to obtain the same results (Figure A3.4)

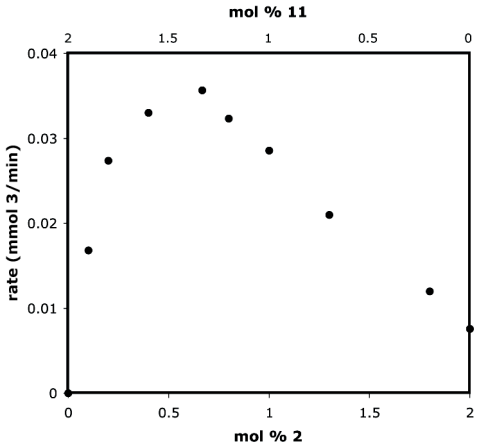

Figure A3.4. Job plot with triethylamine and nickel catalyst, 2% total catalyst loading, 1 mL solvent.

Rate Model—1:1 Ratio

From Equation 5.4:

$$K_{eq} = \frac{[x]}{[\mathbf{2}_o\text{-}x][\mathbf{8}_o\text{-}x]} \qquad \text{(Equation A3.1)}$$

where x represents the amount of complex **2•8** present in the reaction. Equation A3.1 can be rearranged to obtain

$$K_{eq}x^2 - (K_{eq}(\mathbf{2} + \mathbf{8}) + 1)x + K_{eq}\bullet\mathbf{2}\bullet\mathbf{8} = 0 \qquad \text{(Equation A3.2)}$$

in the form $ax^2 + bx + c = 0$, where $a = K_{eq}$, $b = -(K_{eq}(\mathbf{2} + \mathbf{8}) + 1)$, and $c = K_{eq}\bullet\mathbf{2}\bullet\mathbf{8}$. The quadratic equation can be solved by

$$x = \frac{-b \pm (b^2 - 4ac)^{0.5}}{2a} \qquad \text{(Equation A3.3)}$$

and the values for [**2**•**8**] (x) and [**2**] ($\mathbf{2}_o$-x) can be plugged into Equation A3.4 to model the rate.

$$d[\mathbf{3}]/dt = k_1[\mathbf{2}\bullet\mathbf{8}] + k_2[\mathbf{2}] \qquad \text{(Equation A3.4)}$$

Rate Model—2:1 Ratio

From Equation 5.6:

$$K_{eq} = \frac{[x]}{[\mathbf{2}_o\text{-}x][\mathbf{8}_o\text{-}2x]^2} \qquad \text{(Equation A3.5)}$$

where x represents the amount of complex **2**•**8** present in the reaction. Equation A3.5 can be rearranged to obtain

$$(K_{eq}((\mathbf{2}_o - x)(\mathbf{8}_o - 2x)^2)) - x = 0 \qquad \text{(Equation A3.6)}$$

which can be solved in Microsoft Excel and plugged into Equation A3.4 or A3.7 to model the rate.

$$d[\mathbf{3}]/dt = k_1[\mathbf{2}\bullet\mathbf{8}]^{0.5} + k_2[\mathbf{2}] \qquad \text{(Equation A3.7)}$$

APPENDIX 4

Supporting Information for Chapter 6

α-Aminoxylations of aldehydes in the presence of additives

General Procedure: The general procedure is described in the Experimental Section of Chapter 6.

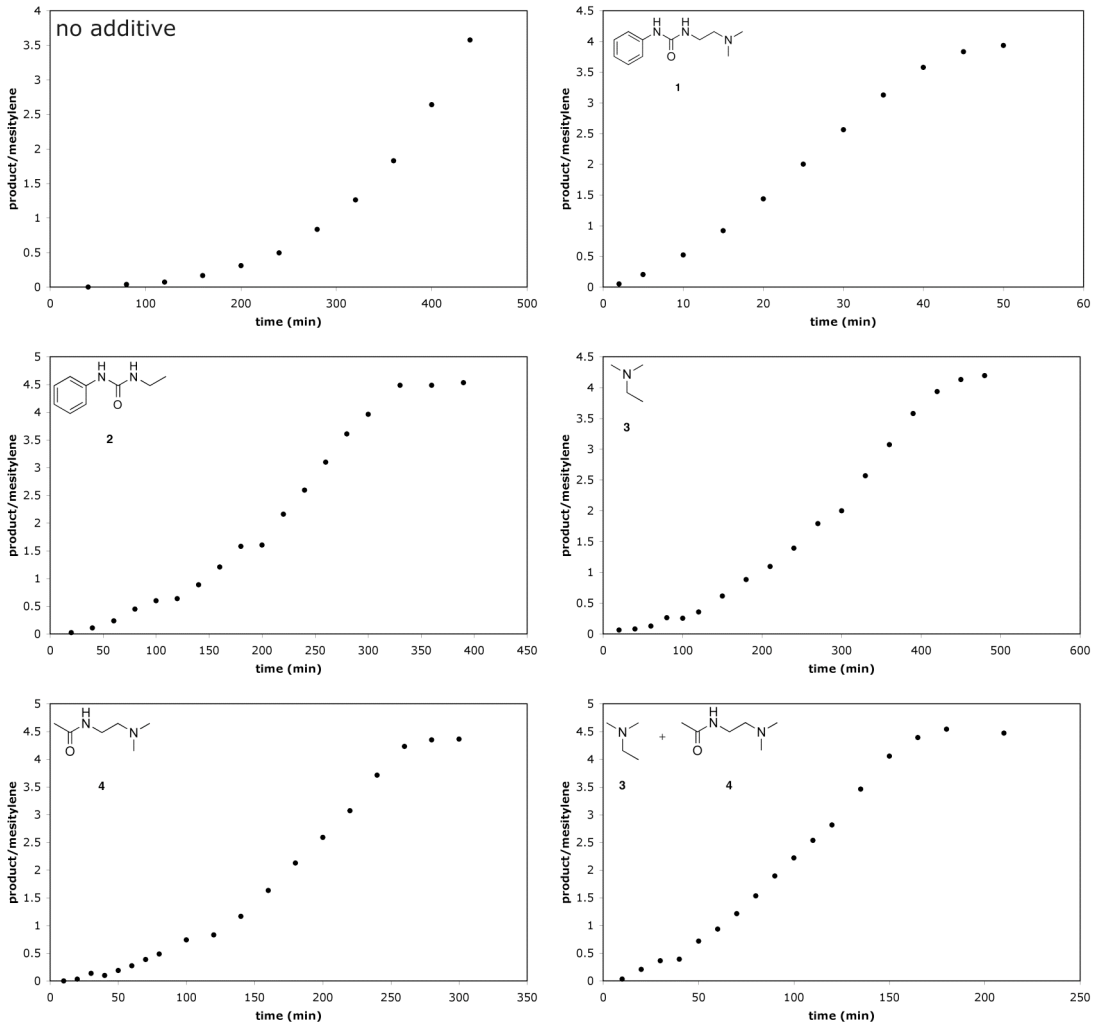

Figure A4.1. Reaction profiles for α-aminoxylations in ethyl acetate.

Examination of other ureas

General Procedure: The reaction was performed as described in the general procedure in the Experimental Section of Chapter 6.

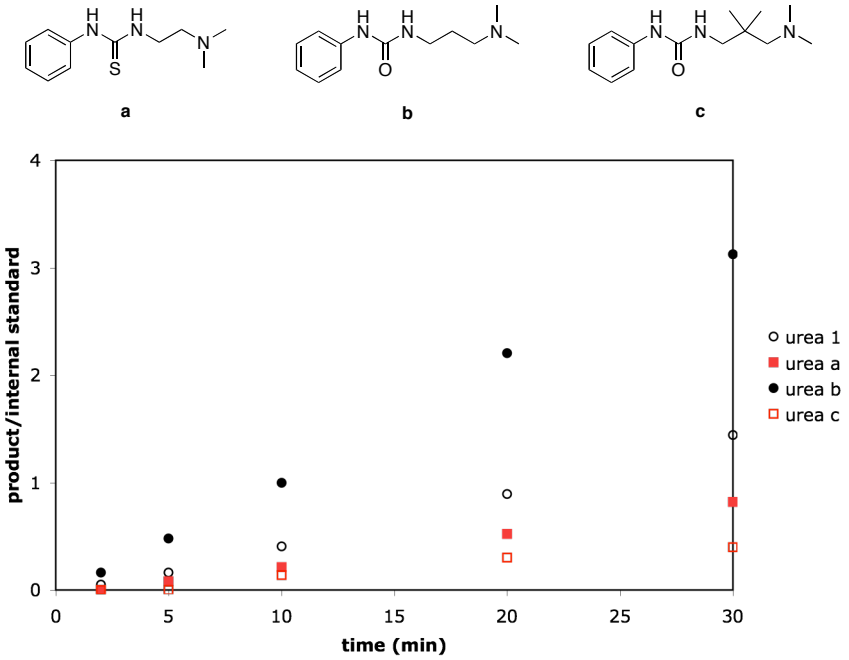

Figure A4.2. α-Aminoxylation of hexanal using ureas **a-c**.

Mannich reaction between benzaldehyde N-Boc imine and propionaldehyde

Benzaldehyde *N*-Boc imine was prepared as reported in the literature.[1]

The Mannich reaction was modified from the procedure reported by Yang et al.[2] A solution of additive (0.05 mmol, 0.05 eq) in 1 mL solvent was added to (L)-proline (5.8 mg, 0.05 mmol, 0.05 eq) in a 1 dram screw cap vial. The vial was sonicated for 1 min and stirred at 0 °C for 15 min. 1 mL of a stock solution of benzaldehyde *N*-Boc

imine (1.0 M) and mesitylene (0.1 M) was added, followed by propionaldehyde (72.2 μL, 4 mmol, 4 eq) and the reaction was stirred at 0 °C. Reaction conversion was monitored by withdrawing aliquots from the reaction, diluting into dichloromethane, and analyzing by GC with reference to mesitylene.

Table A4.1. Reaction times for Mannich reaction in the presence of additives.

additive	time (h)
none	10
urea **1**	2.5
ethyl phenyl urea **2**	9
N,N-dimethylethylamine **3**	4
2 + **3**	2.5

^{1}H-NMR solubility studies

To (L)-proline (17.3 mg, 0.15 mmol) and urea (31.1 mg, 0.15 mmol) in a 1 dram screw cap vial was added mesitylene (5 mM in $CDCl_3$). As a control a vial was prepared in the same way without urea. The vials were rocked at room temperature. After 2 h, the solution was filtered through a 0.45 μm PTFE membrane and assessed by ^{1}H-NMR spectroscopy at 24 °C using the following parameters:

sfrq	300.073
tn	H1
at	1.666
np	16360
sw	4909.2
fb	not used
pw	10
tpwr	56
d1	60.000
tof	685.1
nt	1
gain	28

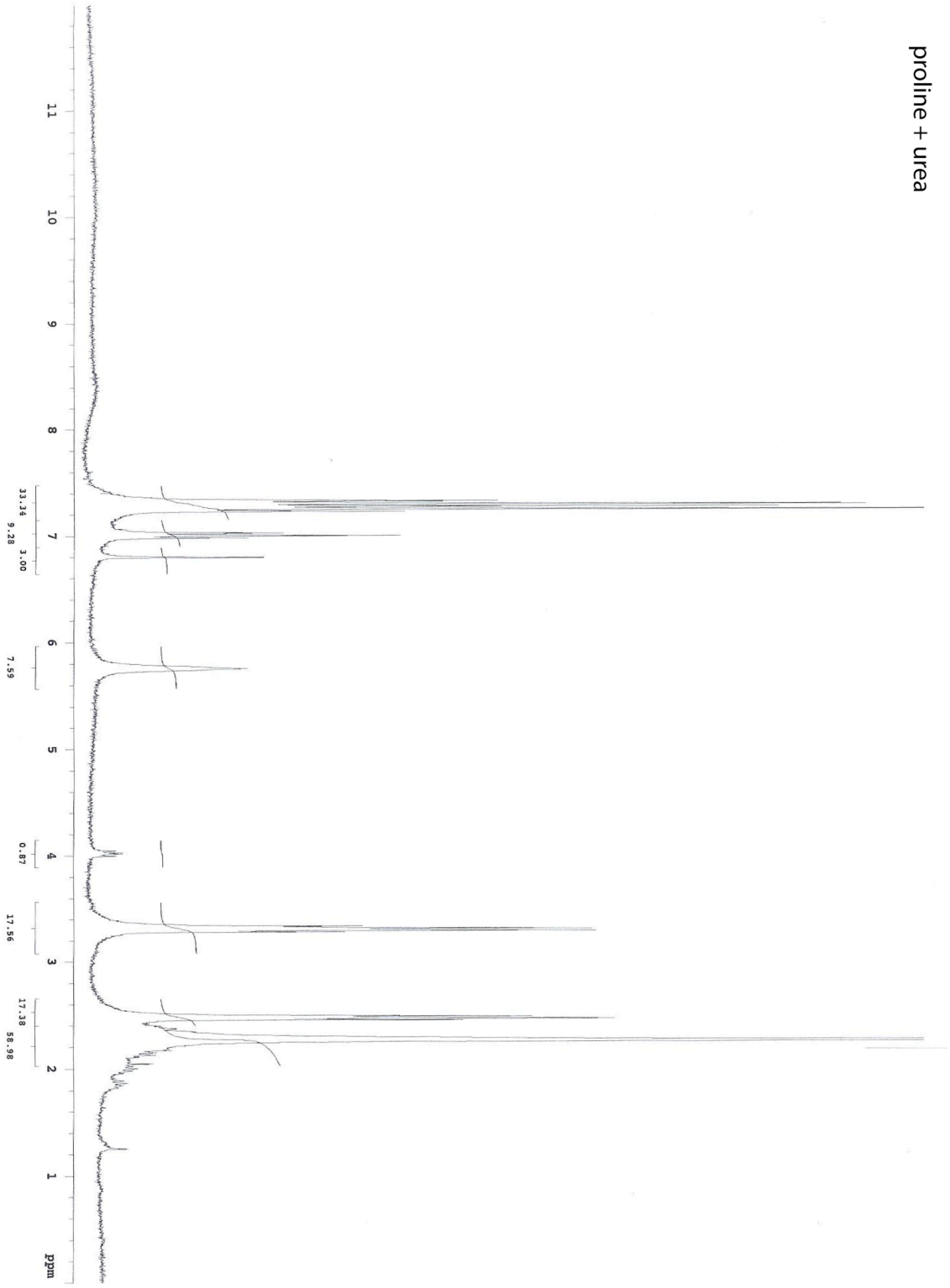

Figure A4.3. ^{1}H NMR spectrum of a 1:1 mixture of proline and urea **1**.

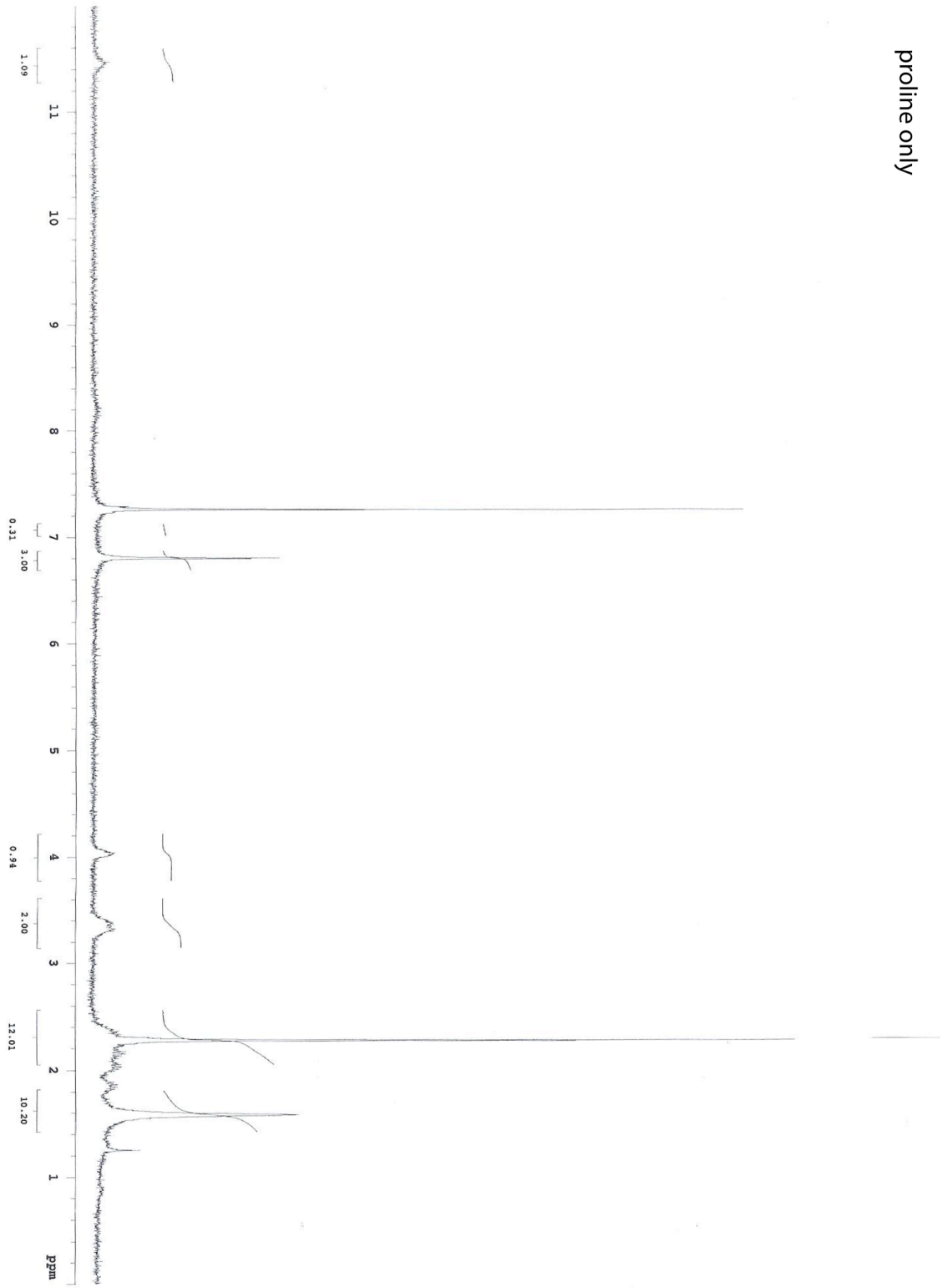

Figure A4.4. ^{1}H NMR spectrum of proline.

Comparison of the aromatic mesitylene proton shift (δ = 6.80) with the proline proton at δ = 4.02 indicates that there is no difference in the extent of dissolution in the two cases:

	mesitylene : proline	proline concentration (M)
proline + 1	3.00 : 0.87	0.0044
proline only	3.00 : 0.94	0.0047

Proline solubility of 0.0045 M is consistent with literature values.[3]

Calculations for iminium-enamine exchange

The 2+2 cycloadduct proposed in Scheme 4 was investigated using the following isodesmic equation. The values provided were computed using the density functional B3LYP with a 3-21G basis set. Thought this is a low level of theory performed in the gas phase, we feel that the relatively similar energies of the sum of the starting materials and product indicate that formation of the intermediate is plausible.

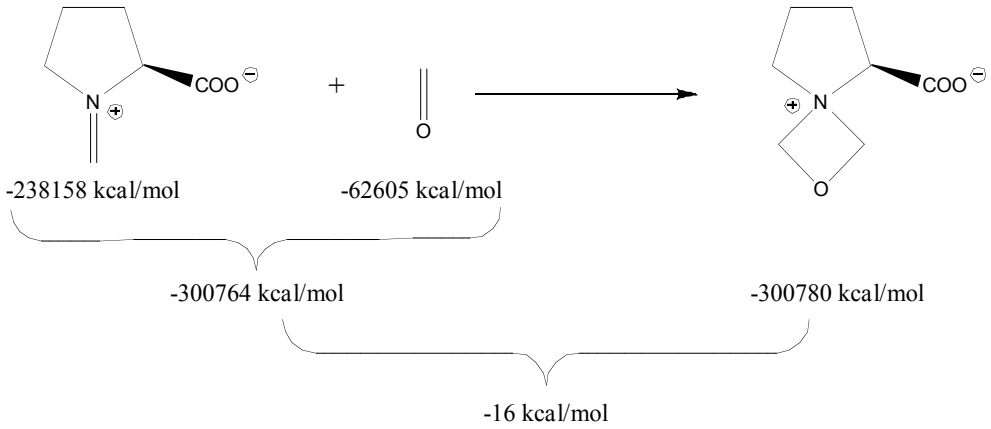

Figure A4.5. Calculations for iminium-enamine exchange.

REFERENCES

1. Wenzel, A. G.; Jacobsen, E. N. *J. Am. Chem. Soc.* **2002** *124*, 12964

2. Yang, J. W.; Stadler, M.; List, B. *Angew. Chem. Int. Ed.* **2007**, *46*, 609.

3. Iwamura, H.; Wells, D. H., Jr.; Mathew, S. P.; Klussmann, M.; Armstrong, A.; Blackmond, D. G. *J. Am. Chem. Soc*. **2004**, *126*, 16312.